ISSN 2458-973X

# JSCMT

# Journal of Sustainable Construction Materials and Technologies

Volume 6
Number 4
Year 2021

YTÜ PRESS

www.jscmt.yildiz.edu.tr

**Journal of Sustainable Construction Materials and Technologies**
Web page info: https://jscmt.yildiz.edu.tr

JSCMT
Journal of Sustainable Construction Materials and Technologies

## Editor In Chief

Assoc. Prof. Dr. Orhan CANPOLAT
Yildiz Technical University

## Assistant Editor

Khizar NAZIR
Yildiz Technical University

## Contact

Journal of Sustainable Construction

Materials and Technologies (JSCMT)

Yildiz Technical University
Civil Engineering Department, 34220 Esenler
Istanbul – Turkey

Web: http://dergipark.gov.tr/jscmt/

E-mail: jscmt@yildiz.edu.tr

**Journal of Sustainable Construction Materials and Technologies**
Web page info: https://jscmt.yildiz.edu.tr

JSCMT
Journal of Sustainable Construction Materials and Technologies

## Honorary Editorial Advisory Board

Tarun R. NAIK
University of Wisconsin-Milwaukee, USA

## Editor-In Chief

Orhan Canpolat
Yildiz Technical University, Turkey

## Co-Editors

Rakesh KUMAR
Central Road Research Institute, India

Benchaa BENABED
University of Laghouat, Algeria

## Editorial Board

Messaoud SAIDANI
Coventry University, UK

Xiaojian GAO
Harbin Institute of Technology, China

Muammer KOÇ
Hamad bin Khalifa University (HBKU), Qatar

Mohiuddin M KHAN
Washington State University, USA

Mustafa ŞAHMARAN
Hacettepe University, Turkey

Roman RABENSEIFER
Slovak University of Technology in Bratislava, Slovakia

Soofia Tahira Elias ÖZKAN
Middle East Technical University, Turkey

Ali Naji ATTIYAH
University of Kufa, Iraq

Asad-ur-Rehman KHAN

**Journal of Sustainable Construction Materials and Technologies**
Web page info: https://jscmt.yildiz.edu.tr

JSCMT
Journal of Sustainable Construction Materials and Technologies

NED University of Engineering & Technology, Pakistan

A.S.M. Abdul AWAL
Universiti Teknologi Malaysia, Malaysia

Aravind Krishna SWAMY
Indian Institute of Technology Delhi, India

Mohammed Mosleh SALMAN
College of Engineering Al-Mustansirya University, Iraq

Mohammed ARIF KEMAL
Aligarh Muslim University, India

Sepanta NAIMI
Altinbas University, Turkey

**Language Editors**

Mohiuddin M KHAN
Washington State University, USA

Mukhallad M.M. AL-MASHHADANI
Istanbul Gelisim University, Turkey

**Assistant Editor**

Khizar NAZIR
Yildiz Technical University, Turkey

Journal of Sustainable Construction Materials and Technologies
Web page info: https://jscmt.yildiz.edu.tr

JSCMT
Journal of Sustainable Construction Materials and Technologies

# TABLE OF CONTENTS

Journal of Sustainable Construction Materials and Technologies
Web page info: https://jscmt.yildiz.edu.tr
DOI: 10.14744/jscmt.2021.01

JSCMT
Journal of Sustainable Construction Materials and Technologies

Original Article

# Plaster of Paris containing zero valent iron particles: Designing a permeable reactive barrier, used for remediation of 4-nitroaniline pollution

**Saliha BOUDIA[1,2], Farida FERNANE[1], Patrick SHARROCK[2,3], Marina FIALLO[2*]**

[1]*Mouloud Mammeri University, Natural Resources Laboratory, Tizi-Ouzou, Algeria*
[2]*Chemistry department, Université Toulouse 3 Paul Sabatier, Castres, France*
[3]*RAPSODEE, Ecole des Mines, Albi, France*

## ARTICLE INFO

*Article history*
*Received: 19 July 2021*
*Accepted: 10 November 2021*

**Key words:**
Groundwater remediation, zero valent iron, nitroaniline, permanent reactive barrier, plaster, pollutants, precast wall block

## ABSTRACT

Permeable reactive barrier (PRB) containing zero valent iron (ZVI), plaster and additives to make a porous composite structure, was tested to remove an organic nitro compound as model pollutant. An aqueous solution of 4-nitroaniline (PNA) was passed through a porous plaster column and chemical degradation quantified by UV-Vis spectroscopy. PNA was reduced to p-phenylenediamine and the rate of the reduction was strongly related to ZVI amount, pollutant volume, and the contact rate with the metal particles. The PBR could be controlled by design and operation. Test columns were made to evaluate the materials for making precast plaster blocks containing ZVI. The results showed that such porous plaster blocks could be efficient as retaining funneling walls for environmental applications. Thus economical Calcium sulphate solids can be used for making remediation columns for depolution with reactive products such as iron metal with capacity for treating unwanted toxic nitrates, or chlorinated-solvents present in waterways. A reactive permeable barrier containing zero valent iron will last as long as some iron particles remain to react.

**Cite this article as:** Boudia S, Fernane F, Sharrock P, Fiallo M. Plaster of Paris containing zero valent iron particles: Designing a permeable reactive barrier, used for remediation of 4-nitroaniline pollution. J Sustain Const Mater Technol 2021;6:4:124–134.

## 1. INTRODUCTION

Permeable reactive barrier (PRB) is a cost-effective technology for groundwater remediation [1]. It is an implementation of filtration consisting in porous material, which passively captures a plume of contaminants through immobilization or transformation of pollutants, releasing decontaminated water to the other side of the barrier [2]. PRB is generally composed of inexpensive filler materials, doped with specific reagents for remediation of unwanted compounds. It was reported that zero valent iron (ZVI) is particularly effective in chemical degradation of persistent chlorinated compounds into non-toxic and harmless by-products [3–5].

Nitroarenes can be reduced to corresponding anilines, in presence of ZVI, in Bechamp reduction [6]; moreover, in organic synthesis other methods were found to be more specific and to reduce by-pass products [7]. For instance,

***Corresponding author.**
*E-mail address: marina.fiallo@iut-tlse3.fr

Published by Yıldız Technical University Press, İstanbul, Turkey
Copyright 2021, Yıldız Technical University. This is an open access article under the CC BY-NC license (http://creativecommons.org/licenses/by-nc/4.0/).

silver nanoparticles were developed for in situ catalytic reduction method of PNA [8]. However, in order to be integrated in a PRB low cost reactant, ZVI has already shown to be a good candidate for reduction of different pollutants [9–11]. Efficiency of a PRB is related to the nature and flow of polluted plume [12, 13].

Calcium sulfates (plaster, $CaSO_4.0.5H_2O$, and its dihydrated product, gypsum, $CaSO_4.2H_2O$) were chosen as "inert substrate" in order to prepare porous composites. They are low cost building materials, sometime considered as a waste when containing phosphogypsum [14, 15]. We researched the possibility of using plaster for making PRB with ZVI as a low cost reactive component. Our aim was to verify if ZVI retains its redox properties when included in a solid shell, shaped as a column and with 4-nitroanilineas pollutant model.

Key factors for all-in-one design of composites for PRB were investigated as follows: permeability of solid plaster, as inert support for PRB, was determined and improved (giving "porous" plaster). "Porous" plaster was tested for its mechanical properties and the best formulas chosen. ZVI was inserted in "porous" plaster and new composites were optimized for all parameters. Reduction of 4-nitroaniline was performed batchwise with ZVI and its degradation to p-phenylenediamine (PDA), was quantified by UV spectroscopy. Reduction of 4-nitroaniline was performed in a downflow column: breakdown and exhaustion points were determined for specific experimental conditions.

## 2. MATERIALS AND METHODS

### 2.1. Chemicals

Plaster, in chemical form of $CaSO_4.0.5H_2O$, was a commercial powder (plaster of Paris quality) from Parexlanko, France; iron powder (ZVI, 325 mesh, 99%), $H_3PO_4$ (85%), and $CaCO_3$ (99%) were from Acros (France), 4-nitroaniline (p-nitroaniline, PNA, 98%), p-phenylendiamine (PDA, 98%), o-phenanthroline (98%) and KSCN (97%) from Aldrich (France).

### 2.2. Plaster Samples Preparation

Plaster slabs were made by adding plaster powder (50 g) to appropriate amounts of distilled water. After 5 minutes of mixing, preparations were poured into PET (polyethylene terephtalate) or PE (polyethylene) cylindrical molds to make samples for flow experiments (in 2.8-cm- diameter, 2-cm-high) and for mechanical tests and density measurements (in 2.6-cm-diameter, 5-cm-heigh). All solid samples were dried at 60°C for 24 hours before their use. All samples were weighted and "apparent" density calculated from geometrical parameters.

### 2.3. Material Characterization

#### *2.3.1. XRD and SEM Analysis*

Solid samples were characterized by powder X-ray diffraction (XRD) with a Bruker D2 X'PertPRO diffractometer using Cu Kα radiation (40 kV and 40 mA). Crystallographic identification of $CaSO_4.2H_2O$ was accomplished by comparing the experimental XRD pattern to COD 2300259 of gypsum standard (point group 2/m). Plaster samples were observed by scanning electron microscopy (SEM) Zeiss Supra 55VP.

#### *2.3.2. Mechanical Tests*

Indirect tensile stress diametral compression tests were carried out with a Zwick Roll Z020 testing machine (Zwick Roell, France) at a cross-head speed of 10 mm/min, until failure. Using initial height (L [m]) and diameter (D [m]) of each sample, and measuring the reciprocated force (F [kg m/s$^2$]) from compression, indirect (or Brazilian) tensile strength, $\sigma_T$ ([kg/m s$^2$]), was calculated from its definition in equation 1:

$$\sigma_T=2F/(\pi LD) \quad (1)$$

#### *2.3.3. Porosity Determination*

Porosity was determined from the ratio of experimental "apparent" density of each sample and gypsum density, $CaSO_4.2H_2O$, 2.308 g/cm$^3$ [16] with equation 2:

$$porosity\ (\%)=(density_{exp}/density_{gypsum})*100 \quad (2)$$

#### *2.3.4. Permeability Coefficient Measurements*

Permeability coefficient measurements were done on plaster samples (2.8-cm diameter, 2.0-cm heigth) with a water pressure column of 5 cm. Discharge of water (Q [m$^3$/s]), percolating under a constant head difference (H [m]) through a sample of porous material of cross area S ([m$^2$]) and length L ([m]), was determined for several samples. Permeability coefficients K (hydraulic conductivity, [m/s]) were calculated from Darcy's law, following equation 3:

$$K = (QL)/(SH) \quad (3)$$

### 2.4. Bechamp Reduction

#### *2.4.1. Spectroscopic Analysis*

Vis-UV spectra were used to quantify 4-nitroaniline (PNA) and p-phenylendiamine (PDA) concentrations. They were recorded between 200 and 700 nm in aqueous solution on a HP 8453 spectrophotometer with quartz cells of 0.2 and 1 cm of path-length. Spectra of pure 4-nitroaniline (PNA) and p-phenylendiamine (PDA) were recorded in aqueous solution giving the following spectroscopic features: PNA: 380 (ε=73.3 l mol$^{-1}$cm$^{-1}$), 227 (35.5), 204 (63.0) nm. PDA: 305 (ε=13.7 l mol$^{-1}$cm$^{-1}$), 240 (49.3), 210 (58.7) nm. PNA concentrations in solution were determined by measuring absorbance at 380 nm. PDA formation (in Bechamp reduction) was checked from band at 240 nm (PDA maximum absorption).

#### *2.4.2. Determination of PNA Degradation*

Degradation of PNA, meaning the disappearing of its characteristic absorption band at 380 nm, was calculated from the UV-Vis spectra (Fig. S1) with equation 4:

$$degradation\ (\%)=(A_{380}-A_{600})/(A°_{380}-A°_{600})*100 \quad (4)$$

where $A_{380}$ and $A_{600}$ are the absorption values of each sample at the noted wavelengths, and $A°_{380}$ and $A°_{700}$ the absorption values of starting solutions. Absorption values were corrected at 600 nm in order to avoid diffusion effects from cloudy solutions. At 380 nm the absorption contribution for presence of PDA in aqueous solutions was insignificant.

#### *2.4.3. ZVI in Batch*

Batch experiments were conducted inside 250 ml Erlemeyer flasks under continuous magnetic stirring (500 rpm) and the overall time of experiments was 7 hours. Batch experimental initial conditions were: temperature; 25°C, PNA concentration; 30 mg/l, water volume; 100 ml. Specific variables in batch experiments included pH (initial pH acidic or neutral) and the amounts of ZVI (1, 2 and 3 g). Sampling was conducted within accumulative time of 15 minutes during first three hours, then of 1 hour for last four in batch experiments. For analysis, 2 ml samples were withdrawn by a 5 ml syringe, their Vis-UV spectra registered using a 1 cm quartz cell, then returned to batch. Initial pH was adjusted, or not, using 95% phosphoric acid. Degradation percentage was calculated from absorbance values at 380 nm.

#### *2.4.4. Column Preparation*

100 g of plaster, mixed with appropriate amounts of ZVI and 0.2% $CaCO_3$, were added to 70 ml of distilled water, containing 0.4 g of phosphoric acid, then all reagents were mixed together and the viscous mixture poured into PET (polyethylene terephtalate) cylindrical molds (in 5.0-cm-diameter, 15-cm-heigh) used as percolator system. PET shells were thermally fixed to plaster columns in order to avoid leaking from their extremities.

#### *2.4.5. ZVI in Column*

PNA-containing aqueous solutions (100 ml aliquots) were passed by percolation through columns. Fractions of 100 ml were recovered post-column: 2 ml of each fraction were checked by UV-Vis spectrum between 200 and 700 nm and absorbance values at 380 nm for used to calculate PNA concentration in each fraction.

#### *2.4.6. Identification of Ionic Species*

Samples of plaster-based composites (2.8-cm diameter, 2.0-cm heigth) were soaked in distilled water (25 ml) and pH was measured as a function of time. KSCN (1%) and o-phenathroline (0.5%) in aqueous solution were used to check by colorimetry presence of Fe(II) or Fe(III) species, respectively.

## *3. Results and Discussion*

Hemihydrate calcium sulphate ($CaSO_4.0.5H_2O$), named plaster, became gypsum when hydrated ($CaSO_4.\ 2H_2O$). Different formulations prepared, by using plaster, water, chemical porogen ($CaCO_3$) and ZVI in different proportions, were realized as expected. For each sample, density, porosity, permeability, and mechanical properties were determined in straightforward fashion. Figure 1 indicated effects of plaster slab chemical composition on mechanical properties and porosity. Detailed values, as well as densities as a function of chemical composition, were reported in Tables A.1, A.2 and A.3.

### 3.1. Properties of Plaster-Based Composites

#### *3.1.1. Effect of Water*

Water/plaster ratio was modified, and physical and mechanical properties were measured for each sample (Fig. 1a, Table A.1). It was reported that water amount determined porosity in plasters blocks [17, 18]; as reported in Figure 1a, indirect tensile strength of plaster was reduced as a function of water content whereas porosity increased. During reaction between plaster ($CaSO_4.0.5H_2O$) and water to form gypsum ($CaSO_4.2H_2O$), part of water was consumed by hydration reaction during material setting and remainder slowly evaporated leading to porosity [19]; hardening of plaster paste lead to porous structure, made of entangled needle-shape gypsum crystals [20].

#### *3.1.2. Effect of Porogen ($CaCO_3$+$H_3PO_4$)*

Porous samples were prepared by adding fine calcium carbonate with plaster powder, then pouring the powder in phosphoric acid–containing aqueous solution. Calcium carbonate was used as porogen in presence of acid in order to generate open porosity and increase permeability through the column (Fig. 1b); phosphoric acid was chosen because formation of calcium phosphate as secondary product gave composites with enhanced mechanical properties and lower dissolution rates [21].

In presence of increasing amount of $H_3PO_4$, porosity increased while density and mechanical properties decreased. These results are in agreement with cavity formation following $CO_2$ evolution during material setting (Table A.2). Starting from 0.5% acid, porosity was not significantly modified, as well as mechanical properties. However, permeability increased three times in magnitude compared to "compact" plaster. Calcium phosphate, formed by reaction of phosphoric acid with calcium carbonate [22], was dispersed in gypsum matrix with no effects on physical and mechanical parameters. It was reported that weak acids (such as citric acid) play a role as plastifier, retarding setting [23]. In fact, citric acid partially inhibits binder hydration from hemihydrate to dihydrate. Total porosity seemed little affected by increasing the amount of $CaCO_3$, pore dimensions were bigger (Fig. 2) and SEM images of porogen-containing samples showed 1 mm pores.

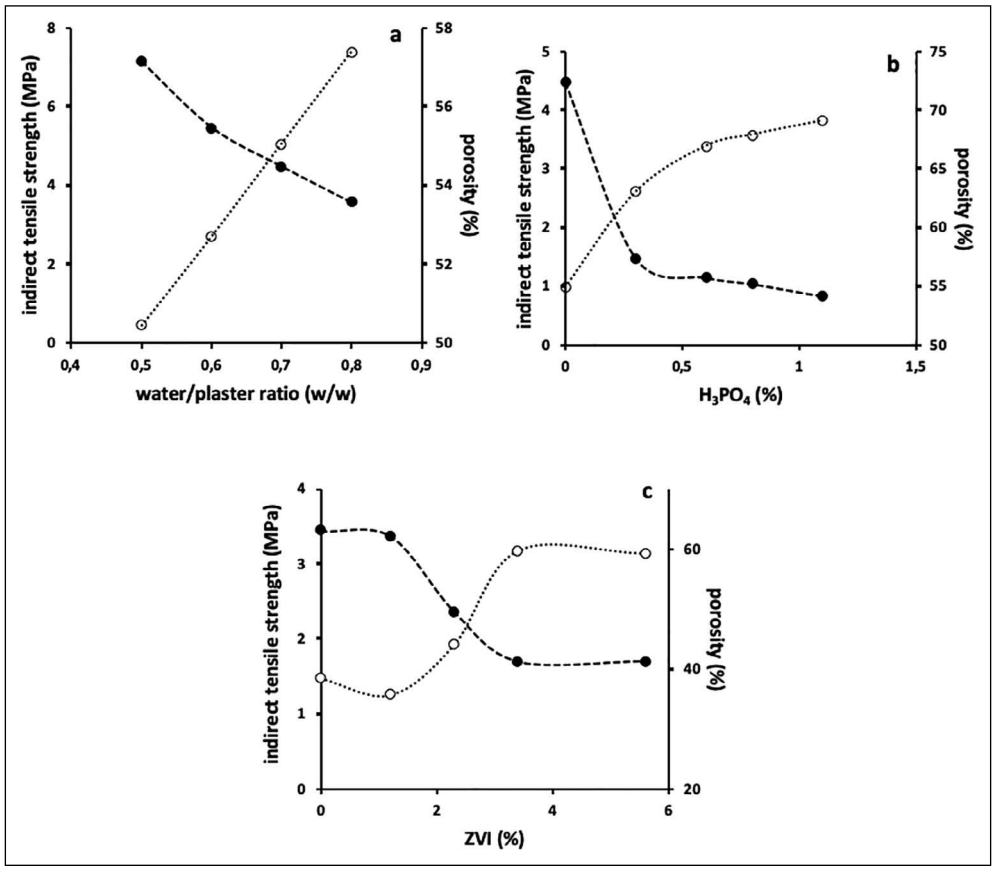


**Figure 1**. **(a)** Indirect tensile strength (closed signet) and porosity (empty signet) as a function of plaster composition as a function of: **(b)** water, (b) $H_3PO_4$, **(c)** ZVI amounts; experimental conditions: plaster (50.0 g).

### *3.1.3. Effect of ZVI*

Different amounts of ZVI were dispersed in solid components (plaster and calcium carbonate) before adding water and phosphoric acid, in order to uniformly scatter the heavier iron particles in the slab. Physical and mechanical properties of different samples obtained were reported in Fig. 1c. Depending on ZVI amounts (Table A.3), density and mechanical properties were increased, and porosity reduced.

### *3.1.4. Effect of Acid*

In classical Bechamp reduction hydrochloric acid is used; for this reason, effect of mineral acid on plaster setting was tested comparing $H_3PO_4$ and HCl. Acidic solutions increased porosity compared to distilled water, but samples with hydrochloric acid were more dense and compact than those made with phosphoric acid (Table A.4). Presence of mineral acids influenced the gypsum crystallization step, promoting formation of large bulky crystals [24]. Particle size was due to increased growth rate [25]. For hydrochloric acid-containing sample the mechanical strength was increased whereas porosity was similar to samples in absence of acid (Table A.3), However, the goal of our research was to increase plaster permeability and not composite mechanical properties. For these reasons hydrochloric acid was not used in further experiments. In presence of $H_3PO_4$ and in absence of carbonate, porosity was higher with respect to samples in Table A.2, indicating that $CaCO_3$ could also act as buffer stopping acid reactivity and controlling porosity.

### *3.1.5. Permeability Coefficient Measurements*

Permeability coefficients were measured for all sample and results reported in Table 1. In order to allow percolation rapidly, porosity obtained only by water evaporation was insufficient to have an acceptable permeability. For samples containing "compact" plaster (series 1 and 3), discharge was very slow and permeability coefficients were estimated from water amount recovered after 24 hours. Using $CaCO_3$ as porogen, plaster permeability increased by three orders of magnitude allowing to run experiments in short times.

In a $^1$H NMR relaxation study of water, confined in porous medium of hardening gypsum (without porogen), coexistence of two water populations were described in permeable and disordered porous plaster structure. The first population (P1) extended uniformly in space while the second one (P2) was more confined and isolated in some clusters of gypsum needles [20]. Distribution of the two populations was related to water-to-plaster ratio (w/p)

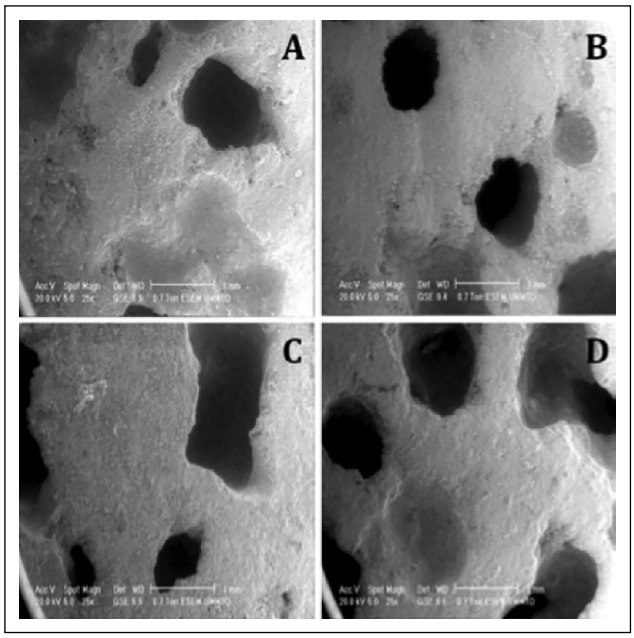


**Figure 2**. SEM photographs showing a view of porogen-containing hardened gypsum samples, prepared with a water-to-plaster ratio of 0.7, as a function of carbonate amounts (with 1.1 % phosphoric acid, w/w). $CaCO_3$: A=0.2%, B=0.5g, C=0.7g, D= 0.9% (w/w); length scale bar is 1 mm and magnification x25).

values: at low w/p value, P2 increased and P1 decreased, in agreement with total porosity observed as a function of w/p. Moreover, from a micro-structural point of view, an intricate percolation networks of needles with different packing density exists in hardened plaster structure where percolation threshold allowing water exchange was about w/p=0.6. Below w/p=0.6, there was an extremely slow exchange rate (almost zero) and the two water populations were almost independent. Above w/p=0.7, there was a small but finite exchange rate between the two water populations, but composite permeability was not sufficient to run PRB kinetic studies in short times.

Porosity of different plaster slabs, obtained from sample densities, with and without porogen, was not so different (62% vs 55%, Table S2), however permeability was extremely dependent on porogen presence, differing by about three orders of magnitude (Table 1).

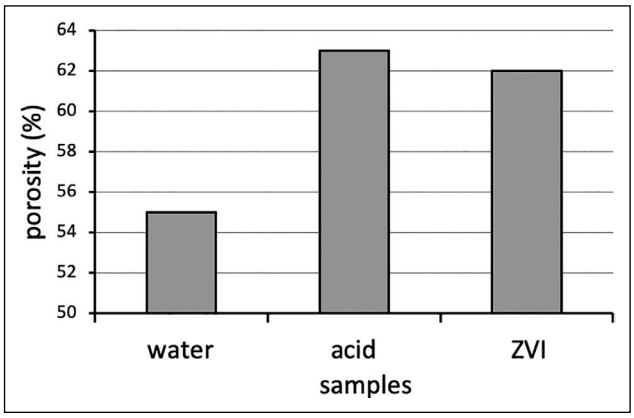


**Figure 3**. Porosity optimization as a function of different components of BRP (water, phosphoric acid and ZVI) plaster (50.0 g, 40.0%); water (56.0%); $CaCO_3$ (0.2%); $H_3PO_4$ (0.2%).

### 3.2. Degradation of 4-Nitroaniline

#### *3.2.1. Column Formulation*

Only composites with a permeability allowing the study of PRB chemical reactivity in a one-day period, were used in pollution removal tests.

Figure 3 reported optimization of all composite components (water, calcium carbonate, phosphoric acid, ZVI) for a fixed amount of plaster to improve different physical properties. Composite formulation, used to mold columns, contained plaster and water with 0.7 ratio, 0.2% $CaCO_3$ and 0.4% $H_3PO_4$ (per 50 g of plaster).

#### *3.2.2. ZVI Reactivity in Batch*

Bechamp reduction was checked batchwise. Experiments were run as a function of ZVI amount, in absence and in presence of phosphoric acid to activate reduction. "Classical" reduction [6] was run with acetic acid (or hydrochloric acid), which does not form insoluble species after oxidation of ZVI to Fe(II) or Fe(III). Yellow PNA aqueous solutions were expected to fade as a function of time, following reduction to PNA (Fig. A1).

As a function of time, yellow solutions turned pale and were cloudy: also in absence of $H_3PO_4$, reduction occurred and after 7 hours almost no PNA remained in solution (Fig. 4). As a function of time, protons were consumed in reduction reaction and solution pH increased (Fig. 5).

**Table 1.** Permeability coefficients of plaster samples as a function of composition. Experimental conditions: plaster (50.0 g, 41.0%); experiments were an average of five samples

| Serie | Water/plaster (w/w) | $CaCO_3$+$H_3PO_4$ (%) | ZVI (%) | pH values | Permeability coefficient (m/s) |
|---|---|---|---|---|---|
| 1 | 0.7 | – | – | 7.1 | $\geq 8.23*10^{-8}$ |
| 2 | 0.7 | 0.4 | – | 7.4 | $2.88\pm0.13*10^{-5}$ |
| 3 | 0.7 | – | 2 | 7.1 | $\geq 8.23*10^{-8}$ |
| 4 | 0.7 | 0.4 | 2 | 7.3 | $2.24\pm0.74*10^{-5}$ |

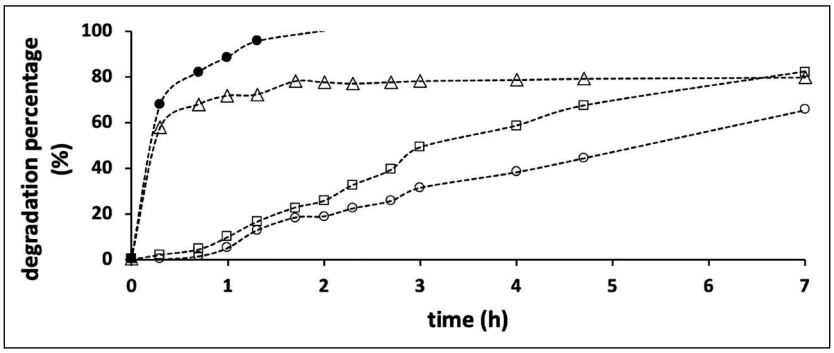


**Figure 4**. Degradation of PNA in Bechamp reduction as a function of time and of ZVI percentage: 1.2 (O); 2.3 (□); 3.4 (Δ); 1.0% + 1.0% $H_3PO_4$ (●); [PNA]=30 mg/l.

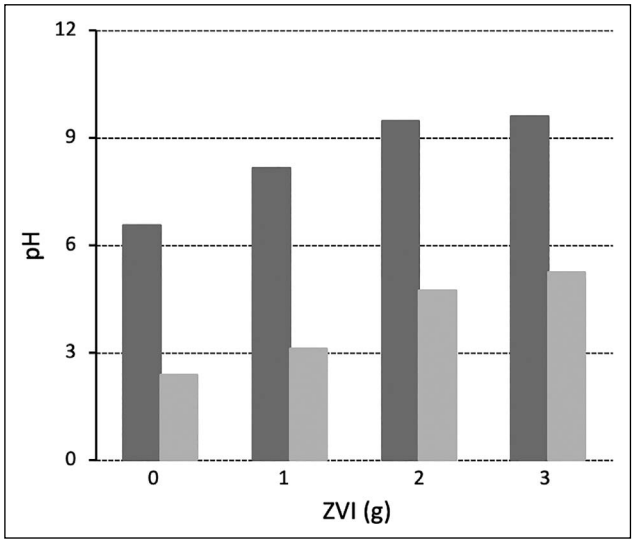


**Figure 5**. Final pH values of solutions in batch Bechamp reduction after 7 hours, as a function of ZVI: without acid (dark grey); with 1 % $H_3PO^4$ (light grey).

In presence of $H_3PO_4$ (0.4%) or higher amount of ZVI (>3%), reaction was faster and total reduction occurred in 1 hour. Solutions were cloudy because of formation of insoluble iron hydroxydes or phosphates. Samples recovered after reduction, with or without acid, became violet by standing: redox reaction was not halted to PDA and polymerization of aromatic molecules also occurred, as usual in presence of metal ions [26, 27].

### *3.2.3. ZVI Reactivity in Column*

PNA solutions were added to columns (Fig. 6) and, after percolation, fractions (100 ml) were recovered and analyzed by Vis-UV spectroscopy. In all experiments, yellow color of PNA solutions disappeared indicating that Bechamp reduction occurred in plaster columns. In order to verify chemical effects in colour fading, UV-Vis spectra were registered between 200 and 700 nm: PNA was reduced to PDA indicating that Bechamp reaction occurred in plaster column. As observed in batch experiments, PDA aqueous solutions were not stable as a function of time: pale yellow solutions

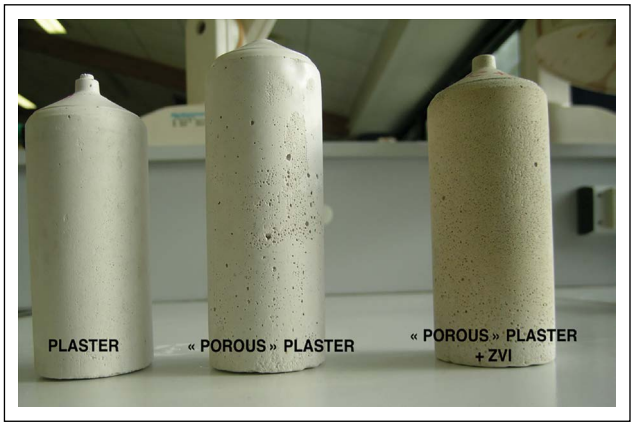


**Figure 6**. Plaster column composition: plaster (50.0 g, 41.0%); water (57.4%); $CaCO_3$ (0.2%); $H_3PO_4$ (1.4%); ZVI (2.3%).

became hazy and violet colored, indicating polymerization of aromatic amines.

Degradation profiles, as a function of time at different concentrations of PNA and ZVI, were reported in Figure 7. The flow through the columns was around 0.3 ml/min.

As expected, breakthrough points in the reduction reaction were dependant on ZVI amount included in plaster column; PNA concentration seemed to have less influence because degradation profiles in Figure 7 (except those with low quantity of ZVI) were almost superimposable.

In degradation reaction, PNA amount reduced to PDA by ZVI (in 2.3 and 3.4% experiments) was estimated: e.g. 1.6 L of aqueous PNA solution at 100 mg/L were treated by 3 g of ZVI, meaning a complete inactivation at around 55 mg of PNA per gram of ZVI, or about $2.2x10^{-2}$ mol PNA per 1 mol Fe(0).

### 3.3. Analysis After Remediation

Plaster columns and solutions recovered were analyzed at the end of remediation process in order to elucidate the role and reactivity of ZVI trapped in solid.

### *3.3.1. Solution Analysis*

Because of the presence of colored species (PNA and

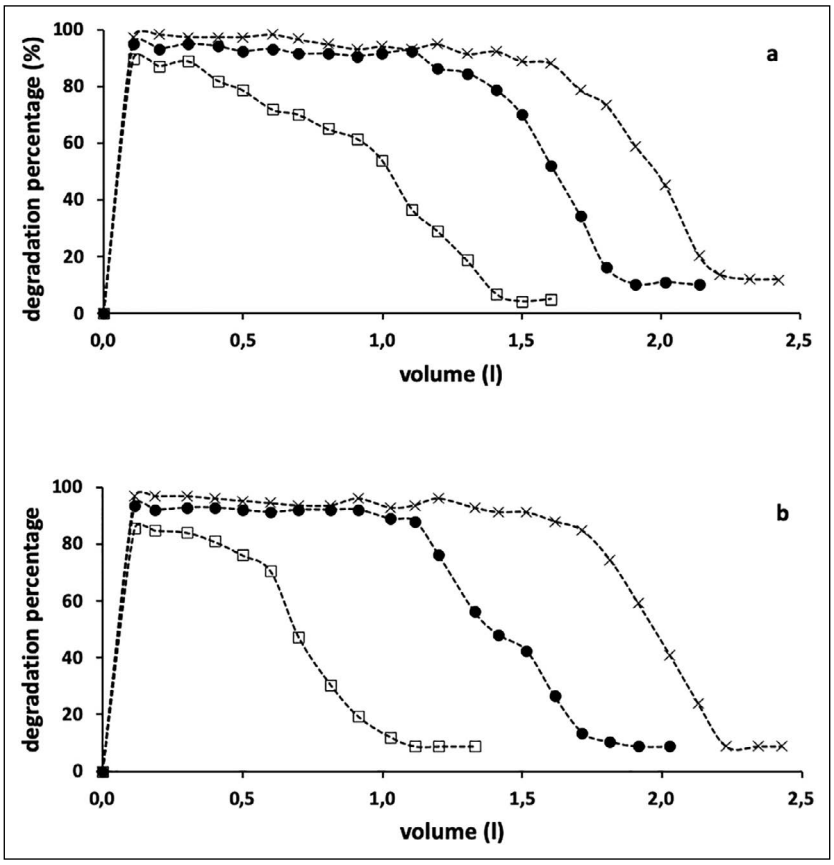


**Figure 7**. Degradation profiles of p-nitroaniline as percentage (PNA=30 mg/L **(a)**, 100 mg/L **(b)**) as a function of elution volume and ZVI percentage. ZVI: 1.2 (□), 2.3 (●), 3.4 % (X); column composition (without ZVI): plaster (200.0 g, 41.0%); water (57.4%); $CaCO_3$ (0.2%); $H_3PO_4$ (1.4%).

PDA), a colorimetric analysis of the solutions in order to follow the fate of ZVI, was not possible. However, this analysis was possible in ZVI composite before any reaction. Samples were soaked in distilled water and pH was measured as a function of time. KSCN and o-phenathroline in aqueous solution were used to check presence of Fe(II) or Fe(III) species, respectively. Because of the low amount of iron ionic species in solution, reagents were used in strong excess for ion identification. Presence of Fe(II) was detected in plaster columns (Table A.5) following the reaction between ZVI and phosphoric acid, whereas Fe(III) was not found by colorimetric method.

In ZVI-containing column, during addition of PNA solutions, the first volume eluted was slightly acid (pH=5.22), probably because of traces of phosphoric acid, whereas, later on, pH was determined by the major organic compound present in solution (PDA, pH=8.07; PNA, pH=6.10 for 30 mg/l aqueous solutions).

### *3.3.2. Solid Analysis*

At the end of reduction process, reddish colour of column indicated presence of $Fe_3O_4$ species, formed because of instability of Fe(II) species in aqueous solution in presence of dioxygen,

XRD diffractograms for plaster samples (Fig. 8) were compatible with those of gypsum (COD 2300259). Typical diffraction angle at 44.8° (2θ) for Fe(0) [28] was not detected by XRD, because in these experimental conditions, iron metal, dispersed in a gypsum matrix, could be observed only at high percentage (>50%). However, in plaster composites containing Fe(0), a diffraction angle at 39.5° was present but disappeared after PNA reduction (Fig. 8).

### *3.3.3. Iron Reactive Species*

Bechamp reduction is a stoichiometric reaction, and not a catalytic one, resulting in a series of parallel reactions, with generation of one or more intermediates and byproducts [29]. ZVI is "consumed" in redox system and passivated during flow of aqueous solutions. Noubactep reported to use the lowest possible Fe(0) loading (e.g. <5 g/l) and work at low temperature (e.g. 15°C) [30]. In an environmental application, it would be possible to alternate in PRB porous plaster blocks (in order to absorb more polluted solution) and ZVI-containing compact plaster blocks (in order to act as reducing agent) to increase the residence time. However, Bechamp reaction in PRB seems to be more complex than in solution. In fact, reduction by Fe(0) occured and contributed significantly to contaminant removal, but the

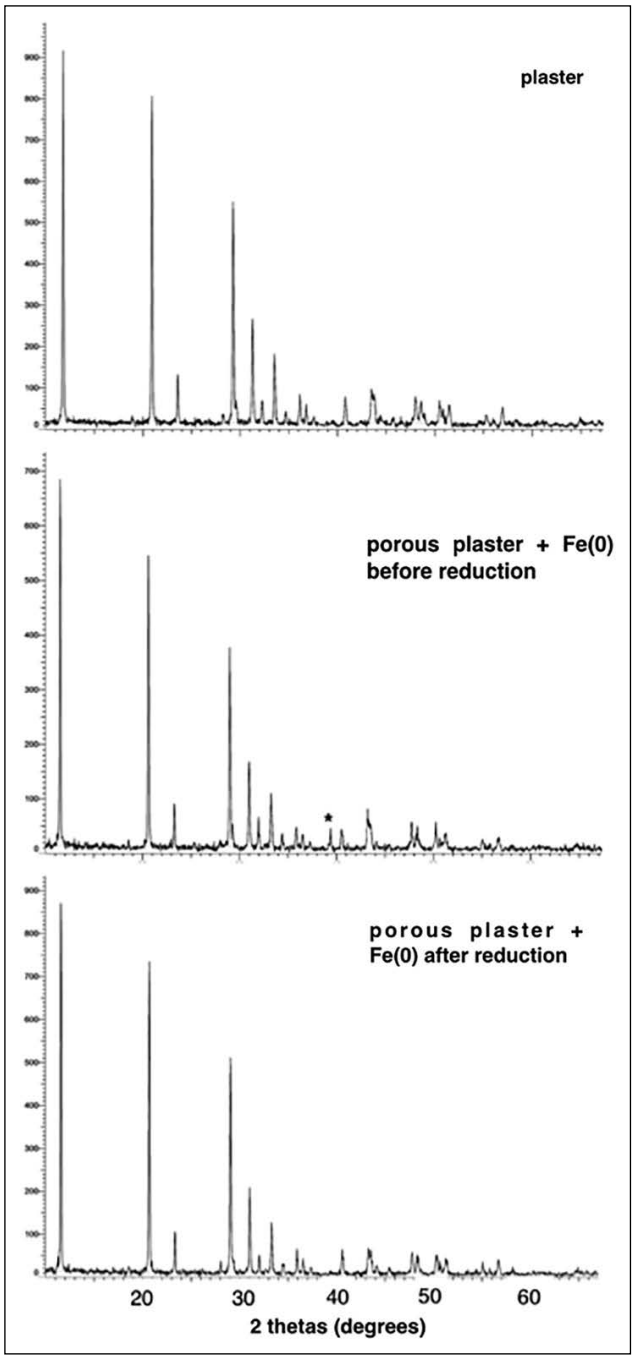


**Figure 8**. DRX of plaster composites, plaster, plaster + Fe(0) before reduction, and plaster + Fe(0) after reduction. Composites were formulated as in Tables S1 and S4.

mechanism remained unclear. It is matter of debate in ZVI depolluting systems, if, between the Fe(II)/Fe(0) or Fe(III)/Fe(II) couples, which one is involved in the redox reactions [31]. In batch experiments, PNA reduction occurred also without acid suggesting that Fe(0) would be directly involved in redox system; however kinetics, in batch and in column, were not the same (in column the reaction was instantaneous) suggesting that preliminary treatment with phosphoric acid acted also on ZVI surface, partially generating Fe(II) species. It means that Fe(II) species could be involved in order to accelerate reduction rate, but remains the question of Fe(II) species stability in presence of dioxygen.

In ZVI reactions, concomitant precipitation of iron hydroxydes absorbing organic compounds has been also suggested [32]. From our experience in pollutant co-precipitation methods [33], we cannot totally reject this mechanism [34], but recovering PDA in solution strongly suggested that redox mechanism was predominant.

Finally, we observed that, as a function of time, downflow through the column increased by 25% indicating that plaster columns were embrittled: columns were sensitive to percolation because of calcium sulfate solubility in water and because iron corrosion products formed in situ were partially disrupting their structure.

### 3.4. Environmental Impact and Cost

An ideal PRB should present the following advantages [35]:

- stability during PRB lifetime in order to minimize lost of efficiency: Plaster of Paris containing zero valent iron particles: is a stable composite
- chemical reactivity, which is related to reactant contact time, depending on flow rate and amount of reactant: ZVI is still actif when included in plaster.
- hydraulic and mechanical performances: PRB permeability has to be higher than aquifer flow in order to not disturb underground flow and not induce polluted flow out of barrier. The supporting material should also be shaped in blocks in order to easily build PRB. Permeability, mechanical properties and shapes of plaster-based PRB can be modulated in formulation step.
- reduced environmental impact in order to avoid pollution effects. PBR has to be mainly constituted by inert and non-toxic materials, producing non-toxic and harmless by-products: if the main problem in using calcium sulfate-based PRB for geological applications is their relative solubility in water, however they will break up with time discharging in environment no toxic species.
- cost of PRB building (in terms of materials and construction process) as low as possible in order to be economically feasible: the cost of plaster-based PRB is estimated to be very low and convenient.

Finally, efficiency of ZVI in plaster based-columns suggests use of these composite as precast plaster wall blocks in environmental applications.

## 4. CONCLUSION

Plaster PRB was used to purify water from soluble organic contaminants, such as 4-nitroaniline. Plaster is one of the most used materials in construction industry. It can be used in PRB and it can incorporate many types of addi-

tives. We have included ZVI to make a reactive component with capacity to remove nitro compounds while the water flow passes through plaster. Use of ZVI as additive in PRB allows removing toxic organic compounds by reduction of nitro function to amino functions. To provide PRB with good flow through properties, formulation of porous plaster with increased porosity was made possible by reaction of calcium carbonate with a small amount of phosphoric acid, which causes evolution of carbon dioxide gas simultaneously with precipitation of calcium phosphate, effectively making plaster less water soluble. Thus improved plaster-based PRB, defining porosity and ZVI particles, can be developed for use in removal of organic compounds from water. This opens possibilities for use of plaster-based PRB in many pollution control technologies where it could be scaled up.

## ACKNOWLEDGEMENTS

SB is grateful to the Algerian Ministry of Education for the fellowship. The authors thank dr. Farid Errassifi (ILIPACK, PEC Department, Université Toulouse 3 Paul Sabatier, Castres, France) for technical assistance in mechanical strength measurements.

## DATA AVAILABILITY STATEMENT

The authors confirm that the data that supports the findings of this study are available within the article. Raw data that support the finding of this study are available from the corresponding author, upon reasonable request.

## CONFLICT OF INTEREST

The authors declare that they have no conflict of interest.

## FINANCIAL DISCLOSURE

The authors declared that this study has received no financial support.

## PEER-REVIEW

Externally peer-reviewed.

## REFERENCES

[1] Henderson, A.D., & Demond A.H. (2007). Long-term performance of zero-valent iron permeable reactive barriers: a critical review. *Environmental Engineering Science*, 24, 401–423. [CrossRef]

[2] Grajales-Mesa S.J., & Malina G. (2016). Screening reactive materials for a permeable barrier to treat TCE-contaminated groundwater: laboratory studies. *Environmental Earth Science*, 75, 772–785. [CrossRef]

[3] Dorathi P.J., & Kandasamy P. (2012). Dechlorination of chlorophenols by zero valent iron impregnated silica. *Journal of Environmental Science*, 24, 765–773. [CrossRef]

[4] Zingaretti D., I.Verginelli, Luisetto I., & Baciocchi R. (2020). Horizontal permeable reactive barriers with zero-valent iron for preventing upward diffusion of chlorinated solvent vapors in the unsaturated zone. *Journal of Contaminant Hydrology*, 234, Article 103687. [CrossRef]

[5] Bortone I., Erto A., Di Nardo A., Santonastaso G.F., Chianese S., & Musmarra D. (2020). Pump-and-treat configurations with vertical and horizontal wells to remediate an aquifer. *Journal of Contaminant Hydrology*, 235, Article 103725. [CrossRef]

[6] Béchamp A. (1854). De l'action des protosels de fer sur la nitronaphtaline et la nitrobenzine. nouvelle méthode de formation des bases organiques artificielles de Zinin. *Annales de Chimie et de Physique*, 42, 186–196.

[7] Schabel T., Belger C., & Plietker B. (2013). A mild chemoselective ru-catalyzed reduction of alkynes, ketones, and nitro compounds. *Organic Letters*,15, 2858–2861.

[8] Farooqi Z.H., Khalid R., Begum R., Farooq U., Wu Q., Wu W., Ajmal M., Irfan A., & Naseem K. (2018). Facile synthesis of silver nanoparticles in a cross-linked polymeric system by in situ reduction method for catalytic reduction of 4-nitroaniline. *Environmental Technology*, 40, 1–30. [CrossRef]

[9] Hu R., Cui X., Gwenzi W., Wu S., & Noubactep C. (2018). Fe0/H2O Systems for environmental remediation: the scientific history and future research directions. *Water*, 10(12), 1739–1755. [CrossRef]

[10] Eljamal O., Thompson I.P., Maamoun I., Shubair T., Eljamal K., Lueangwattanapong K., & Sugihara Y. (2020). Investigating the design parameters for a permeable reactive barrier consisting of nanoscale zero-valent iron and bimetallic iron/copper for phosphate removal. *Journal of Molecular Liquids*, 299, Article 112144. [CrossRef]

[11] Maamoun I., Eljamal O., Eljamal R., Falyouna O., & Sugihara Y. (2020). Promoting aqueous and transport characteristics of highly reactive nanoscale zero valent iron via different layered hydroxide coatings. *Applied Surface Science*, 506, Article 145018.

[12] Wantanaphong J., Mooney S.J., & Bailey E.H. (2006). Quantification of pore clogging characteristics in potential permeable reactive barrier (PRB) substrates using image analysis. *Journal of Contaminant Hydrology*, 8, 299–320. [CrossRef]

[13] Touze S., Chartier R., & Gaboriau H. (2004). Etat de l'art sur les barrières perméables réactives (BPR): Réalisations, expériences, critères décisionnels et perspectives; BRGM Orléans, France.

[14] Saadaoui E., Ghazela N., Ben Romdhanea C., & Massoudi N. (2017). Phosphogypsum: potential uses and problems - a review. *International Journal of Environmental Study*, 74, 558–567. [CrossRef]

[15] Chernysh Y., Yakhnenko O., Chubur V., & Roubik H. (2021). Phosphogypsum recycling: a review of environmental issues, current trends and prospects. *Applied Science*, 11, 1575. [CrossRef]

[16] Rumble J., (Ed.). (2019). *CRC handbook of chemistry and physics* (100th ed.). CRC Press.

[17] Lewry A.J., & Williamson J. (1994). The setting of gypsum plaster: part I. The hydration of calcium sulphate hemihydrate. *Journal of Materials Science*, 29, 5279–5284. [CrossRef]

[18] Adrien J., Meille S., Tadier S., Maire E., & Sasaki L. (2016). In-situ X-ray tomographic monitoring of gypsum plaster setting. *Cement and Concrete Research*, 82, 107–116. [CrossRef]

[19] Diaga Seck M., Van Landeghem M., Faure P., Rodts S., Combes R., Cavalie P., Keita E., & Coussot P. (2015). The mechanisms of plaster drying. *Journal of Materials Science*, 50, 2491–2501. [CrossRef]

[20] Jaffel H., Korb J.P., Ndobo-Epoy J.P., Morin V., & Guicquero J.P. (2006). Probing Microstructure Evolution during the Hardening of Gypsum by Proton NMR Relaxometry. *The Journal of Physical Chemistry B*, 110, 7385–7391. [CrossRef]

[21] Fisher R.D., Hanna J.V., Reesc G.J., & Walton R.I. (2012). Calcium sulfate-phosphate composites with enhanced water resistance. *Journal of Materials Chemistry*, 22, 4837–4846. [CrossRef]

[22] Pham Minh D., Dung Tran N., Nzihou A., & Sharrock P. (2014). Novel one-step synthesis and characterization of bone-like carbonated apatite from calcium carbonate, calcium hydroxide and orthophosphoric acid as economical starting materials. *Materials Research Bulletin*, 51, 236–243. [CrossRef]

[23] Lanzóna M., & García-Ruiz P.A. (2012). Effect of citric acid on setting inhibition and mechanical properties of gypsum building plasters. *Construction and Building Materials*, 28, 506–511. [CrossRef]

[24] Mori T. (1982). The effect of boric acid on the thermal behavior of cast gypsum. *Dental Materials Journal*, 1, 73-80. [CrossRef]

[25] Al-Othman A., & Demopoulos G.P. (2009). Gypsum crystallization and hydrochloric acid regeneration by reaction of calcium chloride solution with sulfuric acid. *Hydrometallurgy*, 96, 95–102. [CrossRef]

[26] Lajoie-Halova B., Brumas V., Fiallo M.M.L., & Berthon G. (2006). Copper(II) interactions with non-steroidal anti-inflammatory agents. III – 3-Methoxyanthranilic acid as a potential OH-inactivating ligand: a quantitative investigation of its copper handling role in vivo. *Journal of Inorganic Biochemistry*, 100, 362–373. [CrossRef]

[27] Sapurina I., & Stejskal J. (2008). The mechanism of the oxidative polymerization of aniline and the formation of supramolecular polyaniline structures. *Polymer International*, 57, 1295–1325. [CrossRef]

[28] Khalil A.M.E., Eljamal O., Amen T.W.M., Sugihara Y., & Matsunaga N. (2018). Scrutiny of interference effect of ions and organic matters on water treatment using supported nanoscale zero-valent iron. *Environmental Earth Science*, 77, 489–501. [CrossRef]

[29] Popat V., & Padhiyar N. (2013). Kinetic study of bechamp process for P-Nitrotoluene reduction to P-Toluidine. *International Journal of Chemical Engineering and Applications*, 4(6), 401–405. [CrossRef]

[30] Noubactep C. (2009). An analysis of the evolution of reactive species in Fe0/H2O systems. *Journal of Hazardous Materials*, 168(2-3), 1626–1631. [CrossRef]

[31] Noubactep C. (2008). A Critical Review on the Process of Contaminant Removal in Fe0–H2O Systems. *Environmental Technology* 29(8), 909–920. [CrossRef]

[32] Noubactep C. (2009). Characterizing the discoloration of methylene blue in Fe0/H2O systems. *Journal of Hazardous Materials*, 166(1), 79–87. [CrossRef]

[33] Lemlikchi W., Sharrock P., Fiallo M., Nzihou A., & Mecherri M.O. (2014). Hydroxyapatite and Alizarin sulfonate ARS modeling interactions for textile dyes removal from wastewaters. *Procedia Engineering*, 83, 378–385. [CrossRef]

[34] Noubactep C. (2007). Processes of contaminant removal in "fe0-h2o" systems revisited: the importance of co-precipitation. *Open Environmental Sciences*, 1, 9–13. [CrossRef]

[35] ITRC. (2021 December 15). Technical Regulatory Guidance Document: Permeable Reactive Barrier: Technology Update (PRB-5, 2011). https://connect.itrcweb.org/HigherLogic/System/DownloadDocumentFile.ashx?DocumentFileKey=fd058d3e-9bdc-4103-8f13-4195efa8499f

**Appendices**

**Table A1.** Physical and mechanical properties of plaster samples (density, porosity, indirect tensile strength) as a function of plaster/water ratio (w/w); experimental conditions: plaster (50.00 g); measurements were an average from ten samples

| Water/plaster ratio (w/w) | Density (g/ml) | Porosity (%) | Indirect tensile strength MPa) |
|---|---|---|---|
| 0.5 | 1.15±0.04 | 50.46±0.40 | 7.14±0.43 |
| 0.6 | 1.10±0.04 | 52.71±0.33 | 5.47±0.41 |
| 0.7 | 1.04±0.06 | 55.06±0.61 | 4.48±0.43 |
| 0.8 | 0.99±0.05 | 57.39±2.00 | 3.57±0.19 |

**Table A2.** Physical and mechanical properties of plaster samples (density, porosity, indirect tensile strength) as a function of $H_3PO_4$ added; experimental conditions: plaster (50.0g, 41.0%); water (58.2 %); $CaCO_3$ (0.2%)

| $H_3PO_4$ (g) | $H_3PO_4$ (%) | Density (g/ml) | Porosity (%) | Indirect tensile strength (MPa) |
|---|---|---|---|---|
| 0 | 0 | 1.04±0.06 | 55.06±0.61 | 4.48±0.43 |
| 0.34 | 0.3 | 0.86±0.06 | 63.08±2.72 | 1.48±0.09 |
| 0.68 | 0.6 | 0.76±0.01 | 66.97±0.35 | 1.15±0.73 |
| 1.01 | 0.8 | 0.74±0.03 | 67.94±2.62 | 1.04±0.25 |
| 1.35 | 1.1 | 0.72±0.01 | 69.13±1.80 | 0.83±0.08 |

**Table A3.** Physical and mechanical properties of plaster samples (density, porosity, indirect tensile strength) as a function of ZVI added; experimental conditions: plaster (50.0 g, 41.0%); water (57.4%); $CaCO_3$ (0.2%); $H_3PO_4$ (0.2%)An example of a table (9pt)

| ZVI (g) | ZVI percentage (%) | Density (g/ml) | Porosity (%) | Indirect tensile strength (kPa) |
|---|---|---|---|---|
| 0 | 0 | 0.86±0.06 | 63.08±2.72 | 1.48±0.09 |
| 1.00 | 1.2 | 0.88±0.29 | 62.19±0.66 | 1.26±0.27 |
| 2.00 | 2.3 | 1.17±0.05 | 49.56±0.37 | 1.93±0.30 |
| 3.00 | 3.4 | 1.36±0.05 | 41.23±0.93 | 3.18±0.88 |
| 5.00 | 5.6 | 1.36±0.06 | 41.32±0.57 | 3.14±0.51 |

**Table A4.** Physical and mechanical properties of plaster samples (density, porosity, indirect tensile strength) as a function of acid added (1.4%); experimental conditions: plaster (50.0 g, 41.6%); water (58.2 %); $CaCO_3$ (0.2%)

| Acid | Density (g/ml) | Porosity (%) | Indirect tensile strength (MPa) |
|---|---|---|---|
| 0 | 1.04±0.06 | 55.06±0.61 | 4.48±0.43 |
| $H_3PO_4$ | 0.52±0.07 | 77.55±0.61 | 1.89±0.65 |
| HCl | 0.94±0.02 | 59.48±0.67 | 5.87±1.90 |

**Table A5.** pH values and qualitative colorimetric results for ionic iron species in plaster-based composites soaked in distilled water

| | pH (t=0) | pH (t=48 h) | Fe(II) test | Fe(III) test |
|---|---|---|---|---|
| Plaster | 6.92 | 6.87 | Negative | Negative |
| Plaster+ZVI | 6.76 | 7.45 | Negative | Negative |
| Plaster+ZVI+$CaCO^3$+$H^3PO_4$ | 6.91 | 7.09 | Positive | Negative |

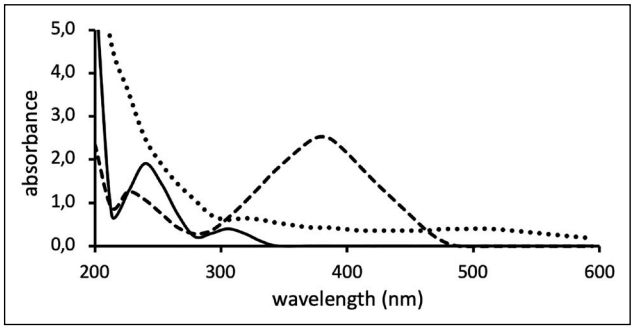


**Figure A1**. (Absorption spectra of PNA (---), PDA (___) and PDA polymerization product (…) in aqueous solutions: [PNA]=[PDA]=30 mg/l; path-length quartz cell=0.2 cm.

Journal of Sustainable Construction Materials and Technologies
Web page info: https://jscmt.yildiz.edu.tr
DOI: 10.14744/jscmt.2021.02

JSCMT
Journal of Sustainable Construction Materials and Technologies

Original Article

# Study of thermal and mechanical properties of typha leaf - clay panels

**Younouss DIEYE[1*], Pape M. TOURE[1], Seckou BODIAN[1], Prince M. GUEYE[1], Mactar FAYE[2], Vincent SAMBOU[1]**

[1]*Laboratoire d'Energétique Appliquée (LEA), Université Cheikh Anta Diop, Dakar-Fann, Sénégal*
[2]*Université Alioune Diop de Bambey, Bambey, Sénégal*

**ARTICLE INFO**

*Article history*
*Received: 18 March 20211*
*Accepted: 04 October 2021*

**Key words:**
Clay, mechanical strength, thermal conductivity, thermal effusivity, typha

**ABSTRACT**

This study contributes to the valorization of typha as local materials of building for thermal insulation. We will examine the influence of the binder content and granulometry on the mechanical and thermal properties of typha - clay panels. The plant of typha is used in different granulometries such as powdered typha and defibrated typha. The results showed that compressive strength, thermal conductivity and effusivity depend on the particle size of the typha and also the binder. The panels of defibrated typha have a better thermal insulation performance (0.085 $W.m^{-1}.K^{-1}$ for 66.66%), which is comparable with many of natural insulating materials. The panels also have low thermal effusivities which show that they have low thermal inertia.

**Cite this article as:** Dieye Y, Toure PM, Bodian S, Gueye PM, Faye M, Sambou V. Study of thermal and mechanical properties of typha leaf - clay panels. J Sustain Const Mater Technol 2021;6:4:135–142.

## 1. INTRODUCTION

Despite a massive industrialization of construction methods with increasingly efficient materials and the use of new technologies in the field of buildings, in recent years we have witnessed the development of a new generation of materials based on renewable plant resources to make in the face of environmental problems. This desire has strongly pushed engineers, researchers and public authorities to organize a reflection on the development of these materials and more particularly in the field of insulation in order to reduce the energy consumption of buildings by using materials with an insulating potential very important and a low economic and environmental cost [1–3]. The synthetic insulation available are imported and expensive [4]. It is therefore necessary to develop insulating materials of plant origin as an alternative to imported insulators.

Many studies have been conducted to investigate thermophysical and mechanical behavior of such bio-based materials. Bruijn et al. [5] studied the mechanical properties of a hemp concrete based on a lime and cement binder. They found that, for the dosages with the presence of the cement, the mechanical strength increases according to the proportion of cement in the mixture of 0.15 MPa to 0.83 MPa. Ashori et al. [6] evaluated the mechanical performance of various panels of eucalyptus, mesquite, saltcedar (Tamarix stricta) and date palm fibers and a formaldehyde resin binder. They concluded that for all types of panels, the modulus of rupture and modulus of elasticity increase as the resin content increases from 9% to 11%. Lertsutthi-

*Corresponding author.
*E-mail address: younouss.dieye@ucad.edu.sn

Published by Yıldız Technical University Press, İstanbul, Turkey
Copyright 2021, Yıldız Technical University. This is an open access article under the CC BY-NC license (http://creativecommons.org/licenses/by-nc/4.0/).

wong et al. [7] studied the mechanical performance of an insulation board based on corn husks and a binder derived from solid waste paper tissue. They concluded that when the binder/fiber mass ratio varies from 0.33 to 3, the modulus of rupture and modulus of elasticity vary respectively from 1.3 to 5 MPa and from 21 to 196 MPa. Cuk et al. [8] studied the influence of two types of binder on the properties of a wood particle board. They showed that the mechanical properties of particle boards produced were better with melamine-formaldehyde resin (flexural strength of 13.42 MPa) than with melamine-urea-formaldehyde resin (11.06 MPa). Cerezo [9] evaluated the evolution of the thermal characteristics of hemp concrete according to the binder dosage. It has achieved an excellent performance of hemp concrete as a thermal insulation with conductivities ranging between 0.06 and 0.19 $Wm^{-1}.K^{-1}$ for densities ranging from 200 to 840 $kg.m^{-3}$. Chikhi et al. [10] investigated the thermal performance of a bio composite based on date palm fibers. They have shown that the increase in the fiber content decreases the density of the material from 1130 to 743 $kg.m^{-3}$ corresponding to 43% and increases its porosity. This reduction in density decreases the thermal conductivity from 0.449 to 0.177 $W.m^{-1}.K^{-1}$. Awwad et al. [11] studied the behavior of three hemp-concrete mixed with about 1%, 2%, and 4% hemp material by concrete volume. The tests results confirm the potential of incorporating raw hemp material in local masonry blocks while satisfying minimum strength (11.7 to 2.6 MPa), and reducing thermal conductivity (1.248 to 0.984 $W.m^{-1}.K^{-1}$) requirements. Chinta et al. [12] have studied the thermal insulation and some mechanical properties and physical properties of a new composite construction material composed of gypsum and natural fibers. The results showed that the incorporated natural fibers changed the rheological and mechanical behavior of the material and increase considerably its ductility and a decrease in thermal conductivity and bulk density is recorded. Moussa et al. [13] have tested a new agromaterial based on hemp and starch. The measured thermal conductivity was 0.08 $W\ m^{-1}.K^{-1}$ at 23˚C. In the paper, authors deal with the study of Typha australis fibers to make a building material. Typha australis is an aquatic plant which is found on wetland and belongs to the Typhaceae family. This plant which can reach a height up to 3 m [14] rapidly spreads via seeds and roots. In very short time it takes over water areas. It is usual to see ponds that are completely surrounded by typha. Typha australis have affected irrigation in the valley of Senegal. It spreads rapidly over the areas and affecting other crops. So, abundant amount of it forced one to find its usefulness in insulation. The global objective of our study is to transform the harmful Typha australis as an opportunity by its transformation as a building material.

Concerning Typha fibers, previous investigations have been carried out to elaborate Typha clay and Typha–cement mixtures [15–17]. Results show that thermal behavior of composite made of Typha fibers and clay has low thermal conductivity ranging from 0.065 to 0.112 $W\ m^{-1}.K^{-1}$ [17]. However, there is no information about the study of lengths of typha fibers on the mechanical and thermal performances of such materials in the literature.

**Figure 1**. Typha leaves powder.

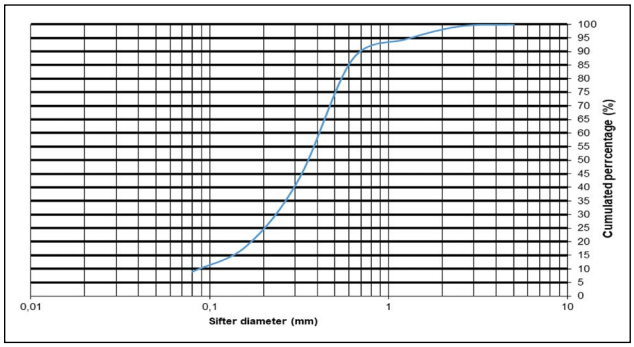


**Figure 2**. Granulometric graph of typha powder used.

The aim of this study is to determine the mechanical and thermal properties of fiber-based construction materials of typha australis. The effect of typha granulometry on properties is also looked at. Then, experimental methods to determine the following properties are detailed: apparent, absolute density, thermal properties (effusivity and conductivity), and the compressive strength. Experimental results are presented and the influence of the granular of Typha and ratio on the material's properties is discussed.

## 2. MATERIALS AND METHODS

### 2.1. Materials

#### *2.1.1 Typha*

The typha used was extracted at the Niayes zone of the Dakar Technopole. The raw material thus extracted was dried for two weeks under the sun before being transformed. We obtained two types of typha leaf granules: powder typha and defibrated typha.

For the powdered typha, the dried typha leaves were cut into small pieces with the aid of an ax as shown in Figure 1. After cutting, the typha pieces obtained were crushed in powder form by an existing grinding machine in the market (Fig. 1). The particle size study of Typha powder was carried out by sieving using standard square mesh sieves with diameters ranging from 5 mm to 0.08 mm. Figure 2

**Figure 3**. Typha leaves defibrated.

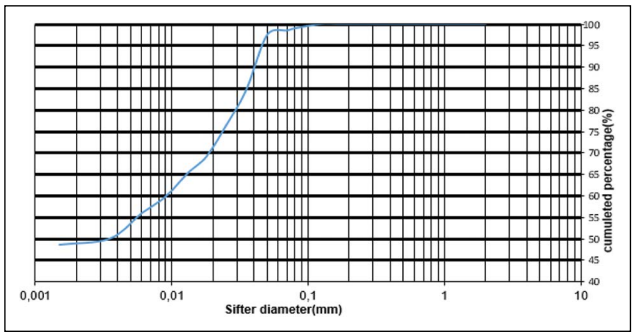


**Figure 4**. Granulometric graph of clay used.

summarizes the particle size distribution that make up the typha powder. The density and the water content of the typha powder are respectively 128.38 kg.m$^{-3}$ and 12.24%. The density was measured according to French standards NF ISO 11272. First, we determined the bulk density by weighing a mass of samples in 500 mL test pieces. The experiment was repeated 3 times. The water content is obtained using an oven at a temperature of 105 °C.

The defibrated typha is also mainly from the leaves. The leaves represent 80% of the mass of the plant; after extraction, they were crushed before being defibrated by hand. The defibrated typha leaves obtained have lengths up to 15 cm as reflect in Figure 3. The length of the leaves of typha defibrated is determined by means of a vernier caliper. The bulk density is 61 kg.m$^{-3}$.

### *2.1.2 Clay*

The clay used is a by-product of local quarries that does not require processing. The clay used as a binder in this study is a clay from the Souvenir Square in Dakar (bulk density of 1400 kg.m$^{-3}$). A grain size analysis is carried out on the clay to determine the dimensions of the grains and the weight percentages of the different families of grains which constitute it. This study was made using sieves with diameters between 0.0015 mm and 2 mm. The granulometric curve obtained is shown in Figure 4. The researchers noted that 99% of the weight of the grains passes the sieve

**Table 1.** Atterberg limits of the clay

| Atterberg limits | Clay |
|---|---|
| Liquid limit, WL (%) | 44. 3 |
| Plastic limit, WP (%) | 17.6 |
| Plasticity index PI (%) | 26.7 |

0.08 mm. The liquidity limit was measured by the method of the dish of Casagrande (WL) and the plasticity limit by the method of the roller (WP). These measures were realized according to NF P94-051 standard. The Atterberg limits were used to determine the plasticity index of the studied materials. The plasticity index (PI) is the difference between the liquid limit and the plastic limit. It is a measure of the plasticity of a soil.

$$PI = WL - WP \quad (1)$$

where PI is the plasticity index; WL is the liquidity limit and WP represents the plasticity limit.

The consistency limits of the clay, which included the plastic limit (WP), liquid limit (WL) and plastic index (PI) are reported in Table 1 The plasticity index shows that the clay is plastic.

### *2.1.3 Formulation of Samples*

#### *2.1.3.1 Preparation of the Binder*

To avoid water competitions between the binder and the typha leaves, the binder is prepared separately. Typha leaves can absorb up to 80% of its weight in water and most of this absorption takes place rapidly. The mixture should contain as much binder as possible and adequate water content to avoid mixing wet typha leaves and dry binder. The binder is prepared so that its adhesion is important and that it has the power to spread easily on typha particles and ensure their bonds. The clay was mixed directly with the corresponding amount of mixing water before being kneaded with an E095 type kneader. The mixer has a specific speed of 62 rpm and a capacity of 5 liters. The mixture was kneaded for 5 minutes in order to have a viscous liquid that sticks, before pouring the amount of typha.

#### *2.1.3.2 Preparation of Samples*

After preparation of the binder, the necessary amounts of typha are poured directly into the binder mixture at the kneader. The weight percentage of the binder was varied and the binder / water ratio set at 1: 1. The mixing time is 5 minutes in total for the mixture to be homogeneous, after preparation of the binder.

The fresh mixture of typha leaf - binder obtained is then put and packed in standardized molds of dimensions 4 cm x 4 cm x 16 cm for mechanical tests and 10 cm x 10 cm x 2 cm for thermal tests (Fig. 5, 6). After sample preparation, the filled molds are placed in the ambient environment of the laboratory of about 27°C, for 24 hours before being demolded. After demolding, the samples were dried in the open air

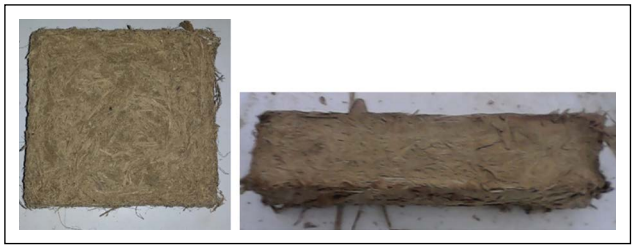

**Figure 5**. Picture of a typha powder sample.

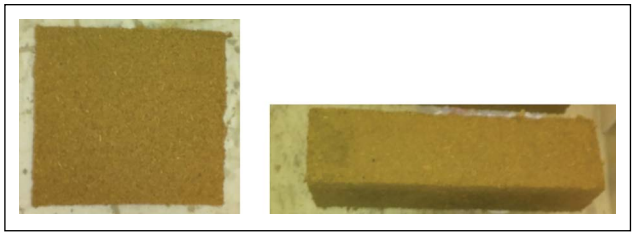

**Figure 6**. Picture of a typha defibrated sample.

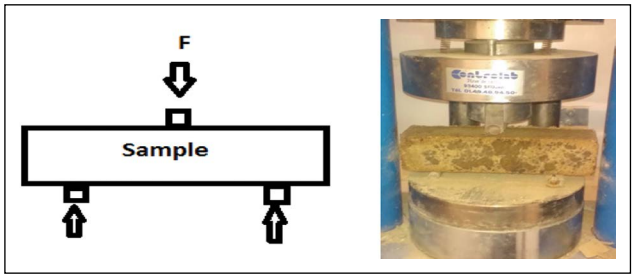


**Figure 7**. Flexural test.

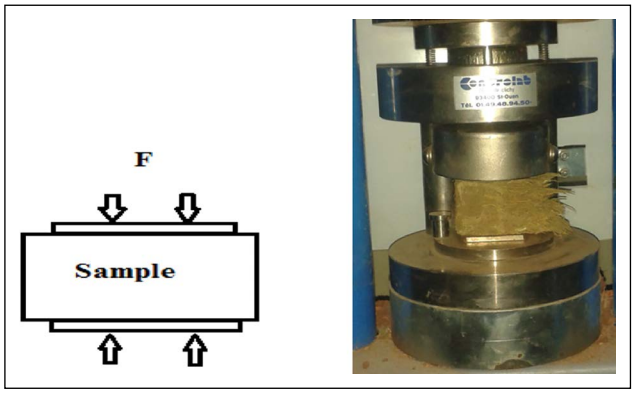


**Figure 8**. Compression test.

under the sun for two weeks, the time they are dried before carrying out the characterization tests. The masses of the different constituents of typha panels are shown on the Table 2. For each formulation, 3 samples were measured.

### 2.2 Methods

#### *2.2.1 Mechanical Characterization*

To characterize the solidity of the material, the mechanical behavior was evaluated by three-point compression and bending tests preceded by the measurement of the apparent density.

**Table 2.** Masses of the different compounds

| Samples | Binder percentage (%) | Clay mass (g) | Typha leaves mass (g) | Water mass (g) |
|---|---|---|---|---|
| $E_1$ | 66.67 | 160 | 80 | 160 |
| $E_2$ | 72.73 | 213 | 80 | 213 |
| $E_3$ | 80 | 320 | 80 | 320 |
| $E_4$ | 88.89 | 640 | 80 | 640 |

*2.2.1.1 Bulk Density*

Apparent density was determined after sample drying using a 0.01 g precision scale for weighing and a 0.01 mm precision vernier caliper to measure sample sizes. For each composition, 5 measurements were made, in order to obtain an average.

*2.2.1.2 Mechanical Test*

Mechanical characterization consists in determining the compressive strength and the tensile strength. This characterization was carried out using a mechanical press type E0160 with a maximum pressure of 250 kPa, in accordance with the standard NF EN 196-1.

2.2.1.2.1 Flexural Test

For the determination of the flexural strength a prismatic sample of dimensions 4 cmx 4 cmx 16 cm was placed on the press as shown in Figure 7 The sample is based on two simple supports, and the load F is applied to the center of the sample as shown in the schema of Figure 7. For each formulation, two samples were tested.

2.2.1.2.2 Compression Test

Compression tests are carried out on dry samples after they are broken for flexural test, at a constant rate of loading of 2 kN/s with the mechanical press. Figure 8 shows the disposition of the sample for the determination of compressive strength. For each composition, 4 trials were used.

These tests involve applying to a standard sample of the material a force F and measuring its breaking stress. The mechanical strength of a material describes its response to applied loads; it is the breaking stress. The maximum stress that the sample can withstand before rupture is called the breaking stress or the resistance to compression or bending. It is defined by:

$$\sigma = \frac{F}{S} \quad \text{(MPa)} \qquad (1)$$

S is the sample section in $mm^2$, F is the force applied (N)

#### *2.2.2 Thermal Characterization*

A measurement of thermal characterization of a material is based on the observation of its response to a thermal disturbance. The hot plane method is used to determine the

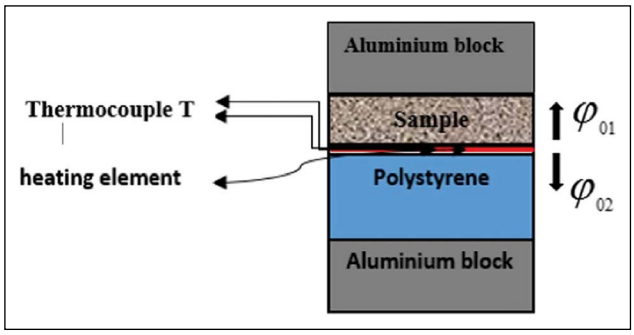


**Figure 9**. Schema of the experimental asymmetrical hot plate device.

thermal conductivity and effusivity of materials. The measuring device is made as shown in Figure 9. The heating element of small thickness is inserted between the sample to be characterized and a polystyrene block of 5 cm thickness and the whole is delimited by two aluminum blocks of 4 cm thickness. The sample of the material to be characterized is parallelepiped with the following dimensions 10 cmx 10 cmx 2 cm. Throughout the experiment, it is assumed that the heat transfer is 1D and that the temperature at the aluminium block is considered constant.

The thermal quadrupole method [18] is used to solve the thermal transfer problem. Indeed, by placing oneself in the Laplace space, the equation of heat depends only on the space variable.

$$\begin{bmatrix}\theta_s\\ \phi_{01}\end{bmatrix}=\begin{bmatrix}1 & 0\\ CsSp & 1\end{bmatrix}\begin{bmatrix}1 & R_C\\ 0 & 1\end{bmatrix}\begin{bmatrix}A & B\\ C & D\end{bmatrix}\begin{bmatrix}0\\ \phi_1\end{bmatrix}\begin{bmatrix}A_1 & B_1\\ C_1 & D_1\end{bmatrix}=\begin{bmatrix}0\\ \phi_1\end{bmatrix} \quad (2)$$

$$\begin{bmatrix}\theta_s\\ \phi_{02}\end{bmatrix}=\begin{bmatrix}A_i & B_i\\ C_i & D_i\end{bmatrix}\begin{bmatrix}0\\ \phi_2\end{bmatrix} \quad (3)$$

With:

$$A=D=\cosh\left(\frac{E}{\lambda}\sqrt{p}\,e\right);B=\frac{\sinh\left(\frac{E}{\lambda}\sqrt{p}\,e\right)}{ES\sqrt{p}};\ C=ES\sqrt{p}\sinh\left(\frac{E}{\lambda}\sqrt{p}\,e\right)$$

$$A_i=D_i=\cosh\left(\frac{E_i}{\lambda_i}\sqrt{p}\,e_i\right);\ B_i=\frac{\sinh\left(\frac{E_i}{\lambda_i}\sqrt{p}\,e_i\right)}{E_i S\sqrt{p}};\ Ci=E_i S\sqrt{p}\sinh\left(\frac{E_i}{\lambda_i}\sqrt{p}\,e_i\right)$$

λ is the sample thermal conductivity; E the sample thermal effusivity; e the sample thickness; $\lambda_i$ the polystyrene thermal conductivity; $E_i$ the polystyrene thermal effusivity; $e_i$ the polystyrene thickness; $\theta_s$ the Laplace transform of the temperature Ts(t); *Cs* the thermal capacity of the heating element per area unit: $Cs=\rho_s c_s e_s$; $R_c$ the thermal contact resistance between the heating element and the sample; $\phi_1$ the Laplace transform of heat flux input on the upper aluminum block; $\phi_2$ the Laplace transform of heat flux input on the lower aluminum block; $\phi_{01}$ the Laplace transform of the heat flux density living the heating element (upstream); $\phi_{02}$ the Laplace transform of the heat flux density living the heating element (downstream)

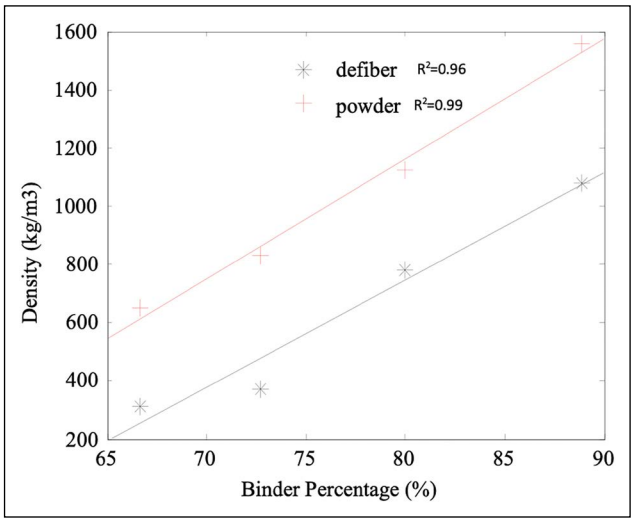


**Figure 10**. Variation curve of density in function of the binder percentage.

After developing the matrix products (2) and (3), the following relations were obtained:

$$\theta_s=\phi_0\frac{1}{\left(\frac{D_1}{B_1}+\frac{D_i}{B_i}\right)} \quad (4)$$

## 3. RESULTS AND DISCUSSION

### 3.1 Mechanical Results

#### *3.1.1 Apparent Density*

The researchers present the evolution of the density according to the binder. We also look at the influence of the type of typha aggregates on the density of the panels. This is illustrated in Figure 10 showing, for the clay binder, the effect of the type of aggregates on the density, but also the change in the density of panels based on typha of powder and defibrated typha according to the percentage of clay binder. The density varies from 314 kg.m$^{-3}$ to 1078 kg.m$^{-3}$ for the defibrated typha and from 652 kg.m$^{-3}$ to 1559 kg.m$^{-3}$ for the powdered leaves, when the mass percentage of clay varies from 66.66% to 88.89%. We observe that the values of the density vary almost linearly as a function of the binder content. This can be explained by the fact that the binder has a higher density. As a result, the greater the amount of binder the more dense the material, the greater the density. The results also show that the type of fibers of the typha leaves influences the density of the panels. Typha powder sheet panels have higher densities. For 66.66% binder, the typha powder board is 2.1 times higher than the defibrated panel and this is due to the fact that the typha powder leaves are denser.

**Figure 11**. Flexural strength.

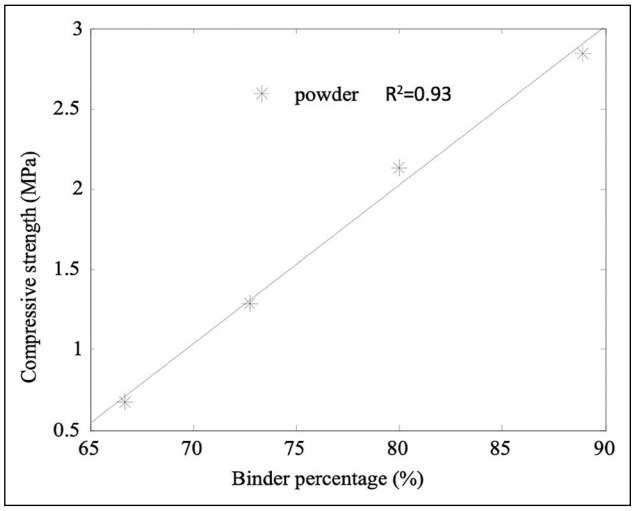


**Figure 12**. Variation curve of compressive strength in function of the binder percentage for typha powder.

### *3.1.2 Flexural Strength*

Typha powder panels have low flexural strength; after applying the load, the panels break quickly. The values are so low that the machine can not display the results and this is due to the particle size of the typha aggregates. In the case of panels based on defibrated typha sheets, the force applied to the panel up to the maximum load causes a deformation of the latter without breaking (Fig. 11). The results obtained are characteristic of a ductile material, which withstands very high deformation levels without breaking. This is due to the particle size of the fibers, the panels have an elastoplastic behavior, a strong deformability under stress and the possibility of recovery efforts even after reaching the maximum mechanical strength. The particle size significantly affects the flexural strength of the panels.

### *3.1.3 Compressive Strength*

The measurement results show an increase in the compressive strength of the panels as a function of the mass concentration of binder. The values of the resistance increase almost linearly according to the percentage of binder Figure 12 illustrates the variation in the compressive strength of the panels based on powdered typha leaves and clay binder. The resistance increases from 0.67 MPa to 2.84 MPa depending on the mass percentage of clay. This can be explained by the fact that, the higher the dosage of the binder, the greater the binding of the fibers is important, thus increasing their mechanical performance. The level of mechanical performance of the panels depends on the thickness of the layer of the binder encapsulating the particles. The mechanical properties of the samples are related to the binder dosage. These results are comparable to those of hemp-lime concrete [5], whose compressive strength values vary from 0.15 MPa to 0.83 MPa as a function of the hemp to binder mass ratio.

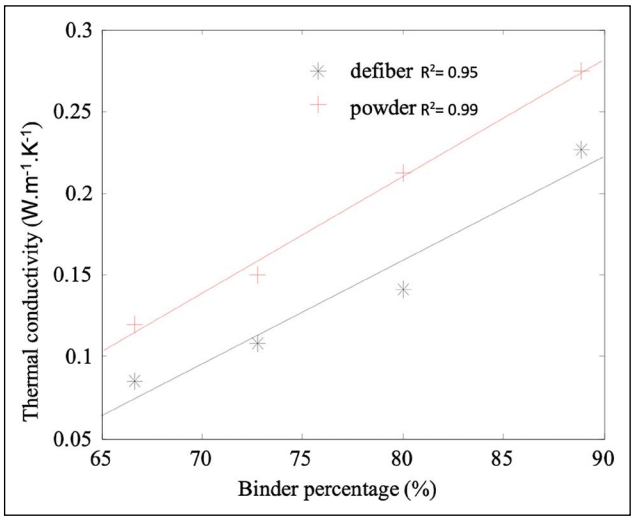


**Figure 13**. Dry panel thermal conductivity in function of the binder.

For the boards of defibrated typha leaves, the application of the load causes a deformation of the materials and not a rupture that is due to the length of the fibers. The defibrated typha boards are ductile compared to those in powder. We can conclude that the particle size of the typha leaves greatly influences the compressive strength.

## 3.2 Thermal Results

### *3.2.1 Thermal Conductivity*

The thermal conductivity λ ($W.m^{-1}.K^{-1}$) is an important quantity that characterizes the thermal insulation capacity of a material. More the material is insulating, the lower is the coefficient λ. The analysis of the curve shows a quasi-linear increase in the thermal conductivity of the dry panels as a function of the amount of binder. The thermal conductivity values of the panels increase as the concentration of binder increases.

Regarding the particle size, for the same type of binder, we have also illustrated in Figure 13 the influence of the length of typha leaf on the thermal conductivity. By comparing the panels of defibrated typha sheets with those of powder for the clay binder, we find that the defibrated typha boards have better thermal insulation properties. The thermal conductivity of the panels varies respectively from 0.085 to 0.227 $W.m^{-1}.K^{-1}$, for the defibrated ty-

pha sheets and from 0.120 to 0.275 $W.m^{-1}.K^{-1}$ for leaves in powder, depending on the binder content. For 66.66% binder, the defibrated typha board is about 41.2% more insulating than the board of typha powder sheets. This difference is due to the difference of the type of fibres, the typha consists essentially of pores which constitute the internal structure of the plant, to which are added the air holes between the particles of typha and in the form of powder, the typha loses its properties.

The results on the conductivity are similar to those obtained on hemp concrete [19] ranging from 0.06 to 0.19 $W.m^{-1}.K^{-1}$ relative to the binder dosage. The values relatively low of the thermal conductivity of typha provide high wall thermal resistances that allow them to meet thermal requirements.

### 3.2.2 Thermal effusivity

Thermal effusivity describes the speed with which a material absorbs and releases heat. The lower is the thermal effusivity, the faster the material will heat up with less energy. The measurement results of the thermal effusivity of the typha panels are shown in the figure. In a similar way to the thermal conductivity, we observe that in the dry state, the thermal effusivity of the panels increases as a function of the increase in the mass concentration of binder. The curve evolves in a quasi - linear way. By increasing the dosage rate by binder, it follows an increase in thermal effusivity which demonstrates the influence of the proportion of binder on the effusivity of the panels. The thermal effusivity of the panels depends on the density, the thermal conductivity and also the heat capacity. By increasing the dosage by bonding panels, we are seeing an increase in density and thermal conductivity thus implying an increase in thermal effusivity.

The figure also illustrates the influence of the type of fibres on thermal effusivity. For the same type of binder, it is clearly observed that the type of the typha fibers have a significant effect on the thermal effusivity of the panels. The effusivity changes respectively by 170.9 $J.m^{-2}.°C^{-1}.s^{-\frac{1}{2}}$ to 473.1 $J.m^{-2}.°C^{-1}.s^{-\frac{1}{2}}$ for the defibrated typha leaves and 265.2 $J.m^{-2}.°C^{-1}.s^{-\frac{1}{2}}$ to 728.2 $J.m^{-2}.°C^{-1}.s^{-\frac{1}{2}}$ for powdered sheets, depending on the percentage of binder (Fig. 4). Comparing the results obtained for the panels of leaves of typha defibrated with those of typha leaves in powder form as in the Figure 14, the researchers notice that the boards based on powdered leaves are more effusive and this can be explained by the fact that the powdered leaves are denser and less porous than those defibrated. For 66.66% binder, the typha powder board is 1.9 times more effusive, this explains the effect of the type of fibres on effusivity.

The values obtained are comparable to those of hemp concrete - lime of 206.9 $J.m^{-2}.°C^{-1}.s^{-\frac{1}{2}}$ for a dry density of 413 $kg/m^3$ [20] and 267 $J.m^{-2}.°C^{-1}.s^{-\frac{1}{2}}$ for a dry density of 440 $kg.m^{-3}$ [21].

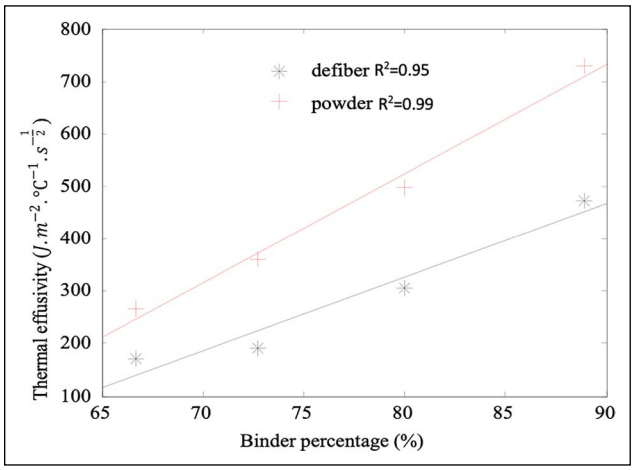


**Figure 14**. Dry panel thermal effusivity in function of the binder.

## 4. CONCLUSION

During this study, we were interested in the development of typha materials for the building while relying on mechanical and thermal characterization.

From a mechanical point of view, the results showed that the flexural strength of panels depends on typha aggregates. The finer is the typha aggregates, the lower is the flexural strength. In the case of compressive strength, the results depend on the nature of the binder and the aggregates used. The panel of typha powder and clay with a binder content of 88.89% and a density of 1559 $kg.m^{-3}$ has the best compressive strength at 2.84 MPa.

The thermal conductivity and effusivity of the panels were evaluated. They increase almost linearly depending on the binder content. The results also showed that the type of typha aggregates affect thermal conductivity. Regarding the influence of the size of the aggregates, it has been shown that for 66.66% of binder content, the panel of defibrated typha sheets is about 41.2% more insulating than the panel of typha powder sheets. Measurement of thermal effusivity has shown that typha panels are weakly effusive. Thermal effusivity increases with increasing binder content. It is concluded that the boards made from powdered leaves are more effusive. The use of these typha panels in the building will contribute to the reduction of energy consumption. This type of material is not also water resistant.

## ACKNOWLEDGEMENTS

We thank the Coordinator of Project of Thermal Insulation Material Production on base of Typha in Senegal (PNEEB/TYPHA) and the director of the Applied Energy Laboratory (LEA).

## DATA AVAILABILITY STATEMENT

The authors confirm that the data that supports the findings of this study are available within the article. Raw data that support the finding of this study are available from the corresponding author, upon reasonable request.

## CONFLICT OF INTEREST

The authors declare that they have no conflict of interest.

## FINANCIAL DISCLOSURE

The authors declared that this study has received no financial support.

## PEER-REVIEW

Externally peer-reviewed.

## REFERENCES

[1] Meukam, P., Jannot, Y., Noumowe, A., & Kofane, T. (2004). Thermo physical characteristics of economical building materials. *Construction and Building Materials*, 18(6), 437–443. [CrossRef]

[2] Millogo, Y., Morel, J. C., Aubert, J. E., & Ghavami, K. (2014). Experimental analysis of Pressed Adobe Blocks reinforced with Hibiscus cannabinus fibers. *Construction and Building Materials*, 52, 71–78. [CrossRef]

[3] Bal, H., Jannot, Y., Quenette, N., Chenu, A., & Gaye, S. (2012). Water content dependence of the porosity, density and thermal capacity of laterite based bricks with millet waste additive. *Construction and Building Materials*, 31, 144–150. [CrossRef]

[4] Tettey, U. Y. A., Dodoo, A., & Gustavsson, L. (2014). Effects of different insulation materials on primary energy and CO2 emission of a multi-storey residential building. *Energy and Buildings*, 82, 369–377. [CrossRef]

[5] de Bruijn, P. B., Jeppsson, K. H., Sandin, K., & Nilsson, C. (2009). Mechanical properties of lime–hemp concrete containing shives and fibres. *Biosystems Engineering*, 103(4), 474–479. [CrossRef]

[6] Ashori, A., & Nourbakhsh, A. (2008). Effect of press cycle time and resin content on physical and mechanical properties of particleboard panels made from the underutilized low-quality raw materials. *Industrial Crops and Products*, 28(2), 225–230. [CrossRef]

[7] Lertsutthiwong, P., Khunthon, S., Siralertmukul, K., Noomun, K., & Chandrkrachang, S. (2008). New insulating particleboards prepared from mixture of solid wastes from tissue paper manufacturing and corn peel. *Bioresource Technology*, 99(11), 4841–4845. [CrossRef]

[8] Cuk, N., Kunaver, M., & Medved, S. (2011). Properties of particleboards made by using an adhesive with added liquefied wood. Materiali in Tehnologije, 45(3), 241–245.

[9] Cérézo, V. (2005). Propriétés mécaniques, thermiques et acoustiques d'un matériau à base de particules végétales: approche expérimentale et modélisation théorique [Doctoral dissertation, Institut National des Sciences Appliquées, Lyon. (French)

[10] Chikhi, M., Agoudjil, B., Boudenne, A., & Gherabli, A. (2013). Experimental investigation of new biocomposite with low cost for thermal insulation. *Energy and Buildings*, 66, 267–273. [CrossRef]

[11] Awwad, E., Choueiter, D., & Khatib, H. (2013). Concrete masonry blocks reinforced with local industrial hemp fibers and hurds. *Proceedings 3rd International Conference On Sustainable Construction Materials And Technology*, Kyoto, Japan, 28, 18–21.

[12] Chinta, S. K., Katkar, P. M., Jafer, M. M. (2013). Natural fibres reinforced gypsum composites. *International Journal of Engineering and Management Sciences*, 4(3), 318–325.

[13] Moussa, T., Maalouf, C., Lachi, M., Umurigirwa, S., Mai, T. H., & Henry, J. F. (2016). Development and performance evaluation of a hemp–starch composite. *Journal of Building Physics*, 40(3), 278–295. [CrossRef]

[14] Ponnukrishnan, P., Thanu, M. C., & Richard, S. (2014). Mechanical characterization of Typha Domingensis natural fiber reinforced polyester composites. *International Journal of Research Science and Technology Engineering Mathematics*, 6, 241-244.

[15] Diatta, M. T., Gaye, S., Thiam, A., & Azilinon, D. (2011). Détermination des propriétés thermo-physique et mécanique du typha australis. In Congres SFT, Perpignan, (France).

[16] Dieye, Y., Sambou, V., Faye, M., Thiam, A., Adj, M., & Azilinon, D. (2017). Thermo-mechanical characterization of a building material based on Typha Australis. *Journal of Building Engineering*, 9, 142–146. [CrossRef]

[17] Niang, I., Maalouf, C., Moussa, T., Bliard, C., Samin, E., Thomachot-Schneider, C., Lachi, M., Pron, H., Mai, T. H., & Gaye, S. (2018). Hygrothermal performance of various Typha–clay composite. *Journal of Building Physics*, 42(3), 316–335. [CrossRef]

[18] Maillet, D., André, S., Batsale, J. C., Degiovanni, A., & Moyne, C. (2000). *Solving the Heat Equation through Integral Transforms*. Wiley.

[19] Collet, F., & Pretot, S. (2014). Thermal conductivity of hemp concretes: Variation with formulation, density and water content. *Construction and Building Materials*, 65, 612–619. [CrossRef]

[20] Collet-Foucault, F. (2004). *Caractérisation hydrique et thermique de matériaux de génie civil à faibles impacts environnementaux* [Doctoral Dissertation, Rennes, INSA].

[21] Evrard, A. (2008). *Transient hygrothermal behaviour of lime-hemp materials* [Doctoral Dissertation, Université catholique de Louvain].

Journal of Sustainable Construction Materials and Technologies
Web page info: https://jscmt.yildiz.edu.tr
DOI: 10.14744/jscmt.2021.03

JSCMT
Journal of Sustainable Construction Materials and Technologies

Original Article

# Calculation of energy consumption and emissions of buildings in capitals of european with the degree-day method

**Okan KON, İsmail CANER***

*Department of Mechanical Engineering, Balıkesir University Faculty of Engineering, Balıkesir, Turkey*

**ARTICLE INFO**

*Article history*
*Received: 06 September 2021*
*Accepted: 18 November 2021*

**Key words:**
Emissions, European capitals, heating and cooling degree-day, insulation thickness, thermal transmittance values of the building envelope

**ABSTRACT**

In this study, firstly, for the building envelope properties of a reference building from TS 825 insulation standard, for 20 capitals selected from Europe, the minimum insulation thicknesses are calculated with different heat transmission coefficients depending on the requirements and/or recommendations thermal transmittance values in the building envelope such as building walls, roofs, floors. Then, $CO_2$ and $SO_2$ emissions, which will be produced by the consumption of coal, natural gas, and fuel-oil fuels, depending on the heating degree-day values and the thermal transmittance values of the building envelope, are investigated for the 20 selected capitals. In the cooling period, depending on the cooling degree-days and the thermal transmittance values of the building envelope, the electricity consumption and the $CO_2$ and $SO_2$ emissions to be released for the coal, natural gas, and fuel oil used in the production of electricity in the power plants are determined. The place of Ankara, the capital of our country, among the selected capitals in European countries has been examined. It has been calculated that Sarajevo, the capital of Bosnia-Herzegovina, has the highest fuel consumption and the highest $CO_2$ and $SO_2$ emissions for three building components and three fuel types for heating. In the study, the highest thermal transmittance value recommended for floor was found to be Athens with 1.90 W/m$^2$.K. Accordingly, it has been determined that the highest electricity consumption for cooling and the highest associated $CO_2$ and $SO_2$ emission values occur in Athens, the capital of Greece.

**Cite this article as:** Kon O, Caner İ. Calculation of energy consumption and emissions of buildings in capitals of european with the degree-day method. J Sustain Const Mater Technol 2021;6:4:143–155.

## 1. INTRODUCTION

Global energy demand has been growing exponentially. It is of international importance to try to reduce the $CO_2$ emissions that will occur due to energy consumption and to reduce climate change. In this context, Europe is responsible for around 40% of the world's total energy consumption. More than 25% of this energy consumption in Europe comes from residences alone and represents the largest energy consumption sector [1, 2]. Within the scope of energy efficiency, the European Union (EU) has set a target of approximately 30% reduction in energy use in buildings and 40% reduction in greenhouse gas (GHG) emissions by 2030 [3].

***Corresponding author.**
*E-mail address: ismail@balikesir.edu.tr

Published by Yıldız Technical University Press, İstanbul, Turkey
Copyright 2021, Yıldız Technical University. This is an open access article under the CC BY-NC license (http://creativecommons.org/licenses/by-nc/4.0/).

The primary purpose of policies and regulations regarding sustainable energy for buildings is to improve the performance of buildings to minimize their energy consumption and reduce their carbon footprint without compromising standard usage requirements such as the thermal comfort of building occupants [4].

The degree days method (DD) is a versatile climate indicator that is widely used in the analysis of building energy performance. With the degree-day method, energy evaluation of existing and new buildings can be made, regional energy consumption can be analyzed, energy consumption estimation analyzes can be developed. The importance of the degree days method is that it can make quick analyzes in various fields and for different purposes [1].

Ozkan D. B. and Onan C. [5], investigated the effects of different insulation thicknesses and the consumption of natural gas and fuel oil fuels on the emissions of pollutants such as $CO_2$ and $SO_2$. deLlano-Paz F., Calvo-Silvosa A., Iglesias Antelo S., Soares I. [6] applied portfolio theory to both economically and environmentally efficient electricity production. With their model, they include all production costs for different technologies and a series of measures related to the risk arising from them and the emission of polluting gases such as carbon dioxide, sulfur dioxide, nitrogen oxides and particulate matter. Çay Y., Gürel A. E. [7] analyzed the effect of insulation thickness on the emission of $CO_2$ and $SO_2$ emissions. D'Agostino D., Cuniberti B., Bertoldi P. [8] presented the overall results of data collected by the Green Building Program (GBP), launched in 2006 to promote and improve energy efficiency in new and existing European non-residential buildings. Rodríguez-Soria B., Domínguez-Hernández J., M. Pérez-Bella J., Coz-Díaz J. J. [9] showed that countries set different permeability values defined on the basis of different degree-day variation intervals for each climate zone. They propose a new methodology that can be used to regulate the thermal insulation of buildings in all countries to ultimately harmonize the energy losses of the building envelope. Christenson M., Manz H., Gyalistras D. [10], in their study, the effect of climate change on Swiss building energy demand was investigated by degree-day method. A procedure was developed, tested and applied to four different Swiss locations to estimate heating degree days (HDD) and cooling degree days (CDD) from monthly temperature data. Rosa M. D., Bianco V., Scarpa F., Tagliafico L. [1] a compared the simplified methods based on reduced climatic data set with reference to the mean daily degree-hour method (MDDH). Rosa M. D., Bianco V., Scarpa F., Tagliafico L. A. [11] proposed a simple dynamic model to simulate heating/cooling energy consumption in buildings. The study analyzed the cooling energy demand on low-cooling days (CDDs) and explained that other factors such as solar radiation play an important role in this case. Ramírez-Villegas R., Eriksson O., Olofsson T. [3] investigate the effect of different building renovation strategies on the energy rating of a selected Building Environmental Assessment Tool and analyze the results in terms of GHG emissions for the local and district heating system. Annunziata E., Frey M., Rizzi F. [12] conducted a survey among 27 European Union Member States on energy efficiency in buildings, energy policy and strategy in Europe. Meng Q., Mourshed M. [13] examined four-year (2012–2016) half-hourly measured gas consumption from 119 non-residential buildings, and their relationship to baseline temperatures and their internal structure parameters using a three-parameter change-point regression model. Al-Hadhrami L.M., [14] in their study, annual and seasonal cooling (CDD) and heating (HDD) degree-day values for Saudi Arabia were presented using long-term average daily temperatures from 38 meteorological stations. Akıner İ., Akıner M. E., Tijhuis W. [15] selected cities from different regions of the country to examine the effects of local climate on energy use in energy-efficient buildings. In the study, Heating Degree Days (HDD) and Cooling Degree Days (CDD) values are used to estimate the energy demand for heating and cooling buildings. Pusat S., Ekmekci I. [16] compared a different climate belt approach proposed by the International Energy Agency (IEA) with respect to both heating and cooling degree-day data obtained from Typical Meteorological Year (TMY) data. Meng Q., Mourshed M., Wei S. [4] in their study, a change point regression technique was proposed to better define the baseline temperature and then applied in buildings with different operational energy use patterns. Spinoni J., Vogt J. V., Barbosa P., Dosio A., McCormick N., Bigano A., Füssel H.-M [17] took into account heating degree-days (HDD) and cooling degree-days (CDD) in relation to energy consumption for heating and cooling of buildings. An N., Turp M. T., Akbaş A., Öztürk Ö., Kurnaz M. L. [18] investigated how the heating and cooling days will change in the future with climate change in Turkey according to the RCP8.5 scenario for intense greenhouse gas emissions. Altun M., Akçamete A., Akgül Ç. M. [19] examined the effect of the outside temperature data on the building heating energy requirement and the validity of the DGBs (Degree day region) created from the TS 825 standard according to the outdoor temperature data. In this context, the validity of DGBs and the effectiveness of the updates made in the standard were examined by evaluating them separately for 81 provinces. Çomaklı, K. and Yüksel, B. [20] examined the effect of air pollution as a result of the burning of fossil fuels used to heat buildings in cold cities such as Erzurum. They found that with low quality fuel consumption, it causes very high air pollution and poor air quality for space heating. In the study, they investigated the environmental effects of thermal insulation used to reduce heat losses in buildings. Bolattürk A. [21] determined the optimum insulation thickness on the exterior walls of buildings. The

study used the degree-hour method of estimating the annual energy consumption of the building. Goggins J., Moran P., Armstrong A., and Hajdukiewicz M. [22] to assess the contribution of changes in building codes to both the construction and operation of buildings' life cycles, they presented the case study for environmental and economic life cycle assessment of buildings in Ireland.

The aim of the study is to investigate the $CO_2$ and $SO_2$ emissions that will occur by using coal, natural gas, fuel-oil consumptions of the buildings heating period and the coal, natural gas and fuel oil used in power plants cooling period, depending on the heating and cooling degree-day values and the building envelope thermal transmittance values for 20 selected European capitals. The different climate and building envelopes with different thermal transmittance values accepted in Europe were selected. Among these 20 capitals, Ankara, the capital of our country, in terms of energy consumption and emission consumption has been examined. In the study, the minimum insulation thicknesses were calculated for the 20 capital cities selected from Europe, for the insulation materials, which are considered different heat transmission coefficients depending on the thermal transmittance values recommended in the building envelope, such as building walls, roofs, floors. It has been examined what can be done to reduce $CO_2$ and $SO_2$ emissions, depending on the thermal transmittance value of the building envelope of Ankara, by comparing it with other selected European countries.

## 2. MATERIAL AND METHOD

### 2.1 Building Envelope Insulation Thickness and Heating and cooling Energy Consumption Equations

Insulation thicknesses for building envelope;

$$d_{ins}=\lambda_{ins}.\left(\frac{1}{U}-R_{si}-R-R_{se}\right) \quad (1)$$

Where U is thermal transmittance value, $R_{si}$ and $R_{se}$ are the internal and external surface thermal resistance, R is other thermal resistance of the structural component and $\lambda_{ins}$ is the thermal conductivity coefficient of the insulation material [20–23].

The amount of fuel consumed per year during the heating period,

$$M_{F_H}=\frac{86400.U.HDD}{H_u.\eta} \quad (2)$$

In the cooling period, the amount of electricity consumed per year,

$$M_{F_C}=\frac{86400.U.CDD}{COP} \quad (3)$$

Here, HDD is degree-day, CDD is cooling degree-day, COP (taken as 2.5) is cooling system coefficient of performance, $H_u$ is lower heating value (LHV) of fuel and η is heating system efficiency [5, 7, 20, 21]. For heating degree-days and cooling degree-days the last three year period were taken into account. Heating degree-days (HDD) cover the days of the months in which the heating is made, these are generally the sum of the days of January, February, March, April, November, and December. Cooling degree-days, on the other hand, cover the days of the months in which the cooling is done; these are generally the sum of the days of June, July, August, and September. May and October are defined as the transition months when heating and cooling are not done.

### 2.2 Combustion Equations

Combustion equation of fuel;

$$C_aH_bO_zS_pN_q + \alpha.\ A.\ (O_2+3.76\ N_2)\ aCO_2 + (b/2)\ H_2O + pSO_2 + B\ O_2 + D\ N_2 \quad (4)$$

Here, A, B and D are;

$$A=(a+b/4+p-z/2) \quad (5)$$

$$B=(\alpha-1)\ (a+b/4+p-z/2) \quad (6)$$

$$D=3.76\ \alpha\ (a+b/4+p-z/2)+q/2 \quad (7)$$

$C_aH_bO_zS_pN_q$ is overall chemical formula of fuel. $CO_2$ and $SO_2$ emissions produced by the combustion of 1 kg of fuel;

$$M_{CO_2}=\frac{a.CO_2}{M} \quad (kg\ CO_2/\ kg\ fuel) \quad (8)$$

$$M_{SO_2}=\frac{p.SO_2}{M} \quad (kg\ SO_2/\ kg\ fuel) \quad (9)$$

If the right side of the above equations is derived by writing the total amount of fuel burned in $M_F$, the total emissions of $CO_2$ and $SO_2$ are found as follows.

$$M_{CO_2}=\frac{44.CO_2}{M}.M_F \quad (kg\ CO_2/m^2year) \quad (10)$$

$$M_{SO_2}=\frac{64.SO_2}{M}.M_F \quad (kg\ SO_2/m^2year) \quad (11)$$

M is the molar weight of the fuel and is found as follows. Where a, b, z, p, q are the combinations of the elements in the chemical formula of the fuels, α is air excess coefficient, which is one of the effective parameters in the combustion of fuel and A indicates the minimum amount of oxygen required for the combustion process [5, 7, 20, 21].

$$M=12.a+b+16.z+32.p+14.q\ (kg/kmol) \quad (12)$$

### 2.3 The values used in the calculations

In the study, the characteristics of the fuels used in European capitals during the heating period are shown in Table 1. In Table 1, LHV is the lower heating value and η is the theoretical efficiency of the combustion system. The lowest recommended thermal transmittance value for the wall is

**Table 1.** The chemical formulas of fuels [7]

| Fuel | Chemical Formula | LHV (Hu) | Efficiency (η) |
|---|---|---|---|
| Coal | $C_{7.074}H_{5.149}O_{0.521}S_{0.01}N_{0.086}$ | $29.295\times10^6$ J/kg | 0.65 |
| Natural gas | $C_{1.269}H_{4.516}O_{0.024}N_{0.012}$ | $34.526\times10^6$ J/m$^3$ | 0.93 |
| Fuel-oil | $C_{7.3125}H_{10.407}O_{0.04}S_{0.026}N_{0.02}$ | $40.594\times10^6$ J/kg | 0.80 |

**Table 2.** Requirements and/or recommendations for cities in Europe thermal transmittance values for walls, roofs and floors (U-value W/m²K) [24]

| City | Country | Wall | Roof | Floor |
|---|---|---|---|---|
| Tirana | Albania | 0.53 | 0.38 | 0.59 |
| Bruxelles | Belgium | 0.60 | 0.40 | 1.20 |
| Sarajevo | Bosnia-Herzegovina | 0.80 | 0.55 | 0.65 |
| Sofia | Bulgaria | 0.50 | 0.30 | 0.50 |
| Prag | Czech Republic | 0.30 | 0.24 | 0.45 |
| Berlin | Germany | 0.30 | 0.20 | 0.40 |
| Madrid | Spain | 0.66 | 0.38 | 0.66 |
| Tallinn | Estonia | 0.25 | 0.16 | 0.25 |
| Helsinki | Finland | 0.25 | 0.16 | 0.25 |
| Paris | France | 0.36 | 0.20 | 0.27 |
| Athens | Greece | 0.70 | 0.50 | 1.90 |
| Budapest | Hungary | 0.45 | 0.25 | 0.50 |
| Roma | Italy | 0.50 | 0.46 | 0.46 |
| Skopje | Macedonia | 0.90 | 0.60 | 0.75 |
| Amsterdam | The Netherlands | 0.37 | 0.37 | 0.37 |
| Oslo | Norway | 0.18 | 0.13 | 0.18 |
| Warschau | Poland | 0.30 | 0.30 | 0.60 |
| Stockholm | Sweden | 0.18 | 0.13 | 0.15 |
| Beograd | Serbia | 0.90 | 0.65 | 0.75 |
| Ankara | Turkey | 0.48 | 0.28 | 0.43 |

**Table 3.** Heating and cooling degree-days for cities in Europe [25]

| City | Country | Heating degree-day 19.5°C | Cooling degree-day 22°C |
|---|---|---|---|
| Tirana | Albania | 1981 | 406 |
| Bruxelles | Belgium | 3247 | 55 |
| Sarajevo | Bosnia-Herzegovina | 3579 | 173 |
| Sofia | Bulgaria | 3232 | 242 |
| Prag | Czech Republic | 3292 | 151 |
| Berlin | Germany | 3407 | 103 |
| Madrid | Spain | 2270 | 583 |
| Tallinn | Estonia | 4678 | 20 |
| Helsinki | Finland | 4833 | 27 |
| Paris | France | 2926 | 115 |
| Athens | Greece | 1413 | 734 |
| Budapest | Hungary | 3293 | 226 |
| Roma | Italy | 1811 | 370 |
| Skopje | Macedonia | 2974 | 369 |
| Amsterdam | The Netherlands | 3194 | 32 |
| Oslo | Norway | 5021 | 13 |
| Warschau | Poland | 3789 | 110 |
| Stockholm | Sweden | 4344 | 22 |
| Beograd | Serbia | 2841 | 310 |
| Ankara | Turkey | 3430 | 264 |

Oslo and Stockholm with 0.18 W/m².K, and the highest value is Skopje and Beograd with 0.90 W/m².K. The lowest recommended value for the roof is Oslo and Stockholm with 0.13 and the highest value is Beograd with 0.65 W/m².K. The lowest recommended value for flooring is Stockholm with 0.15 W/m².K and the highest value is Athens with 1.90 W/m².K. These are given in Table 2.

The highest heating degree-day values occur in Oslo, Helsinki, and Tallinn, and the lowest in Athens, Rome, and Tirana. The highest cooling degree-day values occur in Athens, Madrid, and Tirana, and the lowest in Oslo, Tallinn, and Stockholm. These values and other European heating and cooling degree-day values are given in Table 3. Here, the heating degree-days (HDD) value during the year is the sum of the temperature values 19.5°C below the daily temperature. Cooling degree-days (CDD) is the sum of the temperature values above 22°C of the year. The daily average of the last three years is taken. The building envelope components used to find the minimum insulation thickness depending on the building envelope requirements and/or recommendations thermal transmittance values for European capitals and taken as an example according to TS 825 are shown in Table 4. In Table 5, the $CO_2$ and $SO_2$ emission factors released to the environment for electricity-generating power plants are given.

## 3. RESULTS AND DISCUSSION

### 3.1 Insulation Thicknesses for Different Thermal Transmittance Values

For the thermal conductivity coefficient values between 0.01 to 0.07 W/m.K, the minimum insulation thickness value for the external walls was calculated between 0.004 to 0.026 m in Skopje and Beograd, and the highest thickness between 0.048 to 0.337 m in Oslo and Stockholm. In Helsinki, it was calculated as 0.033–0.228 m. The average value of the minimum insulation thickness of these 20 selected capitals was calculated between 0.019 to 0.133 m. The insu-

**Table 4.** Reference building components for external wall, roof, and floor [23]

| Component | Thickness (m) | Heat conductivity coefficient (W/m.K) |
|---|---|---|
| External wall | | |
| Internal plaster | 0.020 | 1.000 |
| Horizontal brick | 0.190 | 0.360 |
| Insulation | --- | --- |
| External plaster | 0.008 | 0.350 |
| Roof | | |
| Internal plaster | 0.020 | 1.000 |
| Concerete | 0.120 | 2.500 |
| Insulation | --- | --- |
| Floor | | |
| PVC floor covering | 0.005 | 0.230 |
| Screed | 0.030 | 1.400 |
| Insulation | --- | --- |
| Leveling screed | 0.020 | 1.400 |
| Lightweight concrete | 0.100 | 1.100 |

**Table 5.** Gases harmful to the environment and human health (GHEH) emission amounts produced during electricity generation in power plants [6]

| GHEH | Coal | Natural gas | Oil |
|---|---|---|---|
| $CO_2$ (kg/kWh) | 0.7341 | 0.3561 | 0.5465 |
| $SO_2$ (gr/kWh) | 0.0735 | 0.0088 | 0.0547 |

lation thickness for Ankara is calculated between 0.013 to 0.094 m. This value is between the average values of the 20 selected European capitals. These values are given in Figure 1. The minimum value of the insulation thicknesses for the roof was calculated between 0.013 to 0.092 m in Beograd, and the highest thickness between 0.075 to 0.523 m in Oslo and Stockholm. In Helsinki, it is calculated as 0.060–0.422 m. The average value of the minimum insulation thickness of these 20 selected capitals was calculated between 0.035 to 0.248 m. The thickness of the insulation for Ankara is calculated between 0.034 to 0.234 m. This value is also between the average values of the 20 selected European capitals. These values are shown in Figure 2. The minimum value of the insulation thicknesses for the floor was calculated between 0.002 to 0.013 m in Athens, and the highest thickness between 0.063 to 0.443 m in Stockholm. In Oslo, it is 0.052–0.365 m, and in Helsinki, it is 0.037–0.257 m. The average value of the minimum insulation thickness of these 20 selected capitals was calculated between 0.022–0.153 m. The thickness of the insulation for Ankara is calculated between 0.020 to 0.139 m. This value is between the average values of the 20 selected European capitals. These are given in Figure 3. In Scandinavian countries such as Sweden, Norway and Finland, the thermal transmittance values of

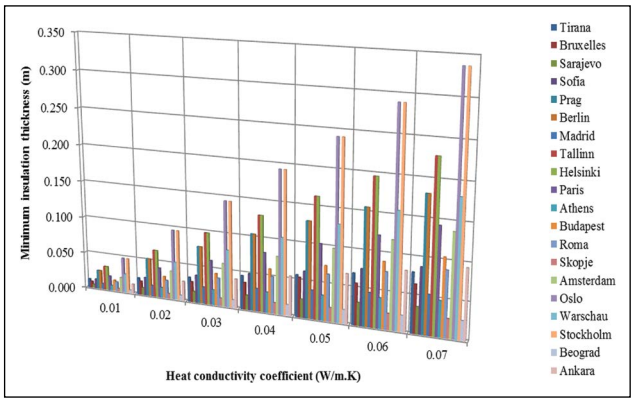


**Figure 1**. Minimum insulation thicknesses for external wall depending on different heat conductivity coefficients.

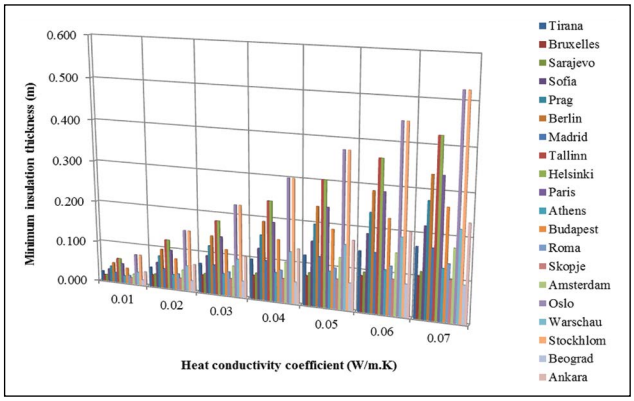


**Figure 2**. Minimum insulation thicknesses for roof depending on different heat conductivity coefficients.

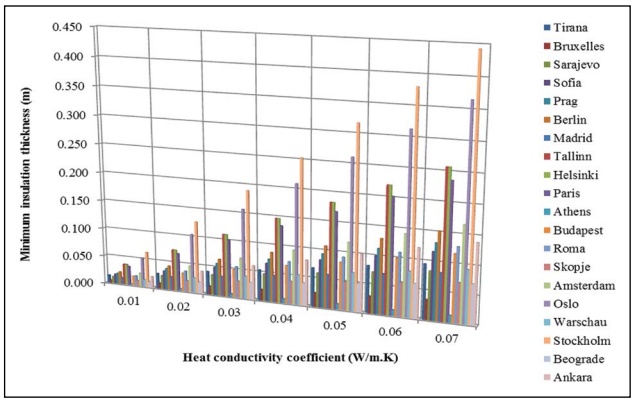


**Figure 3**. Minimum insulation thicknesses for floor depending on different heat conductivity coefficients.

the building shell are much lower than in other countries in Europe and the insulation thicknesses are higher because they have a colder climate.

### 3.2 $CO_2$ and $SO_2$ Emission Values

For the heating period, the highest natural gas consumption is 7.704 kg/$m_2$ in Sarajevo, depending on the wall structure. Based on natural gas consumption, $CO_2$

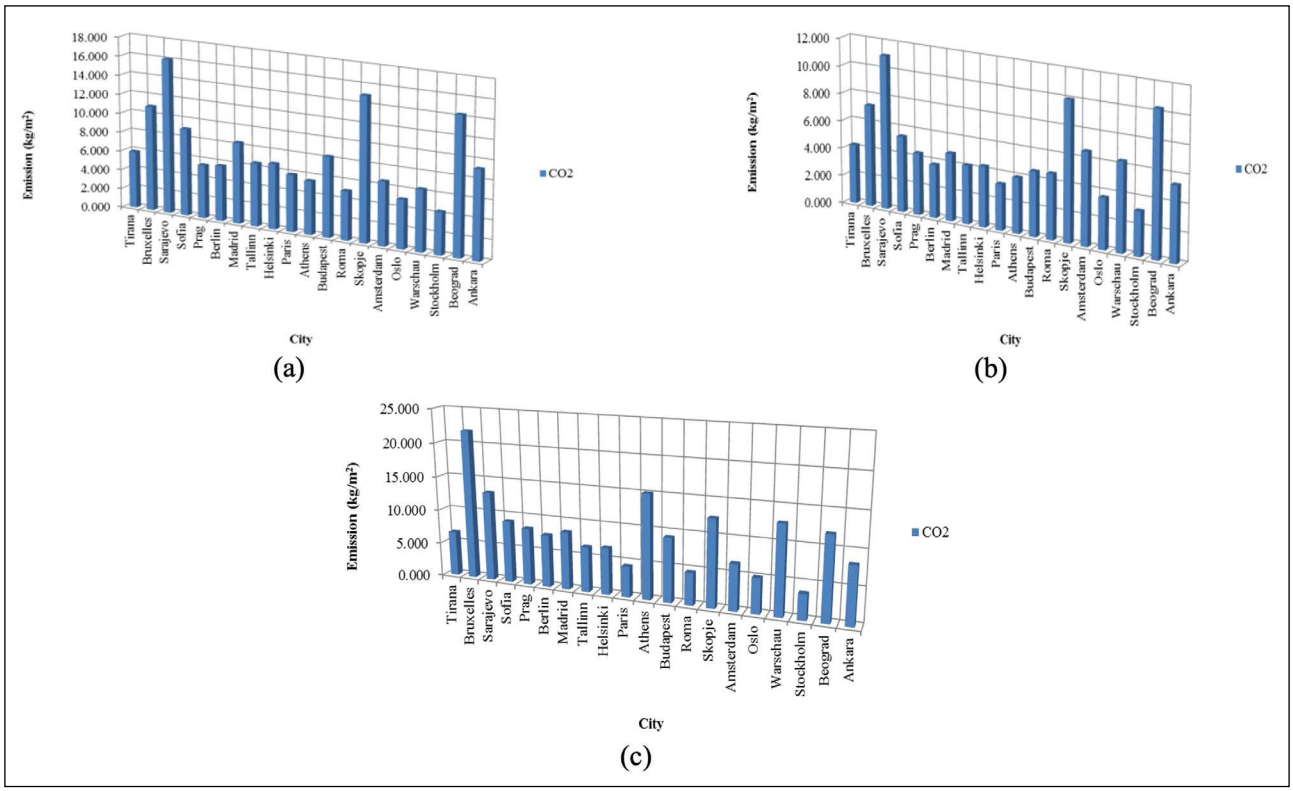


**Figure 4**. $CO_2$ emission to be generated by consuming natural gas for the heating period for **(a)** external wall area **(b)** roof area **(c)** floor area.

emissions are calculated as 16.109 kg/m² in Sarajevo. The lowest natural gas consumption was found in Stockholm as 2.104 kg/m². Based on natural gas consumption, $CO_2$ emissions are calculated as 4.399 kg/m² in Stockholm. The average natural gas consumption for these capitals is 3.858 kg/m², and $CO_2$ emission is 8.067 kg/m². Ankaras' natural gas consumption is 4.430 kg/m² and $CO_2$ emission is 9.263 kg/m². It is higher than the average of the 20 selected European capitals. Depending on the roof structure, the highest natural gas consumption is 5.297 kg/m² in Sarajevo. Depending on the natural gas consumption, the $CO^2$ emission in Sarajevo is calculated as 11.076 kg/m². The lowest natural gas consumption was 1.502 kg/m² in Stockholm. Based on natural gas consumption, $CO_2$ emissions are calculated as 3.178 kg/m² in Stockholm. The average natural gas consumption for these capitals is 2.680 kg/m² and $CO_2$ emissions are 5,604 kg/m². Ankaras' natural gas consumption was found as 2.584 kg/m² and $CO_2$ emission was found as 5,403 kg/m². These are slightly lower than the average of the 20 selected European capitals. Depending on the floor structure, the highest natural gas consumption occurs in Bruxelles as 10.484 kg/m². Depending on the natural gas consumption, the $CO_2$ emission was calculated as 21.922 kg/m² in Bruxelles. The lowest natural gas consumption was found in Stockholm as 1.753 kg/m². Based on natural gas consumption, $CO_2$ emissions are calculated as 3.666 kg/m² in Stockholm. The average natural gas consumption for these capitals is 4.376 kg/m², and $CO_2$ emissions are 9.151 kg/m². Ankaras' natural gas consumption was found to be 3.969 kg/m² and $CO_2$ emission was calculated as 8.299 kg/m2. It is lower than the average of the 20 selected European capitals. These values are given in Figure 4.

Depending on the wall structure for the heating period, the highest coal consumption is 12.991 kg/m² in Sarajevo. Based on coal consumption, $CO_2$ emissions are calculated as 40.480 kg/m² and $SO_2$ emissions 0.083 kg/m² in Sarajevo. The lowest coal consumption was 3.548 kg/m² in Stockholm. Based on coal consumption, the $CO_2$ emission was calculated as 11.056 kg/m² and the $SO_2$ emission was 0.023 kg/m² in Stockholm. The average coal consumption for these capitals is 6.506 kg/m², $CO_2$ emissions are 20.273 kg/m² and $SO_2$ emissions are 0.042 kg/m². Ankaras' coal consumption is 7.470 kg/m², $CO_2$ emission is 23.277 kg/m² and $SO_2$ emission is 0.048 kg/m². It is higher than the average of the 20 selected European capitals. Depending on the roof structure, the highest coal consumption is 8.914 kg/m² in Sarajevo. Depending on the coal consumption, the $CO_2$ emission was calculated as 27.776 kg/m² and the $SO_2$ emission was 0.057 kg/m² in Sarajevo. The lowest coal consumption was found in Stockholm as 2.562 kg/m². Depending on the coal consumption, the $CO_2$ emission was calculated as 7.983 kg/m² and the $SO_2$ emission was 0.016 kg/m² in Stockholm. The average coal consumption for these capitals is 4.519 kg/m², $CO_2$ emissions are 14.080

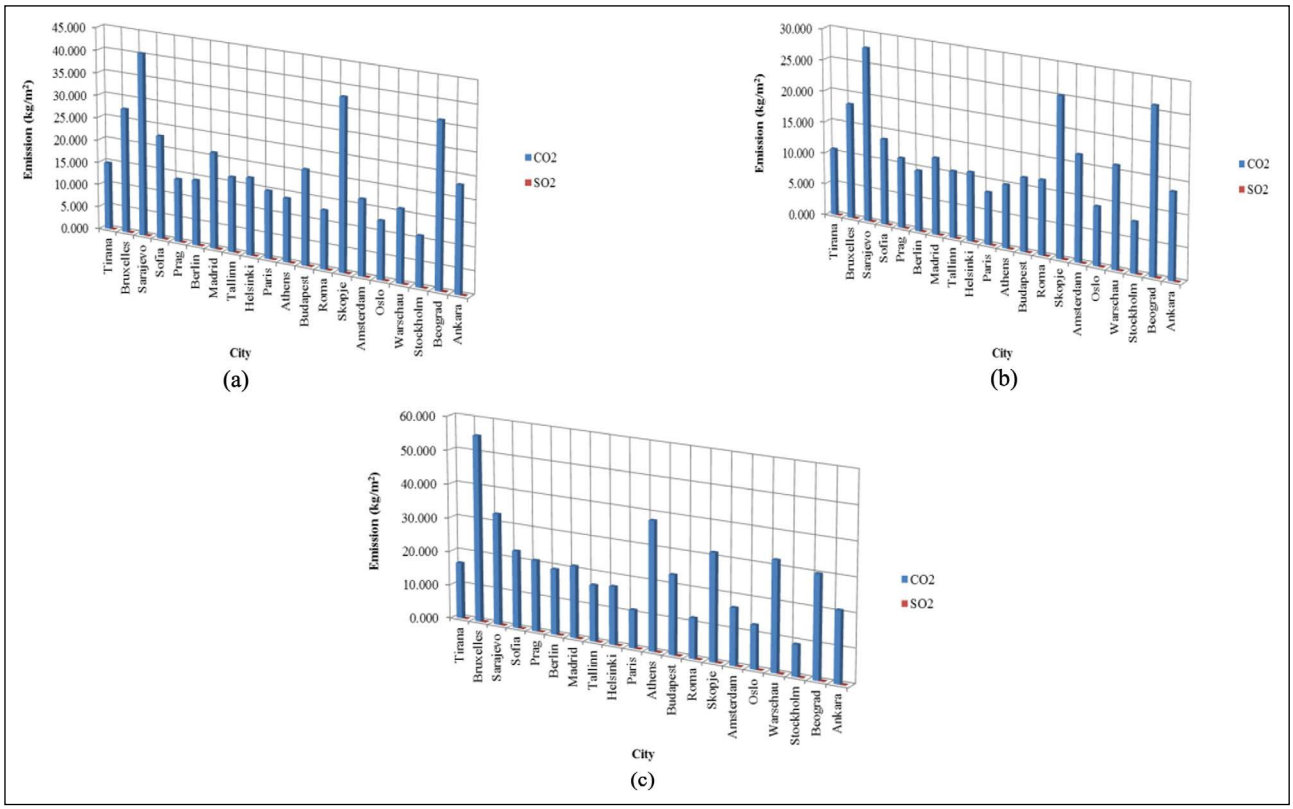


**Figure 5**. $CO_2$ and $SO_2$ emissions that will occur with the consumption of coal for heating period for **(a)** external wall area **(b)** roof area **(c)** floor area.

kg/m² and $SO_2$ emissions are 0.029 kg/m². Ankaras' coal consumption is 4.358 kg/m², $CO_2$ emission is 13.580 kg/m² and $SO_2$ emission is 0.028 kg/m². These are slightly lower than the average of the 20 selected European capitals. Depending on the floor structure, the highest coal consumption is 17.680 kg/m² in Bruxelles. Depending on the coal consumption, the $CO_2$ emission is calculated as Bruxelles 55.091 kg/m² and the $SO_2$ emission is 0.113 kg/m². The lowest coal consumption was found in Stockholm at 2.957 kg/m². Based on coal consumption, $CO_2$ emissions are calculated as 9.214 kg/m² and $SO_2$ emissions 0.019 kg/m² in Stockholm. The average coal consumption for these capitals is 7.380 kg/m², $CO_2$ emissions are 22.996 kg/m² and $SO_2$ emissions are 0.047 kg/m². Ankaras' coal consumption was found to be 6.692 kg/m², $CO_2$ emission was 20.852 kg/m² and $SO_2$ emission was 0.043 kg/m². It is lower than the average of the 20 selected European capitals. These values are given in Figure 5.

Depending on the wall structure for the heating period, the highest fuel-oil consumption is 7.618 kg/m² in Sarajevo. Based on fuel-oil consumption, $CO_2$ emissions are calculated as 24.530 kg/m² and $SO_2$ emissions 0.130 kg/m² in Sarajevo. The lowest fuel oil consumption was 2.080 kg/m² in Stockholm. Based on fuel-oil consumption, $CO_2$ emissions are calculated as 6.698 kg/m² and $SO_2$ emissions 0.035 kg/m² in Stockholm. The average fuel-oil consumption for these capitals is 3.815 kg/m², $CO_2$ emissions are 12.283 kg/m² and $SO_2$ emissions are 0.065 kg/m². Ankaras' fuel-oil consumption was 4.380 kg/m², and depending on fuel-oil consumption, $CO_2$ emission was 14.104 kg/m² and $SO_2$ emission was 0.074 kg/m². It is higher than the average of the 20 selected European capitals. Depending on the roof structure, the highest fuel-oil consumption is 5.237 kg/m² in Sarajevo. Based on fuel-oil consumption, $CO_2$ emissions were calculated as 16.863 kg/m² and $SO_2$ emissions were calculated as 0.089 kg/m² in Sarajevo. The lowest fuel-oil consumption was found in Stockholm as 1.502 kg/m². Based on fuel-oil consumption, $CO_2$ emissions are calculated as 4.836 kg/m² and $SO_2$ emissions as 0.026 kg/m² in Stockholm. Average fuel oil consumption for these capitals is 2.650 kg/m², $CO_2$ emissions are 8.533 kg/m² and $SO_2$ emissions are 0.045 kg/m². Ankara fuel-oil consumption was found to be 2.555 kg/m², and depending on fuel-oil consumption, $CO_2$ emission was found to be 8.227 kg/m² and $SO_2$ emission was 0.043 kg/m². These are slightly lower than the average of the 20 selected European capitals. Depending on the flooring structure, the highest fuel-oil consumption occurs in Bruxelles at 10.366 kg/m². Depending on the fuel-oil consumption, the $CO_2$ emission in Bruxelles is 33.379 kg/m² and the $SO_2$ emission is 0.176 kg/m². The lowest fuel-oil consumption was found in Stockholm at 1.734 kg/m². Depending on the fuel-oil con-

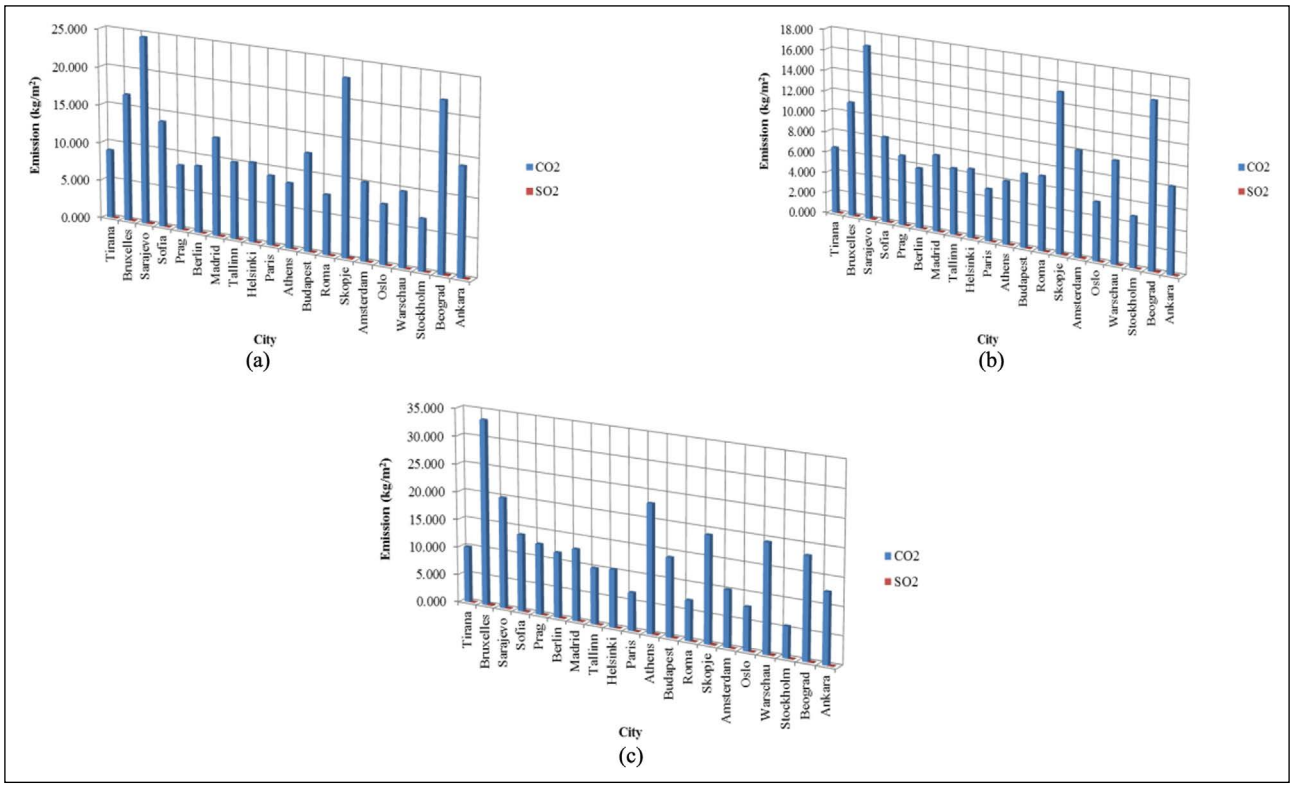


**Figure 6**. $CO_2$ and $SO_2$ emissions from fuel-oil consumption for heating period for **(a)** external wall area **(b)** roof area **(c)** floor area.

sumption, the $CO_2$ emission was calculated as 5.583 kg/m² and the $SO_2$ emission was 0.029 kg/m² in Stockholm. For these capitals, the average fuel oil consumption is 4.327 kg/m², $CO_2$ emissions are 13.933 kg/m² and $SO_2$ emissions are 0.074 kg/m². Ankara fuel-oil consumption was found to be 3.924 kg/m², and depending on fuel-oil consumption, $CO_2$ emission was 12.635 kg/m² and $SO_2$ emission was 0.067 kg/m². It is lower than the average of the 20 selected European capitals. These values are given in Figure 6.

For the cooling period, the highest electricity consumption is 4.936 kWh/m² in Athens, depending on the wall structure. Based on natural gas consumption power plant, $CO_2$ emissions are calculated as 1.758 kg/m² and $SO_2$ emissions as 0.0000434 kg/m² in Athens. The lowest electricity consumption is 0.022 kWh/m² in Oslo. Based on natural gas consumption, $CO_2$ emissions are calculated as 0.008 kg/m² and $SO_2$ emissions as 0.0000002 kg/m² in Oslo. The average electricity consumption for these capitals is 1.254 kWh/m², $CO_2$ emission is 0.447 kg/m² and $SO_2$ emission is 0.0000110 kg/m². Ankaras' electricity consumption is 1.217 kg/m² and $CO_2$ emission is 0.433 kg/m² and $SO_2$ emission is 0.0000107 kg/m² depending on natural gas consumption. It is lower than the average of the 20 selected European capitals. Depending on the roof structure, the highest electricity consumption is 3.526 kWh/m² in Athens. Based on natural gas consumption, $CO_2$ emissions are calculated as 1.256 kg/m² and $SO_2$ emissions 0.0000310 kg/m² in Athens. The lowest electricity consumption was 0.016 kWh/m² in Oslo. Based on natural gas consumption, $CO_2$ emissions are calculated as 0.006 kg/m² and $SO_2$ emissions as 0.000001 kg/m² in Oslo. Average electricity consumption for these capitals is 0.861kWh/m², $CO_2$ emission is 0.307 kg/m² and $SO_2$ emission is 0.000076 kg/m². Ankaras' electricity consumption is 0.710 kWh/m² and $CO_2$ emission is 0.253 kg/m² and $SO_2$ emission is 0.0000062 kg/m² depending on natural gas consumption. It is lower than the average of the 20 selected European capitals. Depending on the floor structure, the highest electricity consumption is 13.399 kWh/m² in Athens. Depending on natural gas consumption, $CO_2$ emissions are calculated as 4.771 kg/m² and 0.0001179 kg/m² in Athens. The lowest electricity consumption was 0.022 kWh/m² in Oslo. Based on natural gas consumption, $CO_2$ emissions are calculated as 0.008 kg/m² and $SO_2$ emissions as 0.0000002 kg/m² in Oslo. The average electricity consumption for these capitals is 1.662 kWh/m², $CO_2$ emissions are 0.592 kg/m² and $SO_2$ emissions are 0.0000146 kg/m². Ankaras' electricity consumption is 1.091 kWh/m² and $CO_2$ emission is 0.389 kg/m² and $SO_2$ emission is 0.0000096 kg/m² depending on natural gas consumption. It is lower than the average of the 20 selected European capitals. These values are given in Figure 7.

Depending on the wall structure for the cooling period, Athens has the highest electricity consumption of 4,936 kWh/m². Depending on the coal consumption pow-

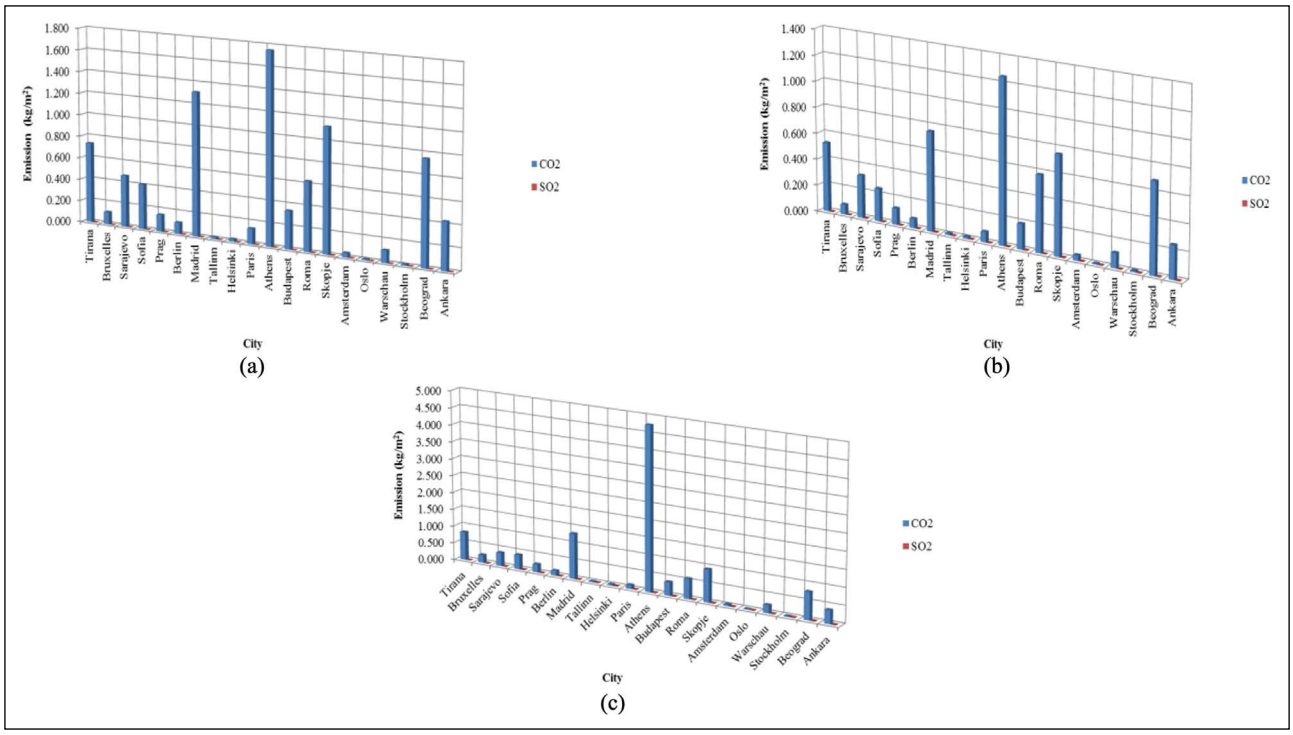


**Figure 7**. $CO_2$ and $SO_2$ emissions for electricity generated by consuming natural gas for cooling **(a)** external wall area **(b)** roof area **(c)** floor area.

er plant, the $CO_2$ emission is calculated as 3.624 kg/m² and the $SO_2$ emission is 0.0003628 kg/m² in Athens. The lowest electricity consumption is 0.022 kWh/m² in Oslo. Based on coal consumption, $CO_2$ emission is calculated as 0.016 kg/m² and $SO_2$ emission is calculated as 0.0000016 kg/m² in Oslo. Average electricity consumption for these capitals is 1,254 kWh/m², $CO_2$ emissions are 0.921 kg/m² and $SO_2$ emissions are 0.0000922 kg/m². Ankaras' electricity consumption is 1.217 kWh/m² and $CO_2$ emission is 0.893 kg/m² and $SO_2$ emission is 0.0000894 kg/m² depending on coal consumption. It is lower than the average of the 20 selected European capitals. Depending on the roof structure, the highest electricity consumption occurs in Athens, at 3.526 kWh/m². Depending on the coal consumption, the $CO_2$ emission is calculated as 2.588 kg/m² and the $SO_2$ emission is 0.0002592 kg/m² in Athens. The lowest electricity consumption was 0.016 kWh/m² in Oslo. Based on coal consumption, $CO_2$ emission is calculated as 0.012 kg/m² and $SO_2$ emission is calculated as 0.0000012 kg/m² in Oslo. The average electricity consumption for these capitals is 0.861 kWh/m², $CO_2$ emissions are 0.632 kg/m² and $SO_2$ emissions are 0.0000663 kg/m². Ankara electricity consumption is 0.710 kg/m² and $CO_2$ emission is 0.521 kg/m² and $SO_2$ emission is 0.0000522 kg/m² depending on coal consumption. It is lower than the average of the 20 selected European capitals. Depending on the floor structure, the highest electricity consumption is 13,399 kWh/m² in Athens. Depending on coal consumption, $CO_2$ emissions are calculated as 9.836 kg/m² and 0.0009848 kg/m² in Athens. The lowest electricity consumption was 0.022 kWh/m² in Oslo. Based on coal consumption, $CO^2$ emission was calculated as 0.016 kg/m² and $SO_2$ emission was calculated as 0.0000016 kg/m² in Oslo. The average electricity consumption for these capitals is 1.662 kWh/m², $CO_2$ emissions are 1.220 kg/m² and $SO_2$ emissions are 0.0001222 kg/m². Ankara electricity consumption is 1.091 kWh/m² and CO2 emission is 0.801 kg/m² and $SO_2$ emission is 0.0000802 kg/m² depending on coal consumption. It is lower than the average of the 20 selected European capitals. These values are given in Figure 8.

For the cooling period, the highest electricity consumption is calculated as 4.936 kWh/m² in Athens depending on the wall structure. Based on fuel-oil consumption power plant, $CO_2$ emissions are calculated as 2.698 kg/m² and $SO_2$ emissions 0.0002700 kg/m² in Athens. The lowest electricity consumption was 0.022 kWh/m² in Oslo. Based on fuel-oil consumption, $CO_2$ emissions are calculated as 0.012 kg/m² and $SO_2$ emissions as 0.0000012 kg/m² in Oslo. The average electricity consumption for these capitals is 1.254 kWh/m², $CO_2$ emissions 0.686 kg/m² and $SO_2$ emissions 0.0000686 kg/m². Ankaras' electricity consumption is 1.217 kg/m² and depending on fuel-oil consumption, $CO_2$ emission is 0.665 kg/m² and $SO_2$ emission is 0.0000666 kg/m². It is lower than the average of the 20 selected European capitals. Depending on the roof structure, the highest electricity consumption is 3.526 kWh/m² in Athens. Based on fuel-oil consumption, $CO_2$ emis-

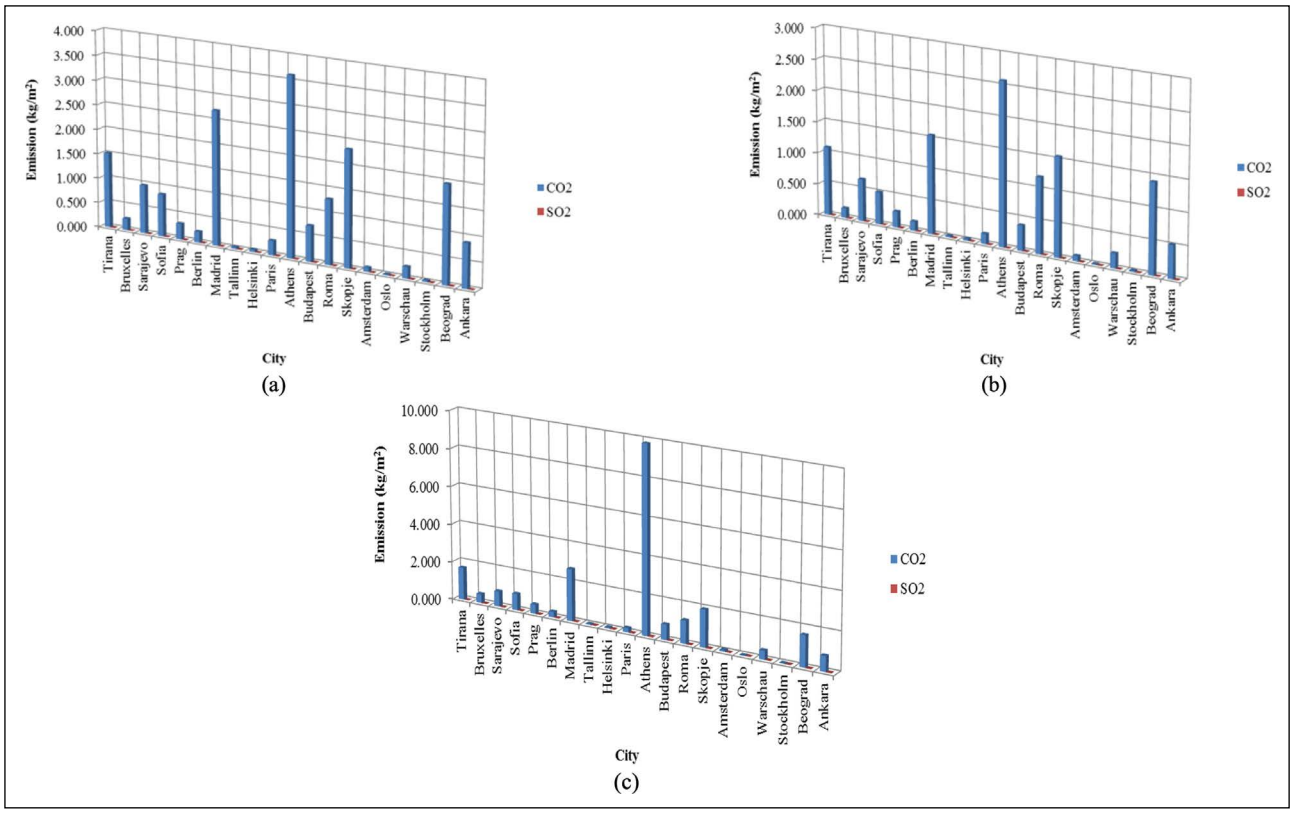


**Figure 8**. $CO_2$ and $SO_2$ emissions for electricity generated by consuming coal for cooling period **(a)** external wall area **(b)** roof area **(c)** floor area.

sions are calculated as 1.927 kg/m² and $SO_2$ emissions as 0.0001929 kg/m² in Athens. The lowest electricity consumption was 0.016 kWh/m² in Oslo. Based on fuel-oil consumption, $CO_2$ emissions are calculated as 0.009 kg/m² and $SO_2$ emissions as 0.0000009 kg/m² in Oslo. Average electricity consumption for these capitals is 0.861 kWh/m², $CO_2$ emissions are 0.471 kg/m² and $SO_2$ emissions are 0.0000471 kg/m². Ankaras' electricity consumption is calculated as 0.710 kWh/m², and depending on fuel-oil consumption, $CO_2$ emission was 0.388 kg/m² and SO2 emission was 0.0000388 kg/m². It is lower than the average of the 20 selected European capitals. Depending on the floor structure, the highest electricity consumption is 13,399 kWh/m² in Athens. Depending on fuel-oil consumption, $CO_2$ emissions are calculated as 7.323 kg/m² and 0.0007329 kg/m² in Athens. The lowest electricity consumption was 0.022 kWh/m² in Oslo. Based on fuel-oil consumption, $CO_2$ emissions are calculated as 0.012 kg/m² and $SO_2$ emissions as 0.0000012 kg/m² in Oslo. The average electricity consumption for these capitals is 1.662 kWh/m², $CO_2$ emissions are 0.908 kg/m² and $SO^2$ emissions are 0.0000909 kg/m². Ankaras' electricity consumption is 1.091 kWh/m² and $CO_2$ emission is 0.596 kg/m² and $SO_2$ emission is 0.0000597 kg/m² depending on fuel-oil consumption. It is lower than the average of the 20 selected European capitals. These values are given in Figure 9.

## 4. CONCLUSION

For the thermal conductivity coefficient 0.01–0.07 W/m.K, the minimum value of the insulation thicknesses for the external walls were calculated between 0.004–0.026 m in Skopje and Beograd, and the highest thickness were between 0.048 to 0.337 m in Oslo. The minimum value of the insulation thicknesses for the roof were calculated between 0.013–0.092 m in Beograd, and the highest thickness were between 0.075 to 0.523 m in Oslo. The minimum value of the insulation thicknesses for the floor were calculated between 0.002 to 0.013 m in Athens, and the highest thickness were between 0.063 to 0.443 m in Stockholm. This is among the average values of the 20 European capitals selected in the Ankara for the entire building envelope. The minimum insulation thicknesses are low in South-eastern Europe due to the higher thermal transmittances value of the building envelope. However, in Northern Europe and Scandinavian countries, the minimum value of the insulation to be made is high due to the lower heat transmission coefficients. This shows that these Scandinavian countries give much more importance to energy saving in buildings. In our country, this is at an average level when the selected European countries are taken into account. However, studies are needed to improve energy savings in buildings.

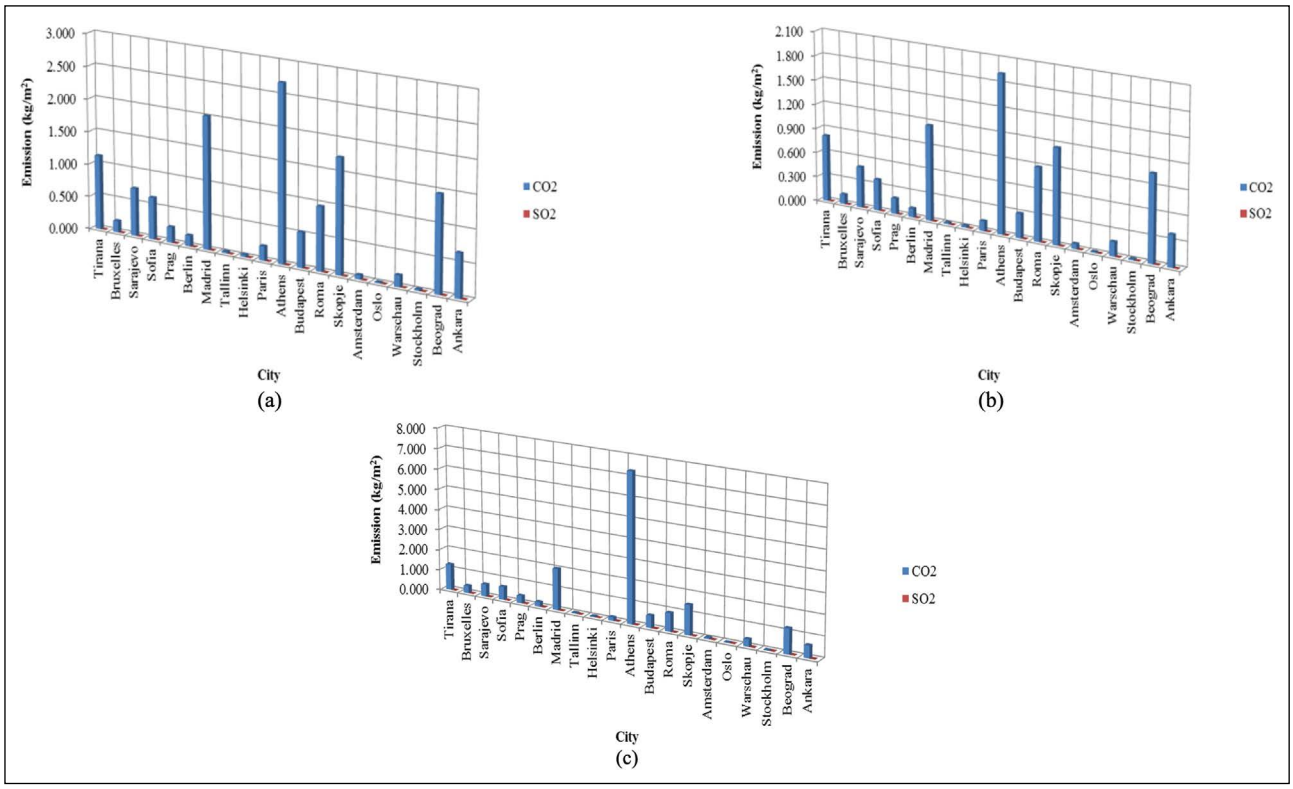


**Figure 9**. $CO_2$ and $SO_2$ emissions for electricity generated by consuming Fuel-oil for cooling period **(a)** external wall area **(b)** roof area **(c)** floor area.

The highest heating degree-day value was determined as 5021 in Oslo, the capital of Norway, and the lowest was 1413 in Athens, the capital of Greece. Requirements and/or recommendations thermal transmittances value for building envelopes are given in the study. Accordingly, it has been calculated that Sarajevo, the capital of Bosnia-Herzegovina, has the highest fuel consumption and the highest $CO_2$ and $SO_2$ emissions for three building components and three fuel types for heating. Although the heating degree-day value of Oslo is high, the thermal transmittances value of the building envelope are kept low, and fuel consumption and therefore emission amounts are low. However, in Sarajevo, the highest fuel consumption and emission amount occurs because an appropriate balance is not established between the heating degree-day and the thermal transmittance value of the building envelope. In Ankara, better results were obtained in terms of fuel consumption and emissions among the 20 selected European capitals. This shows that there is a more balanced situation between the heating degree-day and the building envelope thermal transmittance values. However, when we look at capital cities such as Oslo and Stockholm, it is seen that the thermal transmittance value of the building envelope should be reduced. $CO_2$ and $SO_2$ emissions do not include emissions during the production, transportation, and installation of insulation and materials. It covers only the $CO_2$ and $SO_2$ emissions that will occur as a result of the burning of fuels such as coal, natural gas, and fuel-oil fuels for heating and cooling purposes.

The highest cooling degree-day value was determined as 734 in Athens, the capital of Greece, and the lowest as 13 in Oslo, the capital of Norway. Accordingly, it has been calculated that the highest electricity consumption for three building components and three fuel types for cooling and the highest associated $CO_2$ and $SO^2$ emissions occur in Athens, the capital of Greece. In this case, it is seen that a balance cannot be achieved between both the cooling degree-day value of Athens and the thermal transmittance values of the building envelope. It was determined that the lowest electricity consumption occurred in Oslo, the capital of Norway. It is seen that a balance has been achieved between the cooling degree-day and the thermal transmittance values of the building envelope in Oslo. Ankara, on the other hand, achieved slightly better results than the average values in terms of electricity consumption and emissions among the 20 selected European capitals. This shows that there is a more balanced situation between the cooling degree-day and the building envelope thermal transmittance value. The effect of pollutant emissions such as $CO_2$ and $SO_2$ released into the atmosphere depending on the thermal transmittance value of the building envelope of Ankara, the capital of our country, was investigated and compared with the capitals of other European countries. In this respect, the study has contributed to the literature with a new perspective. The adequacy of the standards in our country on the combustion of the fuels required for the energy needs of

the buildings and the effect of pollutant emissions on the atmosphere has been examined. The important parameter here is the building envelope thermal transmittance values.

As a result, the emissions of fuels to be used when heating and cooling buildings are a very effective parameter in global heating. It is very important to reduce the heat losses of buildings in the formation of these emissions. The most effective way to reduce this is to reduce thermal transmittance values by insulating. With the lower thermal transmittance values of the building envelopes, there will be less heat loss and therefore less emission to the environment. For this purpose, it is considered to carry out different studies on what can be done to reduce building heat losses for future studies. For example, green roof applications, the use of ecological thermal insulation materials, the use of new technological thermal insulation materials with low heat conductivity coefficient, increasing the use of renewable energy such as sun and wind in buildings can be counted.

## DATA AVAILABILITY STATEMENT

The authors confirm that the data that supports the findings of this study are available within the article. Raw data that support the finding of this study are available from the corresponding author, upon reasonable request.

## CONFLICT OF INTEREST

The authors declare that they have no conflict of interest.

## FINANCIAL DISCLOSURE

The authors declared that this study has received no financial support.

## PEER-REVIEW

Externally peer-reviewed.

## REFERENCES

[1] Rosa, M., D., Bianco, V., Scarpa, F., & Tagliafico, L., A. (2015). Historical trends and current state of heating and cooling degree days in Italy. *Energy Conversion and Management*, 90, 323–335. [CrossRef]

[2] Buildings Performance Institute Europe (BPIE). (2011). Europe's buildings under the microscope. https://www.bpie.eu/publication/europes-buildings-under-the-microscope/#

[3] Ramírez-Villegas, R., Eriksson, O., & Olofsson, T. (2016). Assessment of renovation measures for a dwelling area-Impacts on energy efficiency and building certification. *Building and Environment*, 97, 26–33. [CrossRef]

[4] Meng, Q., Mourshed, M., & Wei, S. (2018). going beyond the mean: distributional degree-day base temperatures for building energy analytics using change point quantile regression. *IEEE Access*, 6, 39532-39540. [CrossRef]

[5] Özkan, D., B., & Onan, C. (2011). Optimization of insulation thickness for different glazing areas in buildings for various climatic regions in Turkey. *Applied Energy*, 88, 1331–1342. [CrossRef]

[6] deLlano-Paz, F., Calvo-Silvosa, A., Antelo, S., I., & Soares, I. (2018). Power generation and pollutant emissions in the European Union: a mean-variance model. *Journal of Cleaner Production*, 181, 123–135. [CrossRef]

[7] Çay Y., & Gürel A. E. (2013). Determination of optimum insulation thickness, energy savings, and environmental impact for different climatic regions of Turkey. *Environmental Progress & Sustainable Energy*, 32, 2, 365–372. [CrossRef]

[8] D'Agostino, D., Cuniberti, B., & Bertoldi, P., (2017). Energy consumption and efficiency technology measures in European non-residential buildings. *Energy and Buildings*, 153, 72–86. [CrossRef]

[9] Rodríguez-Soria, B., Domínguez-Hernández, J., M.Pérez-Bella, J., & Coz-Díaz, J., J. (2014). Review of international regulations governing the thermal insulation requirements of residential buildings and the harmonization of envelope energy loss. *Renewable and Sustainable Energy Reviews*, 34, 78–90. [CrossRef]

[10] Christenson, M., Manz, H., & Gyalistras, D. (2006). Climate warming impact on degree-days and building energy demand in Switzerland. *Energy Conversion and Management*, 47, 671–686. [CrossRef]

[11] Rosa, M., D., Bianco, V., Scarpa, F., & Tagliafico, L., A. (2014). Heating and cooling building energy demand evaluation; a simplified model and a modified degree days approach. *Applied Energy*, 128, 217–229. [CrossRef]

[12] Annunziata, E., Frey, M., & Rizzi, F. (2013), Towards nearly zero-energy buildings: the state-of-art of national regulations in Europe. *Energy*, 57, 125-133. [CrossRef]

[13] Meng, Q., & Mourshed, M. (2017). Degree-day based non-domestic building energy analytics and modelling should use building and type specific base temperatures. *Energy and Buildings*, 155, 260–268. [CrossRef]

[14] Al-Hadhrami, L., M. (2013). Comprehensive review of cooling and heating degreedays Characteristics over Kingdom of Saudi Arabia. *Renewable and Sustainable Energy Reviews*, 27, 305–314. [CrossRef]

[15] Akıner, İ., Akıner, M., E., & Tijhuis, W. (2015). A research on environmental rating systems considering building energy performances in different climatic regions of Turkey. *KSCE Journal of Civil Engineering*, 19(5), 1230-1237. [CrossRef]

[16] Pusat, S., & Ekmekci, I. (2016.) A study on degree-day regions of Turkey. *Energy Efficiency*, 9, 525–532. [CrossRef]

[17] Spinoni, J., Vogt, J., V., Barbosa, P., Dosio, A., Mc-

Cormick, N., Bigano, A., & Füssel, H.-M. (2018). Changes of heating and cooling degree-days in Europe from 1981 to 2100. *The International Journal of Climatology*, 38(1), 191–208. [CrossRef]

[18] An, N., Turp, M., T., Akbaş, A., Öztürk, Ö., & Kurnaz, M., L. (2018). Future projections of heating and cooling degree days in a changing climate of Turkey. *Marmara Fen Bilimleri Dergisi*, 3, 227-240.

[19] Altun, M., Akçamete, A., & Akgül, Ç., M. (2020). Dış sıcaklık verisinin bina ısıtma enerji gereksinimine etkisinin ve TS 825 derece-gün bölge kümelendirmesinin geçerliliğinin incelenmesi. *Pamukkale Universitesi Mühendislik Bilimleri Dergisi*, 26(6), 1062–1075.

[20] Çomaklı, K., & Yüksel, B. (2004). Environmental impact of thermal insulation thickness in buildings. *Applied Thermal Engineering*, 24(5-6), 933–940. [CrossRef]

[21] Bolattürk, A. (2008). Optimum insulation thicknesses for building walls with respect to cooling and heating degree-hours in the warmest zone of Turkey. *Building and Environment*, 43(6), 1055–1064. [CrossRef]

[22] Goggins, J., Moran, P., Armstrong, A., & Hajdukiewicz, M. (2016). Lifecycle environmental and economic performance of nearly zeroenergy buildings (NZEB) in Ireland. *Energy and Buildings*, 116, 622–637. [CrossRef]

[23] TS 825, Building Insulation Standard, Turkish Standard, May 2013.

[24] Eurima, the European Insulation Manufacturers Association. (2021, August 16). *U-values in Europe* https://www.eurima.org/u-values-in-europe/

[25] Degree Days. (2021, August 10). *Degree Days Calculated Accurately for Locations Worldwide*. https://www.degreedays.net/

Journal of Sustainable Construction Materials and Technologies
Web page info: https://jscmt.yildiz.edu.tr
DOI: 10.14744/jscmt.2021.04

JSCMT
Journal of Sustainable Construction Materials and Technologies

Research Article

# Assessing the potentials of low impact materials for low energy housing provision in Nigeria

**Oluwafemi K. AKANDE*, Shadrach AKOH, Basil FRANCIS, Solomon ODEKINA, Emmanuel EYIGEGE, Mubarak ABDULSALAM**

*Department of Architecture, Federal University of Technology, Minna Nigeria*

## ARTICLE INFO

*Article history*
Received: 07 December 2021
Accepted: 13 December 2021

**Key words:**
Low impact materials, low energy housing delivery, sandcrete blocks

## ABSTRACT

Due to high energy consumption by building and a resultant increasing cost, it is imperative that a solution be sought after with the aim of achieving low energy housing delivery. This study aimed at assessing the availability, knowledge and importance of low impact building materials in the delivery of low energy housing. Low impact materials suitable for low energy housing delivery and how they are locally obtained in the study areas were identified, occupants' preference in the selection of low impact construction material for housing delivery were examined and the application of low impact material for low energy housing delivery in the study area were determined. The research focused mainly on three states in north central Nigeria namely; Niger, Kogi and FCT Abuja. Quantitative research method was used and weighted mean of responses were ranked in an ordinal manner from 236 respondents. The respondents were not aware of low impact materials as they were only aware and accustomed to using sandcrete blocks and burnt clay bricks. The outcome of the correlation established that the most preferred building material is the sandcrete block, showing a positive relationship with durability and structural performance as the influencers.

**Cite this article as:** Akande OK, Akoh S, Francis B, Odekina S, Eyigege E, Abdulsalam M. Assessing the potentials of low impact materials for low energy housing provision in Nigeria. J Sustain Const Mater Technol 2021;6:4:156–167.

## 1. INTRODUCTION

Due to the continuous increase in urban population in Nigeria, the need and importance of housing in society cannot be overemphasized. According to [1], affordable housing can be achieved through sustainability by incorporating environmentally friendly and community based principles through the choice of construction material. This will go a long way to reduce the negative impact residential buildings can have in the urban environment. All buildings which aim to reduce their impact on the environment could be called, at least, 'lower impact' but the term has come to mean those buildings using largely natural or organic materials. Such as, Compressed Earth Brick (CEB), Hydra Form (Interlocking Bricks), Timber, Clay, Lime, Rammed Earth, Cob, Straw, Hemp, Bamboo and Stone.

***Corresponding author.**
*E-mail address: fkakande225@googlemail.com

Published by Yıldız Technical University Press, İstanbul, Turkey
Copyright 2021, Yıldız Technical University. This is an open access article under the CC BY-NC license (http://creativecommons.org/licenses/by-nc/4.0/).


**Figure 1**. **(a)** stabilized interlocking bricks, **(b)** straw (thatch), **(c)** Adobe, **(d)** Bamboo. Source: [7, 8].

Adequate housing delivery has been the target of many third world countries including Nigeria. The housing deficit of Nigeria falls at the range of 14 million housing units [2] and 17 million housing units. In a third world country like Nigeria, low energy and affordable housing have always been a far cry for an average Nigerian, despite all the strategies formulated by government to overcome shortage of houses by creating low energy and affordable housing scheme [3]. According to [4] it was revealed that 60% of the total housing expenditure goes for the purchase of building materials. Also one of the major challenges to poor housing delivery is high cost of building material, which is as a result of continuous importation of building and construction material from foreign countries.

This paper focused on assessing the availability, knowledge and importance of low impact building materials in the delivery of low energy housing, by identifying low impact materials suitable for low energy housing delivery and how they are locally obtained. It examined occupants' preference in the selection of low impact construction materials for housing delivery and determined the application of low impact materials for low energy housing delivery within three north central states namely; Niger State, Kogi State and FCT Abuja.

## 2. LITERATURE REVIEW

### 2.1 Provision of Low Energy Housing in Nigeria

According to [5] a low-energy new building is a building that is designed to achieve or to come close to the passive house standard and one where passive house or similar quality processes are followed to ensure that design energy use is realised in practice without compromising occupant comfort and satisfaction. In order to realise sustainable housing provision, the housing needs of the Nigerian population have to be put into proper focus and coordinated programmes. This need to be thoroughly worked out, with due consideration given to low impact materials available in Nigeria.

### 2.2 Low Impact Material in Nigeria

The introduction of modern technologies such as the concrete blocks and slabs during the industrial periods had relegated traditional components and methods to the background. Meanwhile, this new material did not provide same comfort as the traditional and locally sourced building material. Native dwellers rather have settled for the high taste of fashion, modernity, expressed of advancement and show of affluence and status in place of the sustainability that local and low impact material have to offer. Recently, more attention is been given to building material that can be very affordable and still deliver the same modern needs [6]. Hence, it is important to pigeonhole materials into five main groupings namely.

- Short term renewable origin (timber, wool, straw)
- Extracted or mined (earth, sand and gravel)
- Extracted and further processed (lime, cement, plaster, slate, stone, brick)
- Extracted and highly processed (steel, glass and plastics)
- Recycled or reclaimed (reused timber, brick, aggregate, steel, glass, insulation)

Some common low-impact building materials that can be sourced locally in Nigeria are shown in Figure 1 above.

### 2.3 Energy Use in Buildings

To achieve a material where the energy needed in the dynamics of that material is low, one needs to understand how this energy is derived in its various components. A building's lifecycle energy comprises its embodied and operational energy [9–14]. Numerous authors such as [13–15] have categorized embodied energy of buildings into three components namely; Initial embodied energy (IEE), Recurrent embodied energy (REE), Demolition embodied energy (DEE).

#### *2.3.1 Initial Embodied Energy (IEE)*

This is the energy consumed in the production process of a product, from the extraction of raw materials and processing of natural resources to the manufacturing and transport of products to building construction sites. It also includes the energy that is directly associated with the construction activities. IEE is thus all the energy that is consumed in the pre-use phase of the building's lifecycle [15].

#### *2.3.2 Recurrent Embodied Energy (REE)*

This refers to the energy required to maintain, repair, and/or refurbish the buildings during their service life. REE is a function of how a building is used by its occupants, the maintenance demands of the occupants, the service life of the building, and the life span and quality of the materials and components [13].

#### *2.3.3 Demolition Embodied Energy (DEE)*

This is the energy consumed to destroy the building at the end of its lifecycle, recycle and re-use some components, and dispose of others by transporting the debris and waste to landfills or incinerators [14].

### 2.4 Operational Energy in Residential Buildings

Among the parameters for assessing sustainable buildings is operation energy. It is described as the energy used in keeping the indoor environment within the acceptable range and other human activities [16]. Operational energy can vary depending on the level of luxury essential to occupants, the predominant climatic environments as well as the operational plan [17]. Meanwhile, the energy expended by the occupants is referred to as delivered energy [18], while the energy embodied in resources found in nature: chemical energy embodied in fossil fuels (coal, oil, and natural gas) is known as primary energy.

### 2.5 Embodied Carbon Emission

According to [19] 8.1 Gt of carbon dioxides is added to the global system as a result of high impact buildings. The global system experiences a harsh impact as a result of high emission of carbon dioxide [20]. The Durban, South Africa, International Union of Architect (UIA) conference held in 2014 by the Architecture profession, jointly projected 2050 as year from which building will experience zero carbon emission. Developed countries are known to generate the greatest emission, however the greatest impact is felt in developing countries. $CO_2$, hydrocarbons, Nitrogen Oxides ($NO_x$) Sulphur dioxide ($SO_2$), Carbon-monoxide (CO) are known as industrial flue gas responsible for greenhouse effect [21]. Energy used during construction and utilization process is largely responsible for $CO_2$ in building [20]. Energy utilization and $CO_2$ emission to our natural environment can be largely traced to procurement and operation of majorly residential building. From the analysis made by [22] approximately 40% global energy utilization, 60% global electricity usage and 30% global GHG emission are traced to buildings.

## 3. RESEARCH METHODOLOGY

### 3.1 The Research Method

The research method adopted in this research process is quantitative research method with comparative research approach. According to [23] comparative analysis is conducted mainly to explain and gain a better understanding of the causal processes involved in the creation of an event, feature or relationship usually by bringing together variations in the explanatory variable or variables.

### 3.2 The Survey Design

Primary data was collected with the aid of a structured questionnaire as the research instrument to determine users' preference as regards the use of low impact materials. To achieve the objectives of this study, a structured questionnaire comprising range of skills established in the literature was designed to determine users' preference in relation to the application of low impact materials. The questionnaire was piloted several times in order to validate and improve the survey.

### 3.3 The Instrument

The survey questions were crafted in simple and straightforward English that is easy to understand to prevent the participants from giving up midway through the survey. It uses two types of closed-ended questions, namely the Checklist and Likert item/scale. The predetermined replies were made comprehensive to capture most materials shared by previous researchers who had done similar study.

### 3.4 Sampling

The target population of the study are general occupants of residential buildings and professionals of the built environment. The sample for the survey span across three regions of North Central Nigeria; namely, Niger State, Kogi State and FCT Abuja. For Niger State the regions of Bosso and Gidan Kwano were surveyed in Bosso Local Government Area, for Kogi state, Lokoja was surveyed and for FCT Abuja, Bwari, Wuse, Amac, Asokoro, Jahi and Garki areas were surveyed. The survey questionnaire was distributed using a convenience sampling method to reach both the professionals and non-professionals in the building industry. Several avenues were employed to send out questionnaires such as emails, personal messages and others posted on social media channels. The respondents were encouraged to share the questionnaires among their network so as to enable the questionnaire to reach beyond the immediate social and professional network of the respondents. This helped to increase the number of respondents as well as enhanced the external validity of the study. This is in accordance with survey strategies employed by [24].

### 3.5 Data Analysis

To achieve the set objectives, comparative analysis with the use of ordinal scale for ranking based on weighted mean and weighted scores and a bivariate correlation were used to analyze the responses gotten from the survey. Descriptive analysis was used to summarize respondents' demographic data while inferential statistics were used to achieve the problems itemized in the objectives.

#### *3.5.1 Validity and Reliability*

Prior to the analyses, a reliability test using Cronbach alpha was undertaken as obtained from SPSS 25. Content and construct validity were used to obtain the reliability and validity of the measurement items used in the study. According to [25] content validity is the extent to which a scale measures a concept that it is intended to measure. Construct validity shows how well a test or experiment

measures up to its claims [26]. For multiple scales, Cronbach alpha measures internal consistency and indicates the consistency of responses [27]. The Cronbach alpha based standardized items obtained is 0.75 (Table 1) which means that the data is reliable.

### *3.5.2 Descriptive Statistics*

Descriptive statistics was used to establish occupants' demographics in form of tables as well as the availability of low impact materials in the study area. According to [28] descriptive statistics is the process that analyzes quantitatively summarized data. Specifically, the weighted scores and the weighted mean of each statement were computed and ranked using the ordinal scale (Table 2). Ordinal ranking makes use of ordinal numbers such as 1,2,3,4, to rank a set of items based on a casual relation in an ascending or descending order.

### *3.5.3 Inferential Statistics*

Inferential statistics was employed to make inferences about a population based on data that was gathered from the sample of the study. Correlation was used to derive inferences based on the relationship between the variables from the sample population. The correlation coefficient in this study was achieved using SPSS 25.

## 4. RESULTS, FINDINGS AND DISCUSSION

A total of 236 respondents were recoded from the 250 questionnaires administered. This shows a response rate of 94.4% [30]. Had a 77% response rate in a study on the built environment. Based on gender, males have a greater outcome with a frequency of 163 respondents as against females with 73 respondents as shown in Table 3. The increase in the male populace is as the result of the dominance of males in the building industry.

According to Table 4 and Table 5, self-employed, regular salaried and students came up with the highest frequencies having a combined percentage of 90.9%, having 79.2% of the respondents' income which falls below N100,000. This is barely enough to build a decent house with the current economic situation.

The Nigerian Government places the minimum wage of every worker at N30, 000 which is very low yet 26.7% of the respondents earn below N20, 000. This agrees with the assessment of World Bank which generally places Nigeria at the low middle class income level as of 2020.

Considering the nature of the study, it is important to validate the understanding of the concept of low energy material through the level of education. 87.7% of the respondents have post-secondary qualification which means that data obtained is from a well-educated sampled populace (Table 6).

Due to the nature of this research, some aspects were covered strictly by professionals. Table 7 shows the distribu-

**Table 1.** Summary of the reliability statistics for the questionnaire survey

| Cronbach's Alpha | Cronbach's Alpha based on standardized items | Number of questions | Number of Items |
|---|---|---|---|
| 0.708 | 0.750 | 17 | 68 |

**Table 2.** Interpretation of Mean Scores for Individual Statements (adapted from [29] p.245)

| Range of mean | Quantitative description | Qualitative description |
|---|---|---|
| 4.21 to 5.00 | 5 | Strongly agree |
| 3.41 to 4.20 | 4 | Agree |
| 2.61 to 3.40 | 3 | Neutral |
| 1.81 to 2.60 | 2 | Disagree |
| 1 to 1.80 | 1 | Strongly disagree |

**Table 3.** Distribution of respondents based on gender

| Gender | Frequency | Percentage |
|---|---|---|
| Male | 163 | 69.1 |
| Female | 73 | 30.9 |
| Total | 236 | 100 |

**Table 4.** Distribution of respondents based on occupation

| Occupation | Frequency | Percentage |
|---|---|---|
| Self-employed/business | 48 | 20.3 |
| Regular salaried (private) | 65 | 27.5 |
| Regular salaried (government) | 40 | 16.9 |
| Casual/daily wage worker | 07 | 3.0 |
| Student | 63 | 26.7 |
| Housewife | 01 | 0.4 |
| Unemployment | 08 | 3.4 |
| Retired | 04 | 1.7 |
| Total | 236 | 100 |

**Table 5.** Distribution of respondents based on income

| Income | Frequency | Percentage |
|---|---|---|
| Below ₦20,000 | 63 | 26.7 |
| ₦20,000–₦50,000 | 42 | 17.8 |
| ₦51,000–₦80,000 | 45 | 19.1 |
| ₦81,000–₦100,000 | 37 | 15.7 |
| N100,000 and above | 49 | 20.8 |
| Total | 236 | 100 |

**Table 6.** Distribution of respondents based on education level

| Educational level | Frequency | Percentage |
|---|---|---|
| Qur'anic education | 04 | 1.7 |
| Primary education | 02 | 0.8 |
| Secondary school | 23 | 9.7 |
| Post-secondary qualification | 157 | 66.5 |
| Post-graduate qualification | 50 | 21.2 |
| Total | 236 | 100 |

**Table 7.** Distribution of respondents that are built environment professionals

| Built environmental professional | Frequency | Percentage |
|---|---|---|
| Architect | 27 | 27.0 |
| Quantity surveyor | 16 | 16.0 |
| Town planner | 13 | 13.0 |
| Builder | 14 | 14.0 |
| Developer | 5 | 5.0 |
| Estate Valuer/surveyor | 12 | 12.0 |
| Civil Engineer | 5 | 5.0 |
| Land surveyor | 3 | 3.0 |
| Project manager | 5 | 5.0 |
| Total | 100 | 100 |

**Table 8.** Years of professional practice of professional respondents

| Professional practice (years) | Frequency | Percentage |
|---|---|---|
| 0–5 | 50 | 50 |
| 6–10 | 27 | 27 |
| 11–15 | 11 | 11 |
| 16–20 | 04 | 04 |
| Above 20 | 08 | 08 |
| Total | 100 | 100 |

tion of 100 professional respondents into the various fields of the built environment with architects (27%) been the highest as they are the ones closest to the clients to influence decisions as regards choice of materials as well as they are the original designers of the houses.

The majority of the professionals have between 0-5 years (50%) which shows a young influx of professionals with 12% at 16 and above years (Table 8). This distribution creates a balance of older experience as well as a young workforce who can implement the adoption of low impact materials for low energy housing delivery.

The result from Table 11 shows the knowledge of how available low impact materials are in the study area. However, the respondents are majorly conversant with sandcrete block which ranks 1st with a weighted mean of 4.64. This agrees with similar studies conducted in Ethiopia by [31] with cement been the widely known and used material. It

**Table 9.** Professional membership of professional respondents

| Professional body membership | Frequency | Percentage |
|---|---|---|
| Nil | 22 | 22 |
| NIA (Nigerian Institute of Architects) | 23 | 23 |
| NIOB (Nigerian Institute of Builders) | 11 | 11 |
| NIQS (Nigerian Institute of quantity surveyors) | 12 | 12 |
| NIS (Nigerian Institute of Surveyors) | 02 | 02 |
| NIESV (Nigerian Institute of Estate Surveyors and valuers) | 11 | 11 |
| NICE (Nigerian Institute of civil Engineers) | 06 | 06 |
| CIPMN(Chartered Institute of Project Managers of Nigeria) | 04 | 04 |
| NITP (Nigerian Institute of Town Planners) | 09 | 09 |
| Total | 100 | 100 |

**Table 10.** Materials used by the respondents in building construction

| Materials used or specified | Frequency | Percentage used | Rank |
|---|---|---|---|
| Straw (thatch from grasses, rice husk) | 70 | 29.7 | 6th |
| Mud bricks | 105 | 44.5 | 3rd |
| Stone | 88 | 37.3 | 4th |
| Bamboo | 20 | 8.5 | 8th |
| Timber | 168 | 71.2 | 2nd |
| Interlocking bricks | 41 | 17.4 | 7th |
| Burnt clay bricks | 80 | 33.9 | 5th |
| Sand crete blocks | 218 | 92.4 | 1st |

further showed that the low impact materials such as mud-bricks, straw, interlocking bricks and bamboo rank 4th, 6th, 7th and 8th respectively are not well known in comparison with sandcrete blocks. Stone and timber rank 2nd and 3rd and respectively [32]. Stated that bamboo is commonly found in the rain forests regions in Nigeria which agrees to it ranking as the least known material in the north central region. Sandcrete block ranked 1st as the most used material from Tables 10 and 12 respectively. This shows that these areas use high impact materials more due to the high content of cement in the sandcrete blocks [22]. Observed from findings that the cement and steel in the usage of sandcrete block alongside with reinforcements amount for 44% from cradle-to-grave energy and 57% of the material energy. This places sandcrete block on a high energy profile. However, mud bricks, timber, stone, bamboo, straw and interlocking bricks which ranks lower compared to sandcrete blocks from both tables in terms of usage have lower embodied energy and embodied carbon emission. According to ICE,

**Table 11.** Knowledge of the availability of low impact materials in the study

| Low impact materials | Weighted score | Weighted mean | Decision rule | Rank |
|---|---|---|---|---|
| Straw (thatch from grasses) | 818 | 3.47 | Quite knowledgeable | 6th |
| Mud bricks | 945 | 4.00 | Quite knowledgeable | 4th |
| Stone | 979 | 4.15 | Quite knowledgeable | 2nd |
| Bamboo | 699 | 2.96 | Barely knowledgeable | 8th |
| Timber | 971 | 4.11 | Quite knowledgeable | 3rd |
| Interlocking bricks | 750 | 3.18 | Barely knowledgeable | 7th |
| Burnt clay bricks | 931 | 3.94 | Quite knowledgeable | 5th |
| Sand crete blocks | 1095 | 4.64 | Highly knowledgeable | 1st |

**Table 12.** Level of usage of the mentioned materials as a walling material

| Low impact materials | Weighted score | Weighted mean | Decision rule | Rank |
|---|---|---|---|---|
| Straw (thatch from grasses) | 543 | 2.30 | Not used | 8th |
| Mud bricks | 793 | 3.36 | Barely used | 4th |
| Stone | 785 | 3.32 | Barely used | 5th |
| Bamboo | 581 | 2.46 | Not used | 7th |
| Timber | 837 | 3.55 | Often used | 3rd |
| Interlocking bricks | 655 | 2.78 | Barely used | 6th |
| Burnt clay bricks | 869 | 3.68 | Often used | 2nd |
| Sand crete blocks | 1121 | 4.75 | Most used | 1st |

**Table 13.** Locations where materials can be obtained

| Material | Source in the study area |
|---|---|
| Straw (thatch from grasses) | Dried grasses and husks from rice farming, typical to FCT Abuja and Niger State |
| Mud bricks | Readily available in local areas of the study areas which entails digging the earth |
| Stone | Quarrying activities are seen in locations like Dutsen Kura, Maikunkele all in Niger State. |
| Bamboo | Pocket of bamboo clumps is found in Niger, Taraba, Plateau and Abuja (Atanda, 2015) |
| Timber | Timber is scarcely found in Abuja and Niger state been in the Sudan Savannah, but can be obtained in Kogi State as it is a derived Savanah (a transition from rain forest to savannah) |
| Interlocking bricks | It is not widely used as its practice in Nigeria is still at the early stage. |
| Burnt clay bricks | Produced in Niger state along Minna- paikoro road chanchaga. |
| Sand crete blocks | Readily available in all block industries in the towns of the study area |

**Table 14.** Respondents preferred choice material for construction

| Low impact materials | Weighted score | Weighted mean | Decision rule | Rank |
|---|---|---|---|---|
| Straw (thatch from grasses) | 448 | 1.90 | Not preferred | 8th |
| Mud bricks | 569 | 2.41 | Not preferred | 7th |
| Stone | 724 | 3.07 | Neutral | 5th |
| Bamboo | 612 | 2.59 | Not preferred | 6th |
| Timber | 837 | 3.55 | Preferred | 3rd |
| Interlocking bricks | 765 | 3.24 | Neutral | 4th |
| Burnt clay bricks | 880 | 3.73 | Preferred | 2nd |
| Sand crete blocks | 965 | 4.09 | Preferred | 1st |

steel and cement have high carbon emission of 2.7 $CO_2$/kg and 1.0 $CO_2$/kg. Timber, bricks, straw and stone on the other hand have carbon emissions of 0.3 $CO_2$/kg, 0.2 $CO_2$/kg, 0.1 $CO_2$/kg and 0.1 $CO_2$/kg respectively.

**Table 15.** Factors that influenced respondents' choice of preferred materials

| Preference | Frequency | Percentage | Rank |
|---|---|---|---|
| Buildability | 38 | 16.1 | 4th |
| Aesthetics | 36 | 15.3 | 5th |
| Structural performance | 44 | 18.6 | 2nd |
| Sustainability | 07 | 3.0 | 7th |
| Reduced total cost of building | 42 | 17.8 | 3rd |
| Durability | 52 | 22.0 | 1st |
| Readily available | 09 | 3.8 | 6th |
| Accessibility | 07 | 3.0 | 7th |
| Lack of knowledge about other materials | 01 | 0.4 | 9th |

**Table 16.** Factors that influenced respondents' choice of preferred materials

| Low impact materials | WS | WM | Decision rule | Rank |
|---|---|---|---|---|
| Straw is easy to maintain | 201 | 2.09 | Disagree | 8th |
| Mud bricks is easy to maintain once plastered | 289 | 3.01 | Neutral | 6th |
| Stone is the easiest to maintain | 322 | 3.35 | Neutral | 4th |
| Bamboo is does not need added treatment for its maintenance | 270 | 2.81 | Neutral | 7th |
| Timber can only be maintained if treated against pest | 351 | 3.66 | Agree | 2nd |
| Interlocking bricks can be easily maintained if the technical skill in construction is high | 323 | 3.36 | Neutral | 3rd |
| Burnt clay bricks can be maintained easily just the way it is | 321 | 3.34 | Neutral | 5th |
| Sandcrete blocks can be easily maintained. | 412 | 4.29 | Strongly agree | 1st |

Occupants preference as seen from Table 14 shows that sandcrete blocks, burnt clay bricks and timber are the preferred materials for building construction with a ranking of 1st, 2nd and 3rd respectively. This finding agrees with [33], who stated that the most common buildings both residential and public in urban centres in Nigeria are built typical with sandcrete blocks, concrete and timber. This further buttresses the fact that the occupants most preferred material has a negative impact to the environment and a need to switch to low impact materials. Low impact materials such as mud bricks, bamboo and straw were not preferred at all and they ranked 6th, 7th and 8th respectively. The occupants were neutral to interlocking blocks as well as stone which ranked 4th and 5th respectively.

Figures from Table 15 indicates that the respondents considered factors that influenced firmness ahead of aesthetics when choosing their materials. Durability and structural performance were the most influencers ranking 1st and 2nd respectively. Reduced total cost of building came 3rd while buildability came 4th, which entails that the respondents do not mind spending a little more on the materials as long as durability, structural performance and buildability are seen in that material. This is the reason why sandcrete blocks and burnt clay bricks were the most preferred materials. Aesthetics came 5th as well as sustainability coming 7th. This shows the level of knowledge that can be found amongst the respondents as regards sustainability and low energy materials. However, the respondents were neutral to interlocking blocks (hydraforms) also known as CSEB (Compressed Stabilized Earth Blocks) and did not prefer bamboo. These two materials can achieve durability, structural performance, buildability factors as well as synergizing aesthetics and sustainability for low energy housing delivery [33]. Stated that hydraforms are easy to build, less expensive [34]. In a test on Hydraform blocks came up with a compressive strength value as high as 4.6 MPa which was higher than the recommended 1 MPa for masonry units for all the blocks in Mettu, Nopa and Hurumu regions in Ethiopia [35]. Established that bamboo is light weight, easy to transport [37]; stated that bamboo has a compressive strength of 23.8 MPa at the top for untreated ones and 36.60 MPa at the top for treated ones. Hydraform blocks and Bamboo are great alternatives to the sandcrete blocks which are as well durable and also have a good compressive strength for residential buildings.

The cost and energy expended in maintaining a building falls under recurrent embodied energy. This influences the total embodied energy of the building. It can be seen from the respondents' responses in Table 16 that sandcrete blocks can be easily maintained as it is the most used and widely known. The neutral response to bamboo, hydraform, bricks and stone shows lack of adequate knowledge of the maintenance culture of materials. This factor influenced the reason why sustainability ranked 7th in the influencers

**Table 17.** Correlation between factors that influenced respondents' choice of preferred materials and the preferred

| Variables | Buildability | Aesthetics | Structural perform. | Sustainability | Reduced total cost of bld. | Durability | Lack of knowl. | Readily avail. | Accessibility |
|---|---|---|---|---|---|---|---|---|---|
| Straw | 0.056 | 0.043 | 0.045 | -0.099 | 0.198*** | -0.237*** | -0.063 | -0.054 | 0.000 |
| Significance | 0.392 | 0.512 | 0.493 | 0.131 | 0.002 | 0.000 | 0.337 | 0.405 | 0.998 |
| Mudbricks | 0.097 | 0.079 | -0.095 | -0.020 | 0.159** | -0.152** | 0.039 | -0.157 | 0.031 |
| Significance | 0.136 | 0.224 | 0.148 | 0.765 | 0.014 | 0.020 | 0.553 | 0.016 | 0.633 |
| Stone | -0.041 | -0.067 | 0.114* | 0.029 | -0.185*** | 0.062 | 0.105 | 0.096 | 0.056 |
| Significance | 0.532 | 0.308 | 0.080 | 0.662 | 0.004 | 0.345 | 0.109 | 0.140 | 0.388 |
| Bamboo | -0.019 | 0.217*** | -0.082 | -0.071 | 0.359*** | -0.344*** | -0.075 | -0.058 | -0.035 |
| Significance | 0.770 | 0.001 | 0.210 | 0.278 | 0.000 | 0.000 | 0.251 | 0.376 | 0.590 |
| Timber | 0.009 | 0.165** | -0.221 | -0.013 | 0.199*** | -0.078 | -0.050 | -0.068 | -0.013 |
| Significance | 0.885 | 0.011 | 0.001 | 0.845 | 0.002 | 0.231 | 0.445 | 0.301 | 0.845 |
| Interlocking | -0.024 | -0.008 | 0.164** | 0.098 | -0.040 | -0.164** | -0.064 | -0.045 | 0.160** |
| Significance | 0.709 | 0.907 | 0.012 | 0.134 | 0.546 | 0.011 | 0.326 | 0.494 | 0.014 |
| Burnt clay | -0.052 | -0.022 | 0.146** | 0.077 | -0.002 | -0.139** | -0.093 | -0.012 | 0.137** |
| Significance | 0.429 | 0.742 | 0.025 | 0.240 | 0.978 | 0.033 | 0.154 | 0.849 | 0.035 |
| Sandcrete | -0.005 | -0.066 | 0.031 | 0.023 | -0.330*** | 0.255*** | 0.067 | 0.115* | 0.023 |
| Significance | 0.936 | 0.315 | 0.640 | 0.727 | 0.000 | 0.000 | 0.307 | 0.079 | 0.727 |

**Table 18.** Importance of low impact materials

| Potentials/importance | WS | WM | Decision rule | Rank |
|---|---|---|---|---|
| A reduced total embodied energy of the building | 403 | 4.20 | Agree | 1st |
| A reduced total embodied carbon emission | 398 | 4.15 | Agree | 2nd |
| Reduces the cost of construction | 395 | 4.11 | Agree | 3rd |
| Reduces the cost incurred in day to day heating and cooling processes.(operational energy) | 390 | 4.06 | Agree | 4th |
| Reduces environmental pollution through reuse of materials | 369 | 3.84 | Agree | 5th |

of preferred materials. Bamboo needs treatment which does not only improves its life span as a result of improved maintenance, it increases it compressive strength [36]. Mud bricks are easy to maintain once plastered. However, [37], iterated that steel moulded bricks bounded with mud plaster and plastered with sandcrete, gives the least amount of cracks compared to those moulded with wooden moulds.

From the table of correlation in Table 17, buttresses the fact that the users' preferred choice of building material been sandcrete have a relationship with topped ranked influencers been durability and structural performance. An alpha level of coefficient of correlation (r) for relationship within the bivariate data is placed at 0.01 and the level of significance (p) is placed at 0.05. There exists a positive relationship between sandcrete block and durability based with a r value of 0.225. This relationship is statistically significant. It means that the major reason for choosing sandcrete block is due to its durability, with high cost been the real cost. Reduced total cost showed a negative relationship with sandcrete blocks with a r value of -0.330. This shows that there is a relationship between cost and sandcrete blocks but a high cost is needed to achieve it.

Burnt clay bricks ranked 2nd from the weighted mean and it showed a positive relationship with structural performance (r=0.146) and a negative relationship with durability (r=-0.139) with both showing statistical significance. Both burnt clay bricks and sandcrete block have a higher impact compared to bamboo and hydraform. Bamboo showed a positive relationship with aesthetics (r=0.217) and reduced total building cost (r=0.359), both outcomes are statistically significant. It showed a relationship between durability but a negative one. This means that the bamboo is a material that is durable, cost effective and aesthetically pleasing. Hydraform showed a positive relationship with structural performance (r=0.164) and accessibility (r=0.160). This means structurally it is ok. It is easily accessible as it is produced on site. It however showed a negative relationship with durability (r=-0.139). The correlation that bamboo and hydraform has shown with structural performance and durability shows that it can serve as an adequate alternative to sandcrete blocks and burnt clay which have a higher impact on the environment.

When the importance and advantages of low energy materials are established, application becomes possible as it will be

**Table 19.** Respondent's agreement to the strategies of infusing low impact materials to building

| Statements | WS | WM | Decision rule | Rank |
|---|---|---|---|---|
| Public awareness as regards the benefits of these materials | 393 | 4.09 | Agree | 3rd |
| Training of specialists in the construction of low energy materials | 422 | 4.40 | Strongly agree | 1st |
| Creating and implementing policies that will improve its usage | 413 | 4.30 | Strongly agree | 2nd |
| Creating a maximum standard for embodied energy to a range of housing types | 386 | 4.02 | Agree | 4th |

Number of professional respondents=96; WS: Weighted score; WM: Weighted mean.

**Table 20.** Respondent's agreement to barriers preventing the integration of low energy materials

| Statements | WS | WM | Decision rule | Rank |
|---|---|---|---|---|
| Lack of awareness by the users | 389 | 4.05 | Agree | 1st |
| Mindset of seeing low energy materials as an indicator of been poor | 361 | 3.76 | Agree | 5th |
| Occupants low income class | 330 | 3.44 | Agree | 7th |
| The poor outlook of the finished product | 351 | 3.67 | Agree | 6th |
| The life span of the material | 368 | 3.83 | Agree | 4th |
| Clients preferred choice as regards the materials | 372 | 3.88 | Agree | 2nd |
| Lack of database on the impact placed by high impact materials on the environment | 372 | 3.88 | Agree | 2nd |

Number of respondents=96; WS: Weighted score; WM: Weighted mean.

**Table 21.** Respondent's level of agreement to strategies for improving the awareness of low energy materials

| Statements | WS | WM | Decision rule | Rank |
|---|---|---|---|---|
| Public enlightenment on the impact of high energy materials. | 411 | 4.28 | Strongly agree | 3rd |
| A constant use of these materials by the building professionals and developers. | 419 | 4.36 | Strongly agree | 2nd |
| Societal Enlightenment as against the mindset that low impact materials is for the poor who cannot afford expensive high energy materials. | 408 | 4.25 | Strongly agree | 4th |
| Integrating the use of low impact materials in the curriculum of Architecture Engineering and Construction (AEC) education | 424 | 4.42 | Strongly agree | 1st |

Number of professional respondents=96; WS: Weighted score; WM: Weighted mean.

easily accepted. Table 18 showed the professional respondents' response with regards to level of agreement with respect to importance of low energy materials. All statements were agreed to which shows that the respondents are well aware of the benefits of these materials. [31] agrees that low impact materials reduce total embodied energy and total embodied carbon emission and reduces environmental pollution through reuse and recycling of materials. [38] agrees that low impact materials result in sustainable homes which is relevant to reduce cost of construction as well as reduce operational energy.

Table 19 shows agreement by the respondents to all the strategies that will infuse low energy materials into the building industry. Training specialists in the construction of low energy materials ranks top as agreed by [31]. This means that the professionals have interest in sustainable construction practices. Policies should be created and implemented by professional bodies backed with the power of the government [39]. Agrees as they suggested government creates a conducive environment that will improve the usage of low energy materials. The public are not left out and as such they should be an enlightenment towards the benefits and use of low energy materials.

Barriers inhibit the progress of any phenomena in a given space. As advantageous as low energy materials are, their use can be hindered. Table 20 shows all possible statements that can prevent the adoption of low energy materials fully for housing delivery. Topping the list is lack of awareness by the end users. These are the clients and they need to be aware of the existence of these materials. Clients preferred choice as established in objective two shows that durability is their prime focus. It also shows that though occupant's income level inhibits the integration of low energy materials, it is not a simile strong inhibitor as long as the client is knowledgeable and satisfied with the output.

As established from Table 20, lack of awareness is the strongest inhibitor to the integration of low energy materials in housing delivery. Table 21 shows strategies to improve awareness. Adding the knowledge of low energy materials to the curriculum of Architecture Engineering and Construction (AEC) education ranks first [39]. Agrees to this

and a review of the AEC curriculum be done. The professionals and developers can help by constantly using low energy materials in construction while ensuring that the public understands the impact high energy materials have on the society. Societal enlightenment against stigma attached to the use of low energy materials has been poor ranked 4th but still has a significant impact.

## 5. RECOMMENDATIONS AND CONCLUSION

### 5.1 Recommendations

From the study, the following recommendations will be of great help which are categorized. Strategies that can result in the integration of low impact materials for low energy housing delivery include;

- Public awareness as regards the benefits of these materials
- Training of specialists in the construction and use of low energy materials
- Creating and implementing policies that will improve its usage by professional bodies and the government
- Creating a maximum standard for embodied energy to a range of housing types.
- The outlook of the finished product should be improved upon to look aesthetically pleasing
- The compressive strength of the materials should be improved so as to improve durability, structural performance and life span of the material.
- The public should be enlightened on maintenance policies and strategies that will make the use of these materials sustainable
- High impact materials should be reused or recycled to reduce the embodied carbon emission as well as embodied energy emitted.

Strategies to improving awareness amongst the masses of the existence and application of low impact materials include;

- Public enlightenment on the impact of high energy materials.
- A constant use of these materials by the building professionals and developers.
- Societal enlightenment as against the mindset that low impact materials is for the poor who cannot afford expensive high energy materials.
- Integrating the use of low impact materials in the curriculum of Architecture Engineering and Construction (AEC) education.

### 5.2 CONCLUSION

The aim of this study focused on assessing the availability, knowledge and importance of low impact building materials in the delivery of low energy housing. In achieving this aim, a threefold objective was set each tied to a research question. The first objective identified low impact materials suitable for low energy housing delivery and how they are locally obtained in the study areas. It was discovered that the occupants in the study area are more conversant with the use of sandcrete blocks and timber in their construction practices. The second objective focused on examining the occupants' preference in the selection of low impact construction materials for housing delivery. Nine variables were considered as influencers in the choice of the most preferred material. Sandcrete blocks and burnt clay bricks came out as the most preferred material with durability and structural performance been the major influencers. Although some of the unknown materials like bamboo and hydraform with good durability and structural performance were not chosen because of lack of knowledge. The third objective focused on determining the application of low impact material for low energy housing delivery in the study areas. The importance of low impact materials was established with strategies that can integrate low impact materials into low energy housing delivery as well as strategies that can improve the awareness of these materials established. Inhibitors to the application of low impact materials were also discovered. Conclusively, low impact materials have the potential to reduce the negative impact on the environment caused by high impact materials as well reducing the embodied energy of the building and operational energy. This is a sustainable construction practice and as such its knowledge and importance should be widely known as well as its application.

## DATA AVAILABILITY STATEMENT

The authors confirm that the data that supports the findings of this study are available within the article. Raw data that support the finding of this study are available from the corresponding author, upon reasonable request.

## CONFLICT OF INTEREST

The authors declare that they have no conflict of interest.

## FINANCIAL DISCLOSURE

The authors declared that this study has received no financial support.

## PEER-REVIEW

Externally peer-reviewed.

## REFERENCES

[1] Gilkinson, N., & Sexton, M. (2007). Delivering Sustainable Homes; meeting requirement: a research agenda. 35th IAHS World Congress on Housing Science, (pp. 4-7). Melbourne, Australia.

[2] Onyike, J. (2007). An assessment of affordability of housing by public servants in Owerri, Nigeria, Journal of Land Use and Development Studies. 8, [Online ahead of print]

[3] Makinde, O.O. (2014). Housing delivery system, need and demand. *Environmental Development Sustainability*, 49–69. [CrossRef]

[4] Yomi, M.A. (2012). Sustainable housing provision: preference for the use of interlocking mansory in housing delivery in Nigeria. *Architecture Research*, 81–86. [CrossRef]

[5] Bruce, T. (2012). *Delivering a low-energy building; making quality a commonplace*. Norwich, UK: Build With Care. Low Carbon Construction, Innovation & Autumn 2010.

[6] Dayaratne, R. (2011). Reinventing traditional technologies for sustainability: contemporary earth architecture of Sri. *Journal of Green Building*, 22–23. [CrossRef]

[7] Arman. H, Heather, C., & Ali, C. (2015). Environmental impacts and embodied energy of construction methods and materials in low-income tropical housing. *Sustainability*, 7, 7866–7883. [CrossRef]

[8] Atanda, J. (2015). Environmental impacts of bamboo as a substitute constructional material in Nigeria. *Case Studies in Construction Materials*, 3, 33–39. [CrossRef]

[9] Praseeda, K.I., Reddy, B.V.V., & Mani, M. (2016). Embodied and operational energy of urban residential buildings in India. *Energy Buildings*, 110, 211–219. [CrossRef]

[10] Dixit, M.K. (2017a). Life cycle embodied energy analysis of residential buildings: A review of literature to investigate embodied energy parameters. *Renewable Sustainable Energy Rev*, 79, 390–413. [CrossRef]

[11] Dixit, M.K. (2017b). Embodied energy analysis of building materials: An improved IO-based hybrid method using sectoral disaggregation. *Energy*, 124, 46–58. [CrossRef]

[12] Nizam, R.S., Zhang, C., Tian, L. (2018), A BIM based tool for assessing embodied energy for buildings. *Energy Buildings*, 170, 1–14. [CrossRef]

[13] Lotteau, M., Loubet, P., & Sonnemann, G. (2017). An analysis to understand how the shape of a concrete residential building influences its embodied energy and embodied carbon. *Energy Buildings*, 154, 1–11. [CrossRef]

[14] Azari, R., & Abbasabadi, N. (2018). Embodied energy of buildings: A review of data, methods, challenges, and research trends. *Energy Buildings*, 168, 225–235. [CrossRef]

[15] Dixit, M.K. Singh, S. (2018). Embodied energy analysis of higher education buildings using an input-output-based hybrid method. *Energy Buildings*, 161, 41–54. [CrossRef]

[16] Chen, T., Burnett, J., & Chau, C. (2000). Analysis of embodied use in the residential building of Honkong. *Energy*, 24(4), pp. 323–340. [CrossRef]

[17] Ezema, I., Opoko, A., & Oluwatayo, A., 2016, De-carbonizing the Nigerian housing sector: The role of life cycle CO2 assessment. *International Journal of Applied Environmental Sciences*, 11(1), 325–349. [CrossRef]

[18] Fay, R., Treloar., G., & Iyer-Raniga, U. (2000). Life Cycle Energy Analysis of Buildings: a case study. *Building, Research and Information*, 28(1), 31–41. [CrossRef]

[19] Jennings, M., Hirst N., & Gambhir A., (2011), *Reduction of carbon dioxide emissions in the global building sector to 2050*. Grantham Institute for Climate Change Report GR. 3, Imperial College, London, UK.

[20] Mohad, H.A., Liman, A.S, Roshida, B.A.M. (2018). Quantifying the embodied carbon of a low energy alternative method of construction (AMC) house in Nigeria. *Chemical Engineering Transactions*, 643–648.

[21] Arocho, I., Rasdorf W., & Hummer, J., (2014). *Methodology to forecast the emissions from construction equipment for a transportation construction project*. Construction Research Congress 2014, 19th-21st May, Atlanta. [CrossRef]

[22] Ezema, I.C., Olotuah A.O., & Fagbenle O.I. (2016). Estimating embodied energy in residential buildings in a nigerian context. *International Journal of Applied Engineering Research*, 44140–44149.

[23] Pickvance, C.G. (2001). Four varieties of comparative analysis. *Journal of Housing and the Built Environment*, 16, 7–28. [CrossRef]

[24] Baltar, F., & Brunet, I. (2012). Social research 2.0: virtual snowball sampling method using Facebook. *Internet Res* 22, 57–74. [CrossRef]

[25] Hasan, M., & Kerr, R.M. (2003). The relationship between total quality management practices and organisational performance in service organisations. *The TQM Magazine*, 15(4), 286–291. [CrossRef]

[26] Shuttleworth, M. (2009). Construct Validity – Does the Concept Match the Specific Measurement? Explorable.com: https://explorable.com/construct-validity. Accessed on Dec 23, 2021.

[27] Saunders, M.N.K., Lewis, P., & Thornhill, A. (2016). *Research Methods for Business Students* (7th ed.). Pearson.

[28] Scherbaum, C.A., & Shockley, K.M. (2015). *Analysing Quantitative Data for Business and Management Students (Mastering Business Research Methods)* (1st ed.). SAGE Publications Ltd. [CrossRef]

[29] Arceňo, R.A. (2018). Motivations and expectations of graduate students of the college of advanced education (CAED). PEOPLE: *International Journal of Social Sciences*, 4(1), 239–256. [CrossRef]

[30] Akande, O.K., Olagunju, R.E., Aremu, S.C., & Ogundepo, E.A. (2018). Exploring factors influencing of project management success in public building projects in Nigeria. *YBL Journal of Built Environment*, 6(1), 51. [CrossRef]

[31] Woubishet, Z.T., & Kassahun A.A. (2019). Embodied energy and CO2 emissions ofwidely used building materials: the ethiopian context. *Buildings*, 1–15.

[32] Anon (2015). http://dreamfundesign.com/restaurant-design/bamboo-for-interior-designing-of-environmentally-friendly-restaurant/attachment/bamboorestaurant-interior-designing2. Accessed on Dec 23, 2021.

[33] Abraham, T., & Albert, A. (2013). Sustainable Housing Supply in Nigeria Through the Use of Indigenous and Composite Building Materials. *Civil and Environmental Research*, 3(1), 79–85.

[34] Beneyam, N.F., Fadilu S.J., & Natinael, B.T. (2021). Study on the Suitability of Soils in Ilu Aba Bora Zone for Hydraform Block Production for Low-Cost Construction. *Journal of Building Material Science*, 3(1), 37–42. [CrossRef]

[35] Klaus, D., (2002). Bamboo as a building Material, In: IL31 Bambus, Karl Kramer, Verlag, Stuttgart,1992.

[36] Norhasliya, M.D., Norazman, M.N, Mohammed, A.Y, Azrul, A.M.A., & Amalina, A.S (2017). The Physical and Mechanical Properties of Treated and Untreated Gigantochloa Scortechinii Bamboo, International Conference on Engineering and Technology (IntCET 2017) AIP Conference Proceedings 1930, 020016.

[37] Musa, Y.P., Ajayi, E.S., & Alabadan, B.A. (2019) Effect of different mud brick moulds and mortar on durability of plaster materials of buildings. *Bayero Journal of Engineering and Technology (Bjet)*, 14(2), 109–122.

[38] Udomiaye, E., Chukwuali, B.C., & Kalu C.K. (2020). Life cycle energy assessment (lcea) approach: a prospect for sustainable architecture in developing Countries. *Civil Engineering and Architecture*, 8(5), 777–791. [CrossRef]

[39] Ikechukwu, O., & Iwuagwu, B.U. (2016). Traditional building materials as a sustainable resource and material for low-cost housing in nigeria advantages, challenges and the way forward. *International Journal of Research in Chemical, Metallurgical and Civil Engineering*, 3(2), 247–252. [CrossRef]

J Sustain Const Mater Technol, Vol. 6, Issue. 4, pp. 168–172, December 2021

Journal of Sustainable Construction Materials and Technologies
Web page info: https://jscmt.yildiz.edu.tr
DOI: 10.14744/jscmt.2021.05

JSCMT
Journal of Sustainable Construction Materials and Technologies

Original Article

# Evaluation of concrete pavers affected by Manavgat wildfires

**Mustafa Altuğ PEKER**

*Alanya Alaaddin Keykubat University, Antalya, Turkey*

## ARTICLE INFO

*Article history*
*Received: 13 December 2021*
*Accepted: 22 December 2021*

**Key words:**
Climate change, concrete, concrete pavers, compressive strength, wildfire

## ABSTRACT

In recent years, wildfires have devastated many regions in many countries, especially in Turkey. In addition to the loss of human lives, villages and business facilities have been destroyed, livestock and domestic animals have perished, and forests and natural assets have burned. The wildfires have affected tourism and agriculture, which account for a large part of economic activity and employment in many of the affected areas. There was also significant destruction of local infrastructure, including roads, power, telecommunications, and community facilities. Some of the paving stones on the roads affected by the Manavgat wildfires were also burnt. The replacement of concrete paving stones used in pavements has both economic and environmental negative impacts. The reuse of these stones is important for the regional economy.

**Cite this article as:** Peker MA. Evaluation of concrete pavers affected by Manavgat wildfires. J Sustain Const Mater Technol 2021;6:4:168–172.

## 1. INTRODUCTION

Global warming is the most serious problem in history which humankind faceoff. Climate change is affecting meteorological balance of weather and threatening food production, water and energy security and causing variability in temperature, precipitation and evaporation patterns. Climate change increases forest fire risk depending on high air temperature and low humidity weather especially in subtropical ecoregions such as Mediterranean climate zones (i.e, Turkey, Greece, Italy, Spain). The expected negative impacts of climate change in these countries are heat waves, increased forest fires and floods, etc. Every year, hundreds of thousands of hectares burn in wild forest fires in European Mediterranean countries. According to Intergovernmental Panel on Climate Change (IPCC) assessment reports and other national and international scientific studies, the impact of climate change in the Mediterranean region, which includes Turkey, will reach a level that would threaten the countries' sustainable development and national security. In light of this knowledge, Turkey is inevitably affected by global warming. The Table 1 shows the city areas in the Mediterranean that are burning [1–3].

Climate change has a number of negative effects that raise the risk of fire in both direct and indirect ways. For example, climate change leads to warmer than average temperatures, which increases evaporation and leads to a moisture deficit at the surface. Low soil moisture increases the amount of dry bushfire fuel available (defined as dead or living vegetation that affects fire intensity and rate). Extreme heat and drought are one of the main triggers of widespread bushfires. Anthropogenic climate change has increased the likelihood of bushfires by at least 30% compared to pre-industrial times, mainly due to extreme heat. Climate change also indirectly affects the bushfire season by influencing large-scale and regional factors [4].

*Corresponding author.
*E-mail address: altug.peker@alanya.edu.tr

Published by Yıldız Technical University Press, İstanbul, Turkey
Copyright 2021, Yıldız Technical University. This is an open access article under the CC BY-NC license (http://creativecommons.org/licenses/by-nc/4.0/).

**Table 1.** Burned city areas by county, 2002–2003 [3]

| | Area (km²) | | Area (km²) |
|---|---|---|---|
| Turkey | 264.7 | Portugal | 10.8 |
| Syria | 232.5 | Serbia | 10.5 |
| Algeria | 106.5 | Lebanon | 9.1 |
| Morocco | 70.5 | Croatia | 5.1 |
| Bulgaria | 63.1 | Macedonia | 4.6 |
| Cyprus | 57.7 | Kosovo | 1.0 |
| Italy | 54.6 | Montenegro | 0.7 |
| Libya | 30.5 | Albania | 0.5 |
| Greece | 30.4 | Bosnia-Herzegovina | 0.3 |
| Israel | 24.7 | Malta | 0.2 |
| Tunisia | 23.5 | Other micro-statesa | 0.2 |
| Egypt | 18.2 | Jordan | 0.0 |
| France | 15.0 | Palestine | 0.0 |
| Spain | 13.2 | Slovenia | 0.0 |

a: Andorra, Gibraltar, Monaco, San Marino, Vatican.

Climate change is extending the fire season in large areas worldwide by prolonging the hot weather of summer. Between 1979 and 2013, an 18.7% increase in the seasonal extent of fires was observed. The global burnable area has doubled, and the frequency of long fire season has increased by 53% of the global vegetated land area [4].

Wildfires are uncontrolled and nonprescribed burns or fires of plants in a natural environment such as forest, grassland, shrubland, or tundra that consume natural fuels and spread due to environmental conditions (e.g., wind, topography). The zone where these fires occur at the edge of the forest and where urban development has occurred is usually referred to as the interface zone. Wildfires in a forested area are referred to as forest fires and can cause great damage if the interface zone spreads to properties or land of economic value and to areas populated by people. In a report published in 2015, Forest fires were the natural disasters that most affected the Canadian economy. The damage of the forest fires to the Canadian economy approached 6.5 billion dollars. Furthermore, in 2007 the worst wildfires in recent Greek history - affecting 270,000 hectares of land - caused estimated total damage of close to 3 billion euros (1.3 percent of nominal Gross Domestic Product) [5–7].

Increasing urbanization and the accompanying urban sprawl have been cited as a major cause of landscape change in many countries around the world. Recent decades show a steady shift of urban populations to the suburbs and the expansion of cities towards forested areas. This change has led to an increase in urban fringe areas that are either in contact with or mixed with forest and rural areas. Especially in the coastal and tourist areas of the European Mediterranean countries, many small towns and resorts have been built in or around natural and forest areas, mainly for their recreational attractions and scenic beauty [8].

**Table 2.** Compressive strengths of concrete paving stones

| Paving stone type | Strength (MPa) | Strength (MPa) | Strength (MPa) |
|---|---|---|---|
| Unburned | 36.24 | 36.01 | 35.87 |
| Half-burned | 48.72 | 49.67 | 50.14 |
| Completely burned | 50.61 | 50.97 | 50.91 |

The presence of residential developments in contact with forested areas increases the vulnerability of these areas to fire damage. Uncontrolled wildfires can have disastrous consequences for properties and land use, and even threaten human life. The contact zone between human infrastructure and wildland vegetation is referred to as the wildland-urban interface (WUI). WUI areas are increasing worldwide as the mixing of urban settlements and forested areas increases due to (i) urban areas colonizing forested areas and (ii) forested areas colonizing rural areas due to rural migration. The WUI is central to the development of wildfire management strategies in the United States, Canada, Australia, and Europe, and extensive research has been conducted on this topic in recent decades [9].

The contact zone between human infrastructure and wild vegetation, the so-called wildland-urban interface (WUI), has increased worldwide in recent decades and is directly related to wildfire risk. Human activities increase the likelihood of wildfires, which can have catastrophic consequences for property and land use and pose a serious threat to human life. A study shows that Galicia has the highest rate of forest fires in Spain. The results show that more than half of the built-up area is in the WUI area and that fires are about twice as likely to break out in WUI areas than in non-WUI areas. Most wildfires occur in non-forested areas of the WUI, while the lowest fire density is associated with isolated buildings. Areas with very dense clusters of buildings surrounded by forested areas, referred to here as near-urban areas, have the highest fire density. This trend highlights the vulnerability of the interface to fire in this region [9].

Natural disasters are a persistent danger to all critical infrastructures. Severe storms, hurricanes, earthquakes, tornadoes, volcanoes, drought, floods, landslides, tsunamis, and wildfires can all cause substantial property and economic damage, as well as obstruct access to key resources like power, water, transportation, and food. Critical infrastructure and services will be damaged or destroyed if they come into contact with a severe wildfire. Transportation networks are disrupted by road closures, with roads directly affected by the flames and heat remaining closed until associated infrastructure can be replaced and trees assessed. Restoring the road network is an important step for many affected communities to begin the economic recovery process, particularly with regard to the tourism industry [10, 11].

**Figure 1**. Manavgat-Oymapınar Neighborhood.

The aim of this study is to help reduce the economic impacts of forest fires on infrastructure through the reuse of concrete pavers. In a previous study on concrete, it was observed that the compressive strengths decreased at certain rates as the temperature increased, but it was observed that the compressive strengths at 250 °C were higher than 100 °C, and even close to the compressive strengths at room temperature [12]. When the studies in the literature about concrete pavers are examined, it is seen that the roads affected by the fire are handled with an only general point of view. Renewal of paving stones creates high costs for municipalities. In this study, concrete paving stone samples affected by forest fires were taken in Manavgat province. Concrete paving stones whose compressive strengths were determined were compared and suggestions were made.

## 2. MATERIALS AND METHODS

Paving stones are natural or artificial floor covering materials, the use of which is increasing day by day for transportation and landscaping purposes, especially on roads where there is no heavy vehicle traffic with the development of urbanization. It is especially seen on roads and pavements, in parking lots, in commercial centers, around factories and similar places that are exposed to intense work. These stones are widely used as they can be produced in various shapes, sizes and colours [13].

**Figure 2**. Pavement in the fire zone.

In order to obtain the materials in this research, the Manavgat fire area was investigated. The area shown in Figure 1 is the Oymapınar neighborhood. It is clearly seen that this region, where forest and habitats are very close to each other, is WUI.

The field marked red in Figure 1 is the area with the most affected pavement from the fire. It was decided to take the samples from this area. When the paving stones were examined, it was seen that there were completely burned, half-burned and unburned concrete paving stones in the same area. It is planned to take three samples from all three combustion conditions to compare them with each other in terms of the mean value of compressive strength. The pavement affected by the fire is shown in Figure 2.

**Figure 3**. Concrete paving stones in different conditions.

As a result of the strength tests to be made, it will be tried to determine whether the burned concrete paving stones can be reused or not. Efforts will be made to obtain the most suitable solution both economically and environmentally.

A sample of the completely burned, half-burned and unburned concrete paving stones taken from the Manavgat wildfire area are shown in the Figure 3.

The paving stones were tested in the pressure machine in the Civil Engineering Laboratory of Alanya Alaaddin Keykubat University. The experimental setup is shown in the Figure 4.

## 3. RESULTS AND DISCUSSION

All experiments were successfully completed, and compressive strengths were obtained in accordance with the standard of BS6717 [14, 15]. The compressive strengths measured as a result of the tests are shown in the Table 2. According to the results obtained, the mean value of compressive strengths of unburned, half-burned, and completely burned stones were 36.04 MPa, 49.51 MPa, and 50.83 MPa, respectively.

It is seen that the compressive strength increases as the amount of combustion increases. Normally, the strength of concrete is expected to decrease when exposed to very high temperatures. The reason for the increase in the strength of concrete paving stones may be that the fire went out before it reached a very high temperature on the pavements in the region. A well-known basic fact in thermodynamics, gases have higher temperatures rise up depending on their low density. Increasing in the strengths of the concrete pavers in the burned regions like heat-treated concrete can be explained using this fundamental thermodynamic law. It is also an indication that the fire does not burn the entire pavement and does not spread to the driveway. These results are also consistent with the study [12] in the literature that concretes treated at 250 °C have higher strength than concretes at room temperature.


**Figure 4**. Compression testing machine.

The results obtained prevent the replacement of paving stones in the region due to strength. However, this result also needs to be evaluated from an architectural point of view. It is clear that the half-burned and completely burned concrete pavers are dirty and have colour mismatch. Therefore, replacement or staining of the stones may be considered.

The cost of only 1 $m^2$ of concrete paving stone is known as 30 TL. When expenses such as transportation, labour and sand are added, the total cost reaches 60 TL/$m^2$. The cost of concrete paint per square meter is 20 TL. The cost of paintwork is 10 TL/$m^2$. Since it is easy to apply to the concrete surface, it can also be done with the municipality's own workers. In this way, it is possible to get no labour cost. In order to better understand the cost difference between renovation and painting, the renovation cost of 1 km long and 1.5 meters wide burnt pavement, including all labour and other expenses, will be approximately 100000 TL. The maximum cost that will occur as a result of painting the same pavement will be 50000 TL. As clearly seen, the cost of renovation is much higher than the cost of painting. Moreover, considering that the existing paving stones must be removed and moved for the renovation process, the cost will be much higher. In addition, the painting process will take much less time than the renovation process. Besides, it is clear that painting of paving stones is a more environmentally friendly solution.

## 4. CONCLUSIONS AND RECOMMENDATIONS

Wildfires have ravaged several parts of the world in recent years, particularly Turkey. Villages and business buildings have been destroyed, cattle and domestic animals have died, and forests and natural assets have been destroyed in addition to human lives lost. Tourism and agriculture, which make for a significant portion of economic activity and jobs in many of the affected areas, have been negatively impacted by the wildfires. Roads, power, telecommunications, and community amenities were all severely damaged. The Manavgat wildfires also burned several paving stones on the highways. Pavement replacement with concrete paving stones has both financial and environmental costs. The economic impact of reusing these stones is significant.

In previous studies, problems such as opening the roads affected by the fire and protecting the existing buildings were mentioned, but no study was conducted on the renewal of paving stones. The goal of this research is to reuse concrete pavers to assist lessen the economic impact of forest fires on infrastructure. Municipalities face substantial costs when pavement stones need to be replaced. Concrete paving stone samples impacted by forest fires were collected in Manavgat province for this research. The compressive strengths of concrete paving stones were compared, and recommendations were made.

Before changing the paving stones at the the fire zones, strength tests should be done on the sample and no change should be made unless a negative situation is encountered. In our study, the strength of the concrete increased with burning. Using burnt paving stones with increased strength will be much more convenient than the cost of replacement.

In addition, the cost of painting the fire-affected concrete paving stones is half of the replacement cost when labour and other costs are taken into account. Considering the use of cement in the concrete stones to be used in the renovation process, it is clear that paint will be the most economical and environmentally friendly solution.

### DATA AVAILABILITY STATEMENT

The author confirm that the data that supports the findings of this study are available within the article. Raw data that support the finding of this study are available from the corresponding author, upon reasonable request.

### CONFLICT OF INTEREST

The author declare that they have no conflict of interest.

### FINANCIAL DISCLOSURE

The author declared that this study has received no financial support.

### PEER-REVIEW

Externally peer-reviewed.

## REFERENCES

[1] Birpinar, M. E., & Tuğaç, C. (2018). *Impacts of climate change on water resources of Turkey. Water resources and wetlands*. 4th International Conference Water resources and wetlands, Tulcea, Romania, 145–152.

[2] Fox, D., Martin, N., Carrega, P., Andrieu, J., Adnès, C., Emsellem, K., Ganga, O., Moebius, F., Tortorollo, N., & Fox, E. A. (2015). Increases in fire risk due to warmer summer temperatures and wildland urban interface changes do not necessarily lead to more fires. *Applied Geography*, 56, 1–12. [CrossRef]

[3] Régis, D. (2015). Mediterranean cities under fire. A critical approach to the wildland–urban interface. *Applied Geography*, 59, 10–21. [CrossRef]

[4] Dey, R., & Lewis, S. C. (2021). Natural disasters linked to climate change. *In the Impacts of Climate Change*, 177-193. [CrossRef]

[5] Agrawal, N. (2018). Defining natural hazards–large scale hazards. *Natural Disasters and Risk Management in Canada*, 49, 1–40. [CrossRef]

[6] PSC (2013/2014/2015) The Canadian disaster database, Public Safety Canada. http://cdd.publicsafety.gc.ca/srchpg-eng.aspx. Acceesed on Dec 27, 2021.

[7] Mitsakis, E., Iraklis, S., Anestis, P., Georgia, A., & Haris, K. (2014). Assessment of extreme weather events on transport networks: case study of the 2007 wildfires in Peloponnesus. *Natural Hazards*, 72(1), 87–107. [CrossRef]

[8] Bento-Gonçalves, A., & Vieira, A. (2020). Wildfires in the wildland-urban interface: key concepts and evaluation methodologies. *Science of the Total Environment*, 707, 135592. [CrossRef]

[9] Chas-Amil, M. L., Touza, J., & García-Martínez, E. (2013). Forest fires in the wildland–urban interface: a spatial analysis of forest fragmentation and human impacts. *Applied Geography*, 43, 127–137. [CrossRef]

[10] Shapiro, L. R., & Maras, M. H. (Eds.). (2019). *Encyclopedia of Security and Emergency Management*. Springer International Publishing.

[11] Stephenson, C. (2010). *A literature review on the economic, social and environmental impacts of severe bushfires in south-eastern Australia*. Victorian Government Department of Sustainability and Environment.

[12] Uysal A. (2004). *Yüksek Sıcaklığın Beton Üzerindeki Etkileri*. Yüksek Lisans Tezi, İstanbul Teknik Üniversitesi, İstanbul.

[13] Kaya, T., & Karakurt, C. (2016). Uygulamadaki Beton Parke Taşlarının Mühendislik Özelliklerinin İncelenmesi. *Düzce Üniversitesi Bilim ve Teknoloji Dergisi*, 4(2016), 469–474.

[14] Öztekin, E., Uyan, M., & Manzak, O. (1989). Beton parke taşları için standart basınç deneyine alternatif iki deney. *1. Ulusal Beton Kongresi, İstanbul, Türkiye*, 354–364.

[15] BS (1986) Precast concrete paving blocks, Part 1: Specification for paving blocks. B.S.I British Standards Institutions (BS 6717).

Journal of Sustainable Construction Materials and Technologies
Web page info: https://jscmt.yildiz.edu.tr
DOI: 10.14744/jscmt.2021.06

JSCMT
Journal of Sustainable Construction Materials and Technologies

Review Article

# Application of finite element method on recycled aggregate concrete and reinforced recycled aggregate concrete: A review

**Hasan DİLBAS**

*Department of Civil Engineering, Van Yüzüncü Yıl University, Engineering Faculty, Van, Turkey*

## ARTICLE INFO

*Article history*
*Received: 18 November 2021*
*Accepted: 11 December 2021*

**Key words:**
Dynamic loading, finite element, recycled aggregate concrete, reinforced recycled aggregate concrete, static loading

## ABSTRACT

In recent years, concrete has become a widely used material for general purposes in the structural area due to its excellent performance and properties. Hence, an increasing number of concrete structures are built, and a huge amount of building stock has been occurred around the world. However, because of the many progress (i.e., natural disasters), some of the concrete structures are demolished and their status is changed into rubble, and hence this becomes an environmental problem threatening the nature. To struggle with the rubbles, – a brilliant idea – recycling concrete is appeared and to disposal the rubbles in concrete works become a subject in the authorities' agenda. Also, according to the brilliant approach, the studies focus on some experiments and simulation works (i.e., finite element modeling) to analyze the use of rubbles as recycled aggregate (RA) in concrete, recycled aggregate concrete (RAC) and reinforced RAC (RRAC) properties. At this point when a deep look is concentrated on the papers on RAC and RRAC, the reviews generally include experimental works of the research but rarely or hardly ever consider the simulation stages of the researche. Hence, this paper is drawn as a state-of-the-art report on modeling works of RAC and RRAC. Also, this paper gives finite element model (FEM) details of the examined research to improve the future studies on RAC and RRAC with helpful comments and directions.

**Cite this article as:** Dilbas H. Application of finite element method on recycled aggregate concrete and reinforced recycled aggregate concrete: A review. J Sustain Const Mater Technol 2021;6:4:173–191.

## 1. INTRODUCTION

Concrete, in present, is widely used due to its excellent structural performance with rebars, strong resistive behavior to harmful environment, low-cost requirements for the maintenance and plastic behavior in fresh state, and a huge amount of structure have been built in the world. Hence, the stock of the reinforced concrete structures has been increased with the urbanization moves of the countries. As a results of the natural disasters, the change in the human demands, and the urban renewal plans etc. many engineering structures have been demolished and their status have been turned into waste [1]. In this situation, it caused million tons of construction and demolished waste (C&DW) in the world [2]. To struggle with C&DW, many countries have taken positions and made new regulations, taken out

*Corresponding author.
*E-mail address: hasandilbas@yyu.edu.tr

Published by Yıldız Technical University Press, İstanbul, Turkey
Copyright 2021, Yıldız Technical University. This is an open access article under the CC BY-NC license (http://creativecommons.org/licenses/by-nc/4.0/).

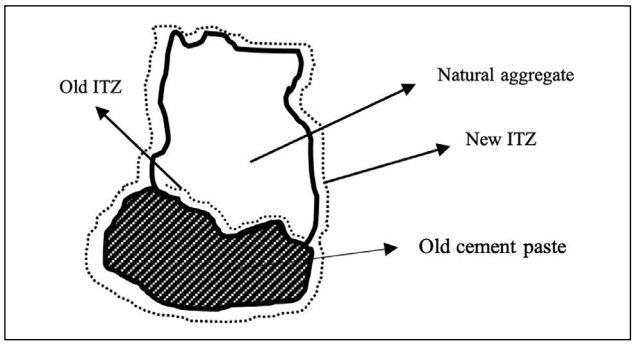


**Figure 1**. The structure of RA.

new laws, and revamped the current urban plans etc. [3, 4]. On the other hand, a huge amount of C&DW and its potential use in concrete as an aggregate (recycled aggregate (RA) inspire the researchers to conduct comprehensive studies. Hence, fully, or partially use of RA is considered in the studies and the effect of RA and other components (i.e., mineral admixtures) widely examined (i.e., [2, 4–8]). The physical and the mechanical properties, and the durability properties of recycled aggregate concrete (RAC) are mainly discussed and valuable comments/recommendations on RAC are stated in the literature [2, 4–8]. For instance, the optimum RA use ratio is mostly suggested by many researchers as 30% in concrete mixtures [2, 5].

On behalf of the studies on RA, it can be said that RA has mainly two parts: Natural aggregate (NA) and adhered old cement paste (OCP). Additionally, interfacial transition zone (ITZ) between NA and OCP can be considered as a part of RA. When the properties of RA are considered, the poor property of RA is usually sourced by OCP which has lower elasticity modulus, lower strength, and more porous structure than NA [2]. On the other hand, if RA is considered to utilize in concrete mixtures, four main things occur (Fig. 1): NA, OCP, new ITZ and old ITZ [2]. Also, SEM observations of RAC in Figure 2 is precisely demonstrated the structure of RA. It can be seen in Figure 2 that there are many cracks and voids between the RA and mortar matrix and it is clear that the components of RA negatively affect the properties of RA and so RAC [2].

In present, the properties of RAC and RRAC can be determined with various instruments using many techniques. As above mentioned, SEM is one of the instruments and it depends on experiments and, mechanical tests (compressive, tensile, etc.) are some the other instruments used in the literature widely. In this perspective, it is well-known that it is possible to estimate the concrete or the reinforced concrete behaviors with simulation models if the model is composed properly. The finite element method is widely used method in modeling research in the literature, and the finite element analysis (FEA) gives consistent results with experiments is proven in many conducted research (i.e., [9–11]).

When a deep look is concentrated on the related literature, the research on RA is usually conducted in two parts: an experimental stage and a modeling stage (i.e., [12–18]). In the research, after or before the experiments, a modeling stage is usually examined, and the theoretical results obtained from modeling part are verified with the experimental results. The results are generally used to show that FE model (FEM) is suitable to estimate the behavior of concrete under various conditions (i.e., static loading). Hence, FEA takes part in the studies and has an importance as much as experiments have; and perhaps the most important thing is that the verified models can supply additional data without conducting any additional experiments to estimate the concrete behavior.

However, when someone sets eye on the review works on RAC and RRAC, the reviews generally report experimental parts and rarely or hardly ever consider the simulation stages of the research (i.e., [2, 13–15]). Hence, to fill the gap in the literature and to summarize the research included finite element (FE) modeling works, this paper is not only drawn primarily as a state-of-the-art report on modeling of RAC, but also written as a state-of-art on mod-

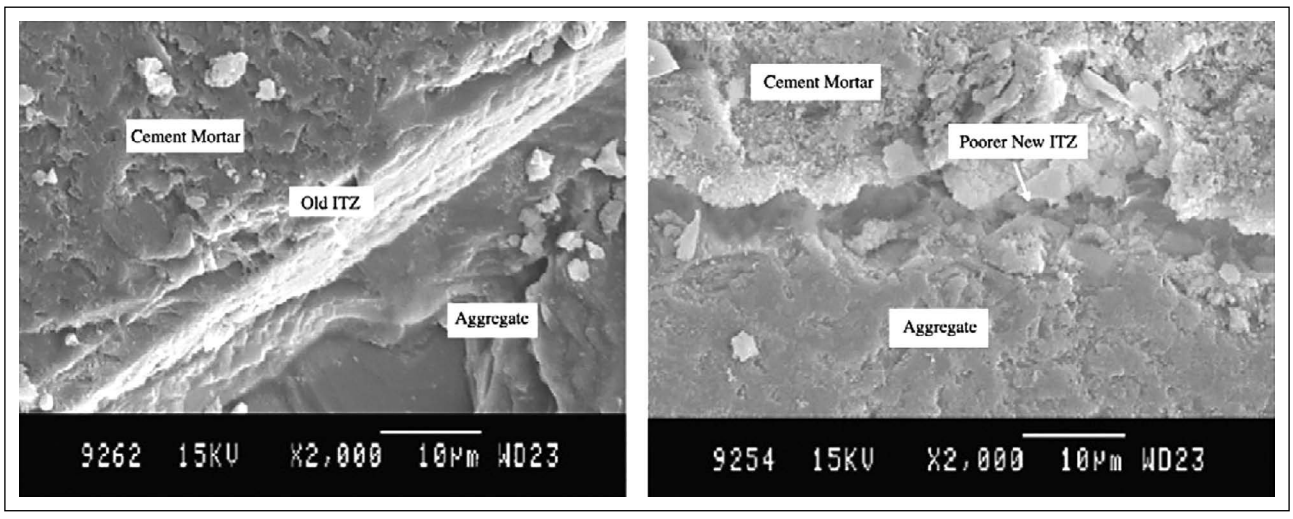


**Figure 2**. The microstructure characteristics of RAC [2].

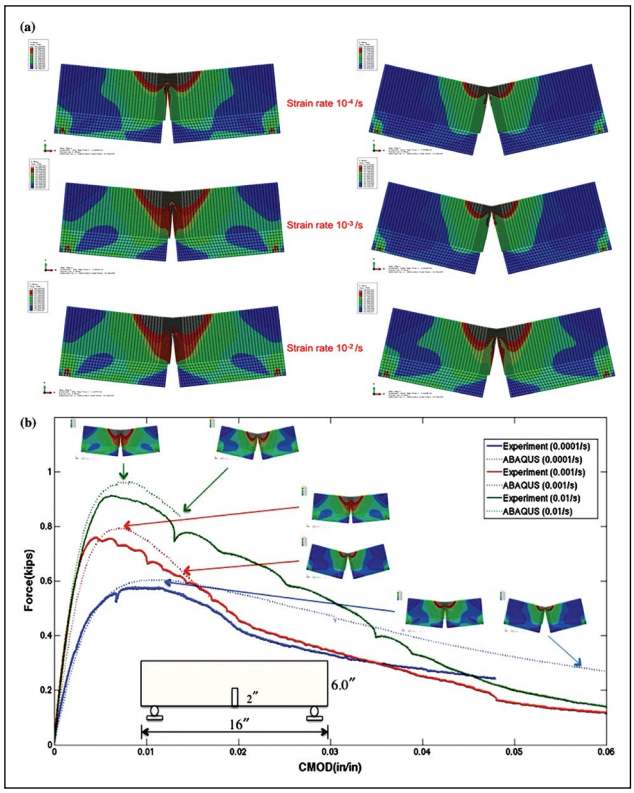


**Figure 3**. Force versus CMOD and stress distributions for Case 1: fixed beam size under three different loading rates, stress distribution at peak loads and final deformed stages for Case 1, Full force versus CMOD curves for Case 1 [23].

eling of RRAC. In addition, this review gives the details of FEMs of the related research to improve the future studies on RAC and RRAC with helpful comments and directions.

## 2. RECYCLED AGGREGATE CONCRETE

It is well-known that RAC has poor properties (low strength [5, 19], low elasticity modulus [19], etc.) in comparison to conventional concrete (NAC)due to its components, and the low properties of RAC usually sourced by RA [20]. RA has lower strength, elasticity modulus and porous structure with cracks [13] and ITZ is a crucial component in RAC [5]. Hence, the works on RAC generally concentrate on modeling ITZ and RA in macro-, meso- and micro-scales. In this perspective, the related research is examined in three subsections as given in below.

### 2.1. Modeling of Recycled Aggregate Concrete

#### *2.1.1. Macro-Scale Modeling*

In the literature, researchers examine the macro-scale behavior of RAC in pure concrete state and in confined concrete state (concrete filled steel tube (CFST)). Hence, in this review paper, the subject of "Modeling of Recycled Aggregate Concrete" is divided into two parts as one can see in below considering the details given above.

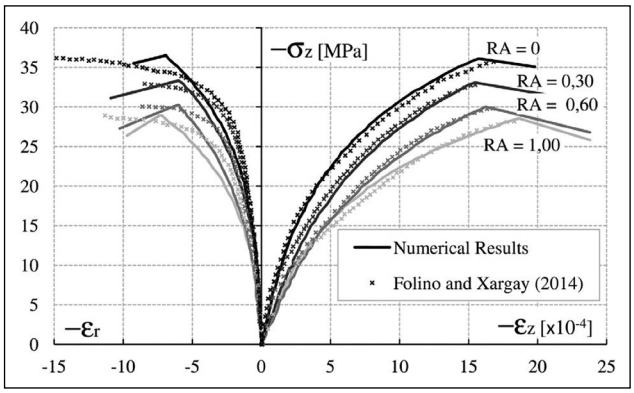


**Figure 4**. Numerical results of uniaxial compression tests against experimental results by Folino and Xargay [24].

*2.1.1.1. Macro-Scale Behavior of RAC in Pure RAC State*

Etse et al. [21] improve a constitutive theory for RAC considering high temperature conditions. The theory is a material model of thermodynamically consistent gradient poroplastic and aims to predict the mechanical behavior of RAC [21]. In the research, the elevated temperatures (20-200-400-600°C) and various RA ratios (0-30-60-100%) are concerned and the RAC simulation of the failure behavior under high temperature and the capability of the theory are demonstrated [21].

Dilbas [4], in his research, conducts some mechanical tests (compressive strength, splitting tensile strength and elasticity modulus) to define the mechanical behavior of RAC obtaining stress-strain data from zero to failure and beyond for mechanical tests [4]. Then, a homogeneous cantilever beam subjected to a point load is modeled in his research using the obtained mechanical properties and the mechanical behavior is examined under static loading conditions in Abaqus [4]. In his research, 3-dimensional (3D) non-linear FEA is considered, and pure plasticity is used to define the RAC properties in Abaqus [4]. Also, the results are verified with SAP 2000 FEA software.

Choubey et al. [22] demonstrate the application of fracture models to RAC (double-K fracture model and fictitious crack model). The required parameters for the models are obtained in the equations given in the related literature and varying content of RA (0-30-50-70-100%) is considered [22]. It is concluded that the fracture models given in the literature for natural aggregate concrete (NAC) is suitable for RAC and the fracture parameters of RAC included RA from 0% to 100% can be determined using the models [22]. Also, some interesting results for NAC and RAC are found that the ratio of Pini/Pu (force when initial crack occurs/ultimate force) and KICini/KICun (initial cracking toughness/unstable fracture toughness) are constant for RAC and NAC [22].

Musiket et al. [23] present the fracture tests on notched RAC beams with different sizes under different high loading rates from 10−4/s to 10−2/s (Fig. 3) considering and combining two material models: viscoelastic model and

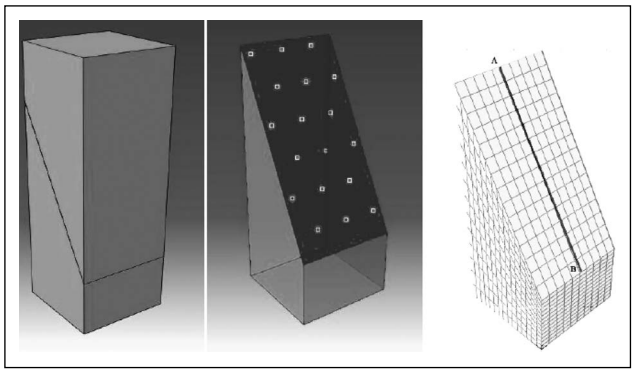

**Figure 5**. Parts assembled (left), surface definition (right) and mean line of the interface [25].

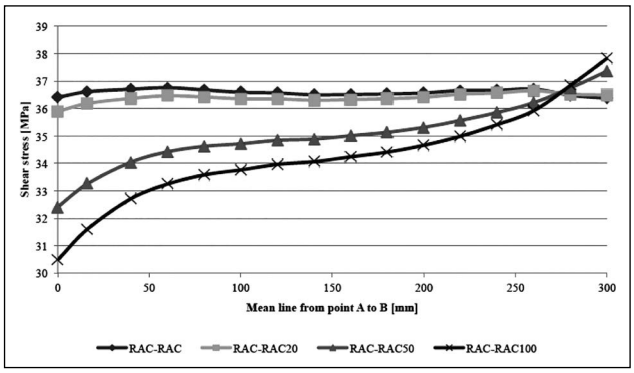


**Figure 6**. Evaluation of the shear stress in the interface [25].

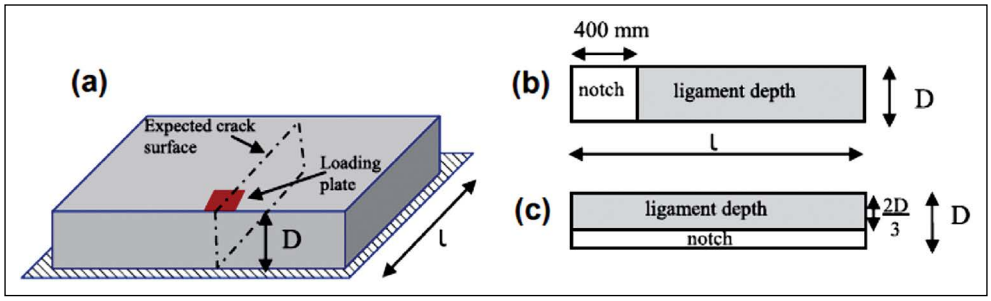


**Figure 7**. **(a)** Slab specimen on soil with expected crack surface; **(b)** edge-notched slab; and **(c)** one-third notched slab. Gray area in **(b and c)** denotes the ligament, while the white area is the pre-existing notch [9].

multi-phase composite model. Combining two material models, the rigidity of RAC is predicted for high loading rate conditions [23]. Force-crack mouth opening displacement (CMOD) curves are obtained from simulations, and the simulation model includes the fracture analysis criteria and eXtended Finite Element Method (XFEM) [23]. As a results, similar distributions of stress in the beams for different sizes are obtained, and the maximum loads estimated by the simulations are not close with test data [23].

Ripani et al. [24] study on a gradient plasticity theory reformulating Leon-Druger-Prager Model. The theory is widened to estimate the mechanical failure behavior of RAC, and the supposed theory is consistent with thermodynamic laws and considers the softening and hardening response behaviors [24]. In the modeling section, the supposed model and some numerical results are compared against experimental results given in the literature and the formulation of dual mixed FE is considered [24]. The formulation includes thermodynamically consistent gradient plasticity [24]. Also, the tests of uniaxial tensile and compression are adopted to FEM [24]. It is stated in conclusion that the proposed constitutive model presents the influence of RA addition on the behavior of failure response and reflects the sensitivity of RA [24] (Fig. 4).

Ceia [25] researches the effect of RA on shear resistance. In the experimental work, many specimens including various RA ratios (0-20-50-100%) are produced [25]. In the 3D modeling section, Abaqus is used, two parts (upper and lower parts) are defined separately to model the shear test and then the parts are assembled in conformity with a behavior of linear elastic material [25] (Fig. 5). Cohesive bonding is considered for the surfaces of the specimens [25]. It is stated that the stiffness of differential in FEA is substantial for shear strength [25] (Fig. 6).

Gaedicke et al. [9] propose an 3D approach which includes three subjects separately: Concrete slab flexural load capacity determination under mode I -the slab lies on elastic foundation-, crack growth and crack initiation. 3D slabs FEM is generated in Abaqus, and the slabs include cohesive crack elements along pre-defined paths [9] (Fig. 7). The bilinear softening for concrete is considered, and the model is simulated. Also, the results are verified experimentally [9]. It is concluded that 3D cohesive crack element can estimate the capacity of slabs under flexural loads on soils [9].

*2.1.1.2. Macro-Scale Behavior of RAC in Confined RAC State*

Tam et al. [26] use RAC in concrete-filled steel tubular (CFST) columns as a filling material and CFST columns has rectangular geometry. Then FEA is considered to model CFST columns in Abaqus [26]. An equation defined for stress-strain data for confined concrete proposed by Han et al. [26] is used in the model as a constitutive model parameter and it is stated that the equation gives good results for models when the damage plasticity model is used in Ab-

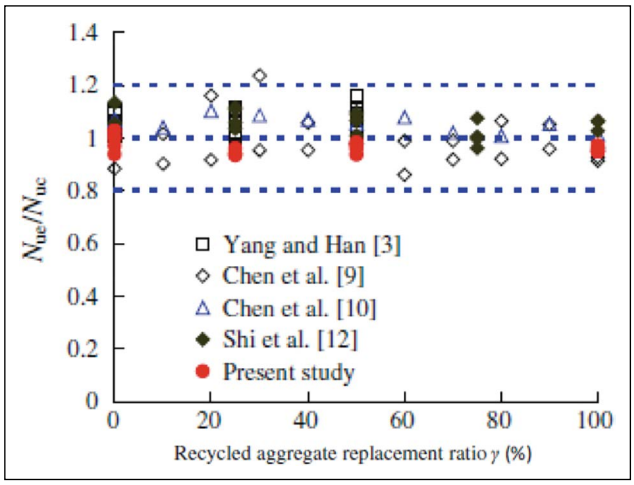


**Figure 8**. Comparison between the predicted and experimental ultimate strength [26].

aqus [26]. In the modeling part, steel jacket and concrete are modeled as shell and solid elements, respectively [26]. Also, surface-based interaction between the steel jacket and concrete is defined: In the normal direction and the tangential direction a contact pressure model and a Coulomb friction model, respectively [26]. In conclusion, it is stated that a FE model simulated for conventional concrete-filled steel tubes is possible to use for CFST with RAC, and satisfactory CFST results are found [26] (Fig. 8).

Yang et al. [27] carry out an experimental and numerical studies on square CFST under lateral impact loads (Fig. 9). In this study, local damages and failure modes of specimens are examined [27]. The non-linear FEM for CFST is simulated in Abaqus, and explicit solver is considered. [27]. Damaged plasticity model is taken into account for modeling nonlinear behavior of concrete [27]. It is found that the failure mode of CFST is generally concave where the loads are applied to, and the shear failure with punching shear failure of CFST is observed [27]. Also, experimental, and numerical results are in good agreements is found [27].

Xiao et al. [28] use glass fiber reinforced plastic (GFRP) tubes and steel tubes to confine RAC in their research and apply axial compression force to concrete-filled tubes to determine the mechanical properties. Then, a concrete-filled tube FEM is simulated to examine the outer tube thickness and the core strength effect [28]. The non-linearity in FEM is accounted in ANSYS [28]. 3D solid element for outer tube is used and the element abilities are creep, plasticity, stress stiffening, swelling, large strain, and large deflection, and the name is solid45 [28]. Also, 3D solid element for core concrete is chosen and the name is solid65 [28]. Solid65 is for solid models including no rebars and the abilities of solid65 are crushing in compression, cracking, creep cracking in tension and plastic deformation [28]. It is concluded that the peak stress of recycled concrete filled steel tube increases when the thickness increases and no effect on the plastic stage is observed [28] (Fig. 10).

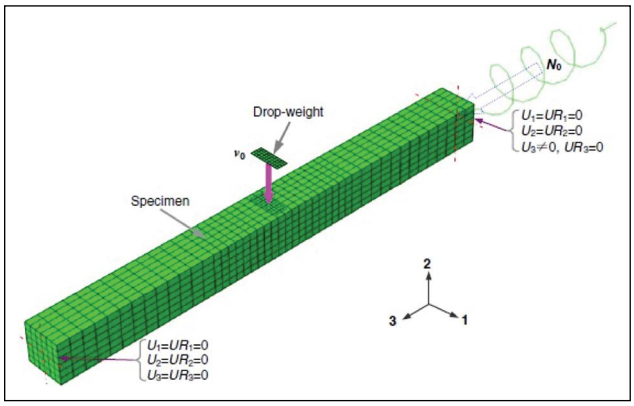


**Figure 9**. A schematic view of the test assembly [27].

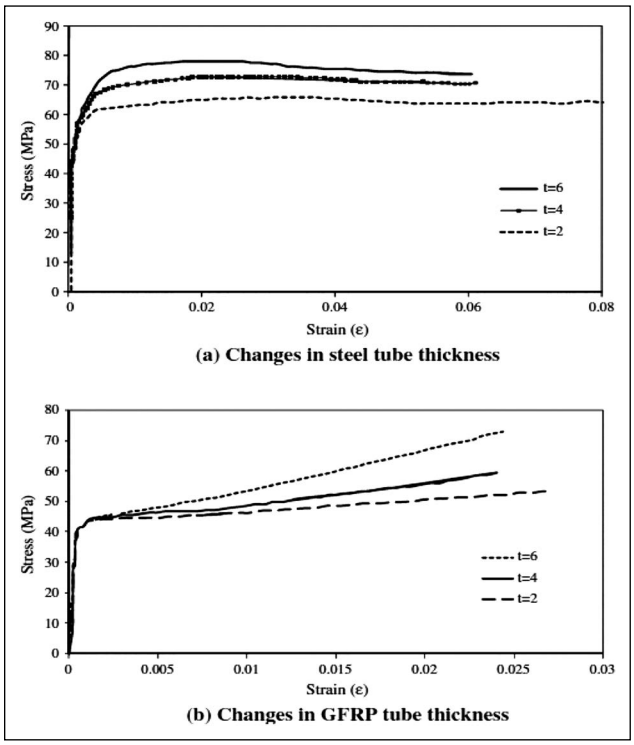


**Figure 10**. Effect of the outer tube thickness [28].

Xiang et al. [29] conduct a theoretical study on recycled aggregate concrete-filled steel tube stub columns. In the study, cold-formed hollow structural square steel tube is used, and nonlinear finite element model is simulated in Abaqus [29]. The stub column is subjected to axial compression. 3D eight-node solid elements with full integration (C3D8) are chosen for rigid plates and RAC, and the cold-formed steel tube is modeled with a shell element (S4) due to the small wall thickness in Abaqus [29]. For modeling the cold-formed steel material behavior, an idealized elastic-plastic stress-strain model proposed by Abdel-Rahman and Sivakumaran is considered [29]. This model indicates a multi-linear isotropic strain hardening rule [29]. The ascending part of RAC equivalent stress-strain is modeled according to Guo and Zhang equation [29]. Concrete damaged plasticity model in Abaqus

**Table 1.** Comparisons of the ultimate compressive strengths determined by different methods [29]

| Specimen | Eurocode 4 | | ACI 318-05 | | ANSI/AISC 360-05 | | Sakino | | Han | |
|---|---|---|---|---|---|---|---|---|---|---|
| | $P_{EC4}$(kN) | $P_{EC4}$ / $P_{TEST}$ | $P_{ACI}$ (kN) | $P_{ACI}$ / $P_{TEST}$ | $P_{AISC}$ (kN) | $P_{AISC}$ / $P_{TEST}$ | $P_{Sakino}$ (kN) | $P_{Sakino}$ / $P_{TEST}$ | $P_{Han}$ (kN) | $P_{Han}$ / $P_{TEST}$ |
| Sa1-1 | 610 | 0.946 | 563 | 0.873 | 559 | 0.867 | 605 | 0.938 | 598 | 0.927 |
| Sa1-2 | 610 | 0.924 | 563 | 0.853 | 559 | 0.847 | 605 | 0.917 | 598 | 0.906 |
| Sa2-1 | 567 | 0.909 | 526 | 0.843 | 523 | 0.838 | 559 | 0.896 | 557 | 0.893 |
| Sa2-2 | 567 | 0.923 | 526 | 0.857 | 523 | 0.852 | 559 | 0.910 | 557 | 0.907 |
| Sb1-1 | 1305 | 1.020 | 1197 | 0.936 | 1191 | 0.931 | 1290 | 1.009 | 1283 | 1.003 |
| Sb1-2 | 1305 | 1.014 | 1197 | 0.930 | 1191 | 0.925 | 1290 | 1.002 | 1283 | 0.997 |
| Sb2-1 | 1207 | 0.966 | 1114 | 0.890 | 1108 | 0.886 | 1192 | 0.954 | 1191 | 0.953 |
| Sb2-2 | 1207 | 0.933 | 1114 | 0.861 | 1108 | 0.857 | 1192 | 0.922 | 1191 | 0.921 |
| Sc1-1 | 2230 | 1.050 | 2038 | 0.960 | 2027 | 0.955 | 2147 | 1.011 | 2191 | 1.032 |
| Sc1-2 | 2230 | 0.996 | 2038 | 0.911 | 2027 | 0.906 | 2147 | 0.959 | 2191 | 0.979 |
| Sc2-1 | 2055 | 0.980 | 1889 | 0.900 | 1880 | 0.896 | 1979 | 0.943 | 2026 | 0.966 |
| Sc2-2 | 2055 | 0.960 | 1889 | 0.883 | 1880 | 0.879 | 1979 | 0.925 | 2026 | 0.947 |
| Mean | | 0.968 | | 0.891 | | 0.887 | | 0.949 | | 0.953 |
| COV | | 0.044 | | 0.040 | | 0.040 | | 0.040 | | 0.044 |

is considered for RAC, and the surface-to-surface contact is used for the relation between the faces of steel jacket and core concrete [29]. In the research section on the friction coefficient, it is stated that the column under compression has no sensitivity with the friction coefficients although various friction coefficients (from 0.2 to 0.6) in FEM is considered [29]. In conclusion it is stated that the square CFST included RAC has similar mechanical behavior with the square CFST included conventional concrete, and the specification Eurocode 4 estimates the ultimate compressive strength of square CFST with a reasonable accuracy [29] (Table 1).

Yang et al. [30] investigate the fire resistance of CFST included RAC (Fig. 11). In the analysis, typical temperature development, failure pattern, fire resistance and axial displacement of the specimens are determined [30]. In the simulation, RAC-filled square steel tubular columns is modeled in Abaqus [30]. According to the research, the model includes two main parts: thermal part (includes temperature development) and mechanical part (includes displacement, failure pattern, and fire resistance) [30]. In the model, the effects of radiation and heat convection on column is taken into account [30]. The thermal contact resistance between the core RAC and steel tube is considered in conformity of the suggestion of Ghojel [30]. In the heat transfer model, the core concrete and the steel jacket are modeled with linear 3D brick elements (DC3D8) and 3D shell elements (DS4), respectively [30]. Under high temperatures, plasticity model is used for steel tubes and the damaged plasticity model for core concrete is adopted [30]. The 'Coulomb friction' and 'hard contact' is chosen for the contact properties between core and steel, and geometric linearity is assumed for large lateral deflections [30]. In conclusion, it is stated that the temperature development and fire resistance, failure pattern and axial displacement of specimens with 50% RA are generally similar behavior with reference CFST, and the estimated response of CFST under fire is generally in good agreement with experiments [30].

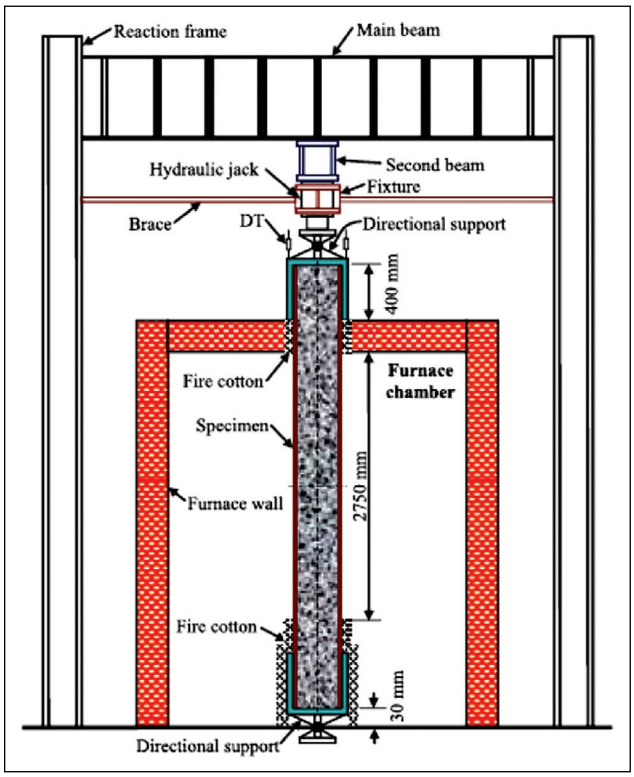


**Figure 11**. Schematic diagram of the test set-up [30].

Geng et al. [31] examine the time-dependent behavior of CFST with RAC (50 MPa). In this paper, a CFST is modeled in Abaqus. Core concrete and steel tubes are considered in Abaqus as Timoshenko beam elements (B31) and the time-dependent behavior of concrete is formed considering the Fathifazl creep model [31]. Under compression, the concrete constitutive model in Abaqus with the UMAT subroutine is used [31]. As a results, FEM gives a good agreement with the numerical results and the FEA results with the maximum deviation 1.9‰ is obtained in comparison to the numerical results [31].

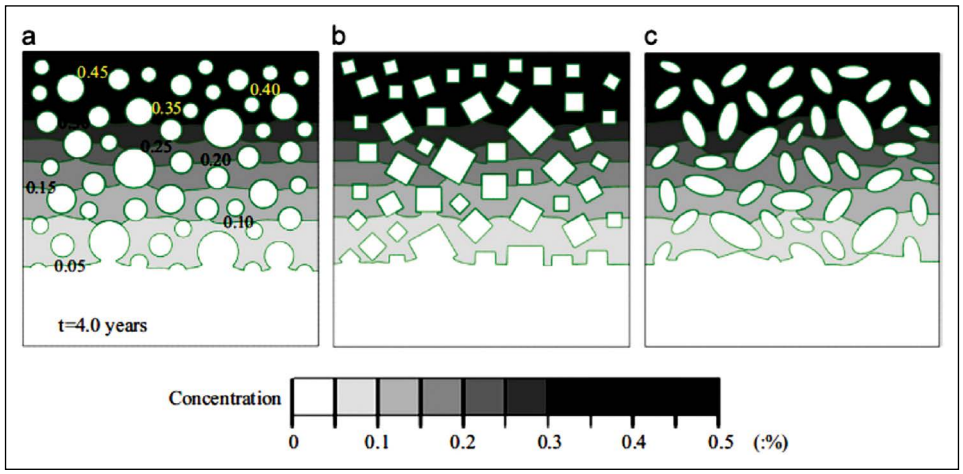


**Figure 12**. Total chloride concentration along the depth of three concrete specimens with different aggregate shapes, after4yearsofexposure [32].

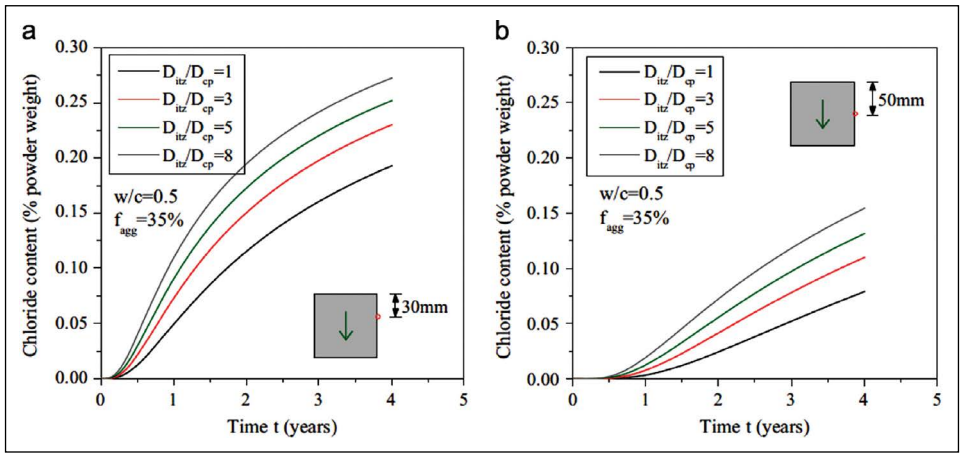


**Figure 13**. Chloride content-time of the specimen: **(a)** at cover depth=30 mmand **(b)** depth=50mm [32].

### *2.1.2. Meso-Scale Modeling*

Du et al. [32], in their research, develop a heterogeneous model including mortar matrix, aggregate, and ITZ to examine chloride diffusivity of concrete, especially RAC [32]. In the model, aggregates are assumed as an impermeable material and the chloride diffusion occurs through the mortar matrix and ITZs [32]. The diffusivity parameters of components, such as mortar matrix and ITZs, are obtained in the literature, and the model simulated in Abaqus is validated with the test given in the literature [32]. The transient analysis is chosen, and the period is 4 years [32]. 4-node linear heat transfer quadrilateral elements are used for concrete [32]. As a results, it is concluded that three different aggregate shape (squared and circular, elliptical) don't affect the chloride diffusion performances of RAC for the same aggregate volume ratio in concrete (Fig. 12) and, the chloride diffusion increases when ITZs thickness increases due to more porous structure and higher water/cement ratio of ITZ in comparison to the cement paste (Fig. 13) [32].

Kim et al. [33] conduct a series of numerical analysis on porous concrete pile (RAPP) produced with RA and compared the results with the numerical simulation results using Abaqus [33]. RAPP is modeled as a vertical drainage in Ref. [33]. In the modeling part, RAPP and the clay formation are simulated by using the Mohr–Coulomb model and the modified Cam clay model, respectively [33]. For all the components, 4-node bilinear displacement and the pore pressure element (CAX4P) is used [33]. It is stated that RAPP considerably contributes to enriching consolidation with supplying radial drainage [33].

Xiao et al. [34] examine the ITZs effects on stress-strain of RAC. In this paper, RAC is modeled in meso/micro scale in Abaqus (Fig. 14). The plastic-damage constitutive models are used, and the model is simulated to determine mechanical behavior (i.e., compression and tension) [34]. In Explicit step, ABAQUS/explicit quasi-static solver is used [34]. While defining the properties of ITZ and other parts, concrete damaged plasticity is considered and the properties of parts are based on experimental data (i.e., nano-indenta-

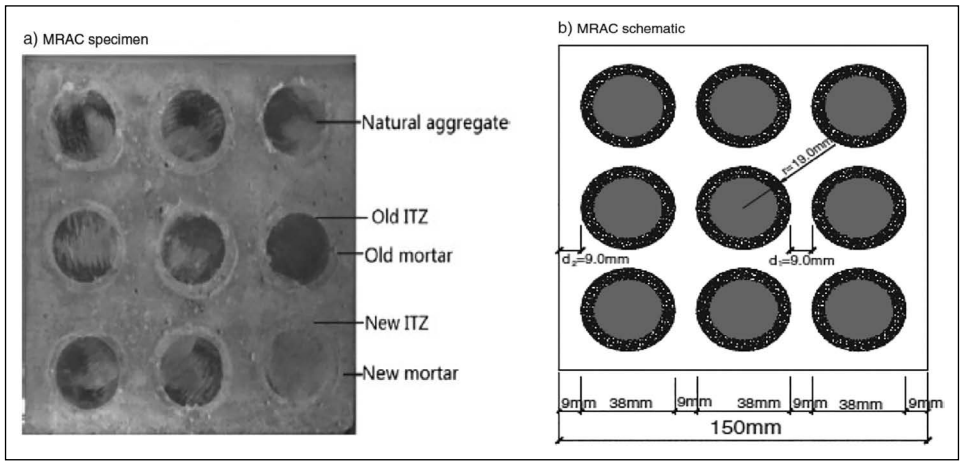


**Figure 14**. Modeled recycled aggregate concrete (MRAC) [34].

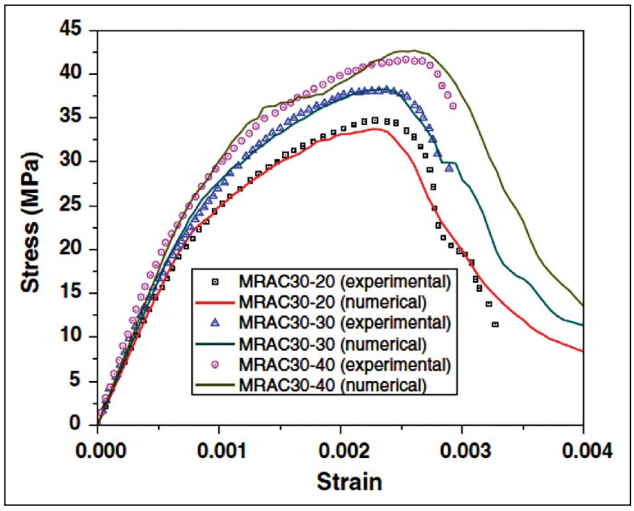


**Figure 15**. Compressive stress–strain curves with different new mortar matrices [34].

tion tests) [34]. It is concluded that the mortar matrixes and ITZs has a significant role on failure patterns and stress–strain relationship of modeled RAC (MRAC) (Fig. 15) [34].

Xiao et al. [35] propose a model to define the RA effect on chloride diffusion in RAC using Abaqus (Fig. 16). In the simulation part, a five-phase composite for RAC is modeled (Fig. 17) (these phases are old and new ITZs, old and new mortar, and original aggregate) [35]. The transient analysis and the 8-node quadratic heat transfer quadrilateral element are chosen for the model [35]. It is stated that the suggested heterogeneous RAC FE model works well and gives realistic chloride diffusion results [35].

Wang et al. [11] study the influence of old concrete carbonation on ITZ properties of RAC. In this paper, old concretes with various water/binder ratios are considered and modeled and are carbonated [11]. Then, the peak load, the load–displacement curves, and the peak displacement are examined to define the effect of carbonation on modeled RAC [11]. The model is simulated in Abaqus and is verified

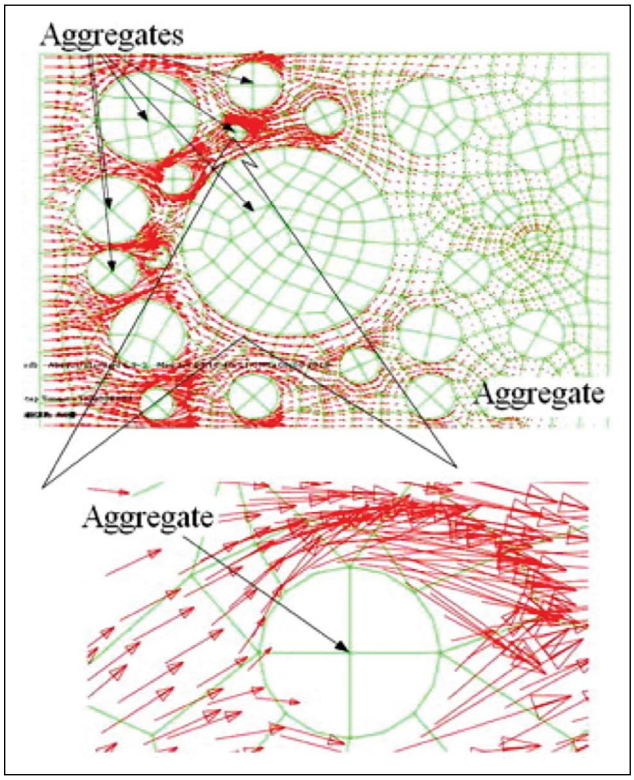


**Figure 16**. The chloride flow in modeling concrete [35].

with the test data [11]. In the modeling of mortar matrix and ITZ, the constitutive relationship of mortar matrix and ITZ is defined with damage plasticity model in Abaqus [11]. It is stated that ITZ properties have similarity with mortar matrix properties, however elastic modulus, and strength of ITZ are lower than the mortar matrix in the model [11]. On the other hand, in the modeling of natural aggregate (NA), NA is considered and modeled as an isotropic material [11]. In FEA, ABAQUS/explicit solver is used to solve FEM equations [11]. As a results, it is stated that ITZ properties of modeled RAC is considerably related with shape of RA, distribution of old mortar, and carbonation depth [11].

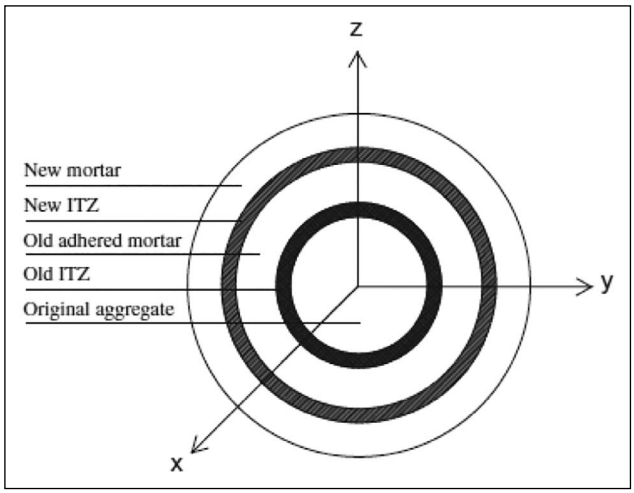


**Figure 17**. Five-phase composite sphere mode [35].

Ying et al. [10] investigate the effect of RA ratio on chloride diffusion in RAC using Abaqus (Fig. 18). The transient analysis and the 8-node quadratic heat transfer quadrilateral element are selected for FEM [10]. It is concluded that the consistent tendency for compressive strength and chloride migration in modeled RAC is observed and FEA results are verified with test results [10].

Xiao et al. [36] investigate RAC stress distribution while a pressure load is applied to RAC model in Abaqus. In FEA, overall mechanical properties, elastic stress distribution, damage localization and stress concentration are examined (Fig. 19) [36]. The static analysis in Abaqus is adopted to FEM and the linearity in the analysis is considered [36]. In conclusion, it is recommended that ITZ presents a strain softening behavior and the non-linearity in the analysis for ITZ should be considered [36].

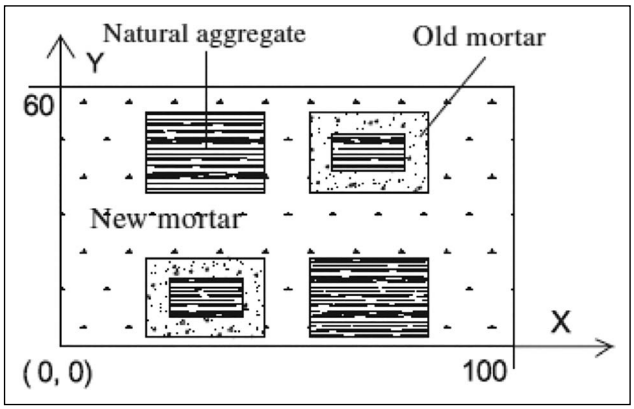


**Figure 18**. The MRAC containing modeled RA and NA [10].

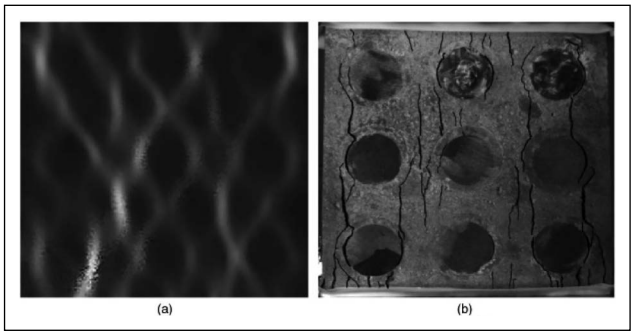


**Figure 19**. Testing results on the MRAC under uniaxial loading by the digital image correlation: **(a)** horizontal field strain contour map; **(b)** crack pattern [36].

### *2.1.3. Micro-Scale Modeling*

Jeong et al. [37] study on the time-dependent hydration phenomenon chemo-thermal modeling of mortars included RA and NA. In this paper experimental and theoretical

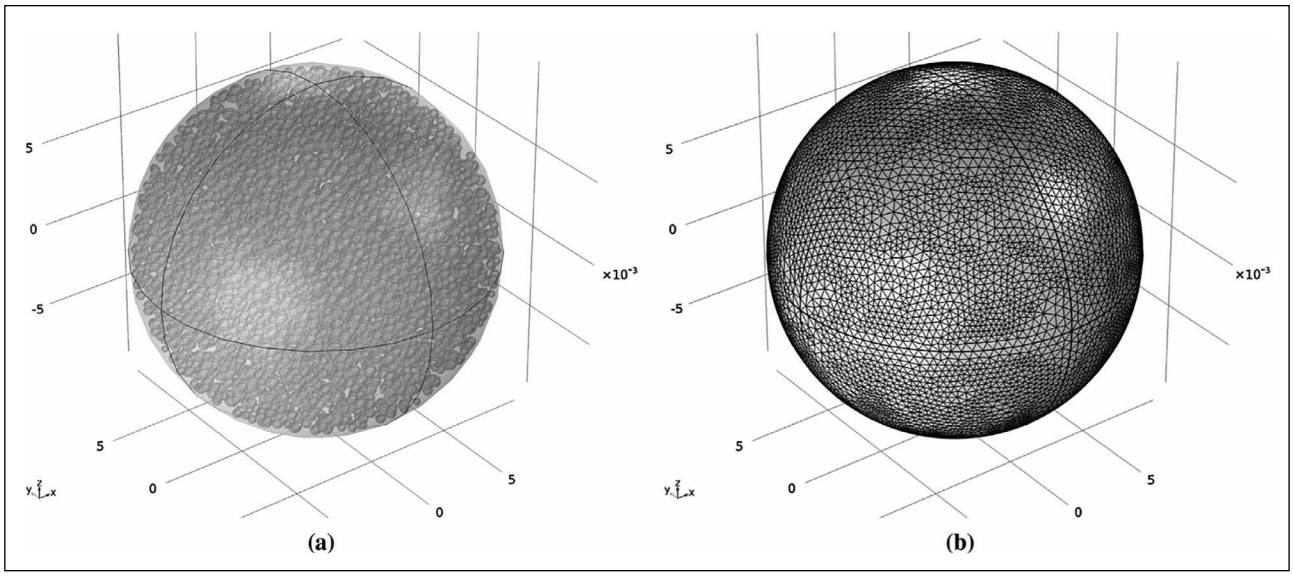


**Figure 20**. Illustration of geometrical configurations of M2-1 numerical EAG specimens, **(a)** cement matrix including 4149 sand grains and **(b)** mesh density [37].

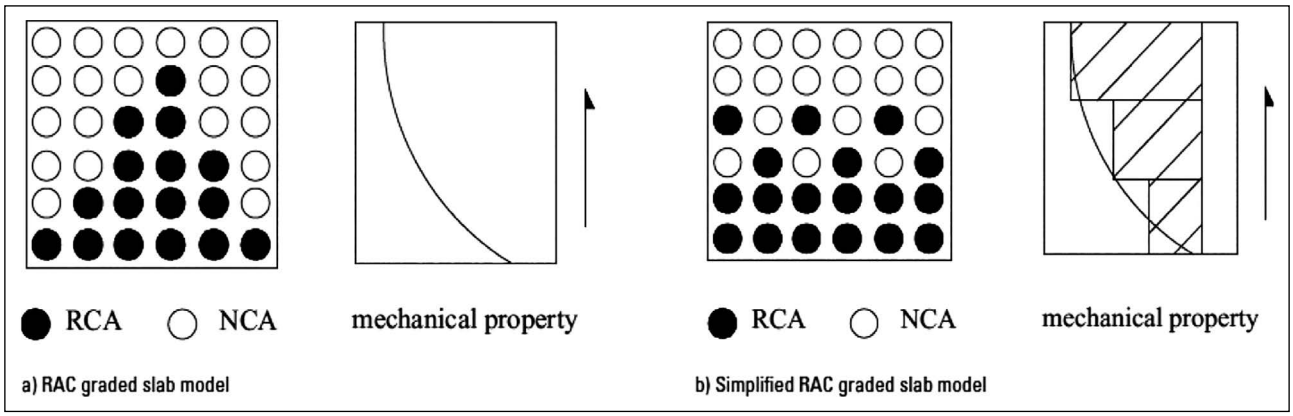


**Figure 21**. RAC graded slab models [38].

**Table 2.** Comparisons between ABAQUS simulation and experiment [38]

| Slab No. | | Yield load (kN) | Ultimate load (kN) | Yield displacement (mm) |
|---|---|---|---|---|
| 5f-1 | Test | 25.2 | 31.6 | 29.2 |
| | ABAQUS | 27.5 | 30.3 | 16.2 |
| 5h | Test | 22.0 | 30.5 | 28.0 |
| | ABAQUS | 26.5 | 29.8 | 17.3 |
| 5f-2 | Test | 18.2 | 29.3 | 27.7 |
| | ABAQUS | 24.4 | 33.4 | 13.3 |
| 7f-1 | Test | 27.8 | 39.6 | 16.7 |
| | ABAQUS | 37.5 | 41.1 | 15.6 |
| 7h | Test | 28.0 | 39.2 | 19.9 |
| | ABAQUS | 28.3 | 41.5 | 14.2 |
| 7f-2 | Test | 26.8 | 39.8 | 12.9 |
| | ABAQUS | 36.1 | 43.4 | 15.3 |

analysis are conducted and the modified Arrhenius' law and 3D FEA are considered [37]. In the modeling section, the Extracted Aggregate Groups (EAGs) concept is formed and has spherical geometry (Fig. 20) [37]. During the hydration process, the isotropic chemo-thermal features in the calorimeter device is considered [37]. Also, the pseudo-random geometric spherical packing algorithm is considered [37]. In this paper, the grains in the mortar are modeled and formed in Matlab-Comsolcode [37]. In the modeling, it is pointed out that the chemo-thermal modeling is in non-linear transient-state because the chemical reactions of cement paste have the non-linear features [37]. In conclusion, according to a user-written Matlab-Comsolcode FEA and the experimental results, the modified Arrhenius' law is not useful for the recycling mortar hydration modeling [37]. Hence, a revision is need for the modified Arrhenius' law if it is used for the recycling mortar hydration modeling [37].

## 3. REINFORCED RECYCLED AGGREGATE CONCRETE

It is well-known that the rebar behavior with concrete works together perfectly, and hence many concrete works included rebars and concrete, and investigations on their behavior are implemented around the world. In the literature, in parallel, the reinforced recycled aggregate concrete (RRAC)behavior is examined widely, and especially the comparative studies on RRAC, and reinforced NAC (RNAC) are done. Researchers are generally inspired to determine the properties of RRAC under the static and the dynamic loading conditions to assess the properties of RRAC (i.e., punching). Hence, in this section, the papers on modeling of RRAC are reviewed in two sub-sections consisted of the static and the dynamic loading conditions.

### 3.1. Modeling of Reinforced Recycled Aggregate Concrete

#### *3.1.1. Behavior Under Static Loading Conditions*

Xiao et al. [38] investigate RRAC graded slabs with 0-50-100% RA. The gradation of RA is done in consideration of the stress state in the element (Fig. 21) [38]. In the FEM, the flexural behavior of the slabs, the grading models effect, and the different reinforcement ratios effect are examined in Abaqus [38]. The rebars are embedded in RAC and the bond slip is not considered [38]. The slab model is divided into 3 parts due to the RRAC graded slab modeling method, and the divided parts have different material properties [38]. As a results, it is concluded that RRAC graded slabs presents a good flexural behavior and is feasible to simulate in a FEM (Table 2) [38].

Pacheco et al. [39] study on concrete structures made with RA to analysis the vertical load effect on the slabs. The two-stories concrete structure is designed according to Eurocode 2 and 8 (Fig. 22) [39]. In the modeling section, a 3D concrete structure is modeled using linear FEM in CSI SAP 2000 v.15, and the elasticity modulus of the concretes is predicted by FEM calibration [39].

Francesconi et al. [40] examine the punching shear behavior RRAC slabs with 30-50-80-100% RA. A linear FE slab model is simulated to obtain the prediction of the slab rotation. It is stated that the reinforcement in slab has an important role [40].

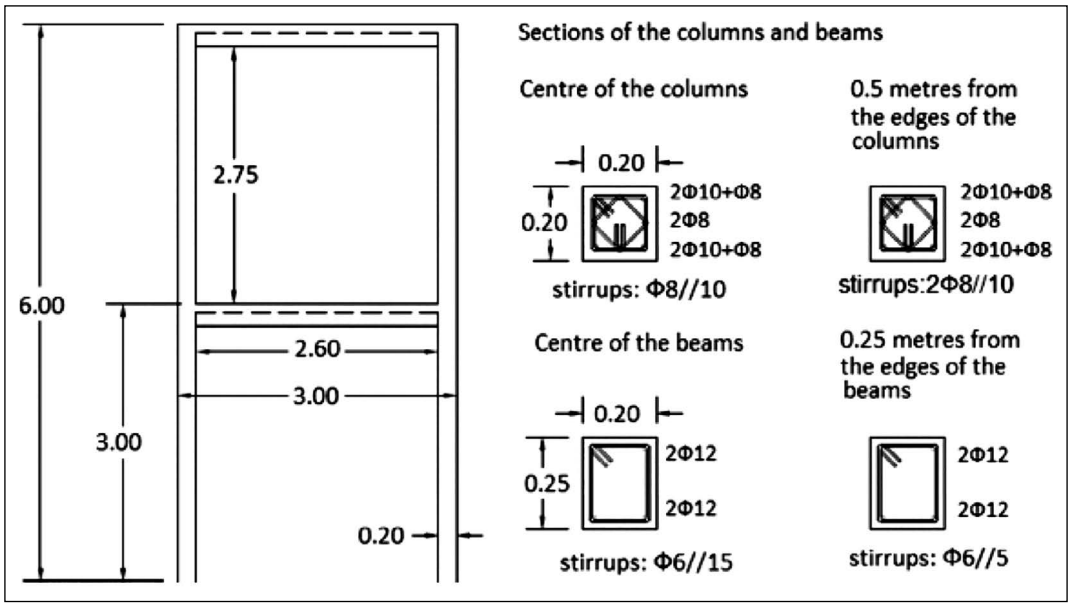


**Figure 22**. Geometry and reinforcement layout of the test-structures [39].

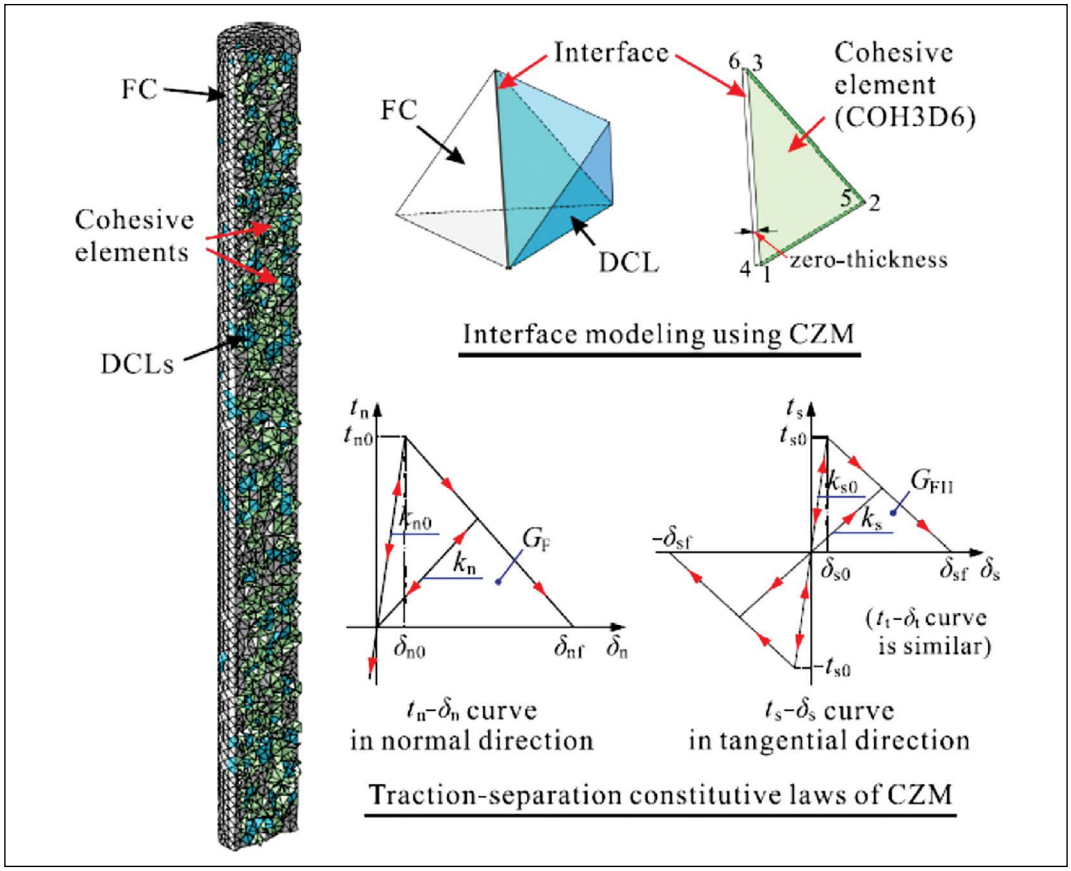


**Figure 23**. Cohesive zone model (CZM) and its traction-separation constitutive laws [41].

Zhao et al. [41] conduct research on thin-walled circular steel tubular columns and the columns indicate demolished concrete lumps (DCLs) and fresh concrete (FC) [41]. Under consideration of Monte Carlo simulation technique, a non-linear 3D FE model is simulated in Abaqus [41]. In the model DCLs are fully bonded and considered to have a random spatial distribution [41]. Also, the cohesive zone model (CZM) is adopted for the zone between DCLs and FC (Fig. 23) [41]. In

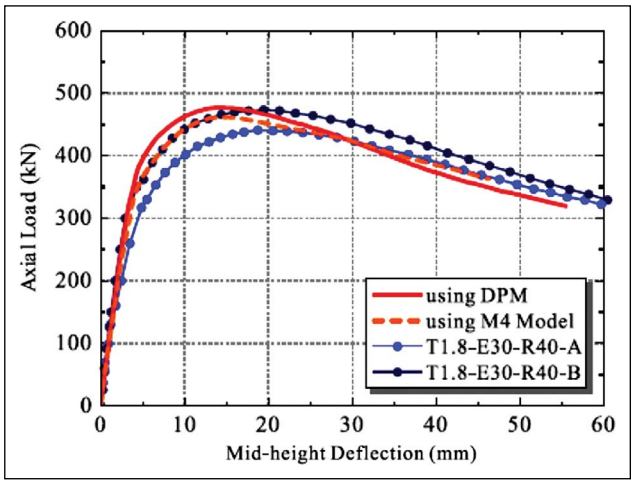


**Figure 24**. Comparison of simulation results using DPM and M4 model against test results [41].

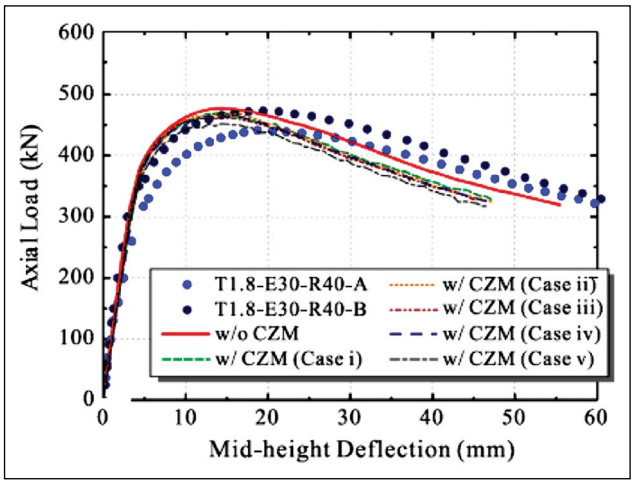


**Figure 25**. Comparison of simulation results with and without CZM against test results [41].

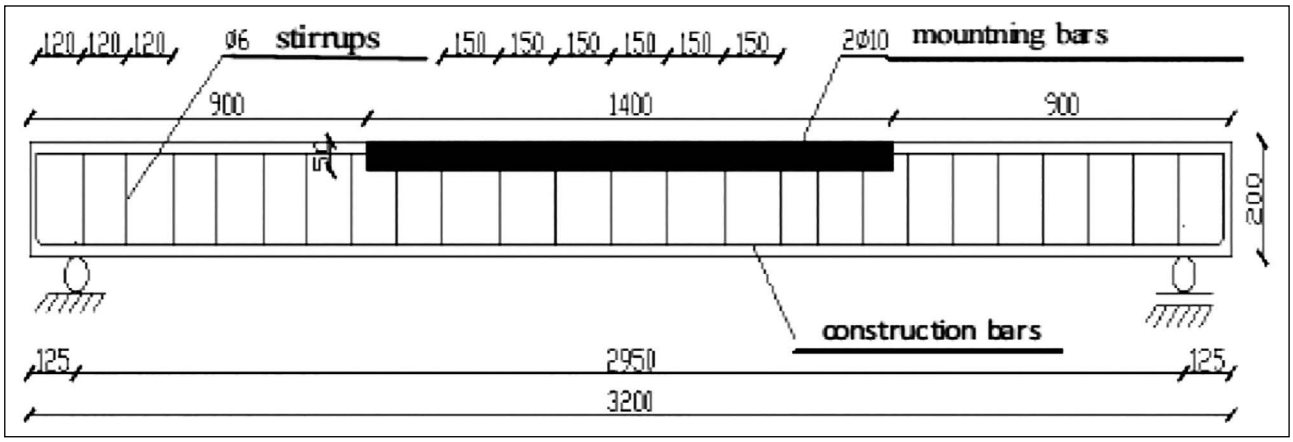


**Figure 26**. The scheme of innovative full-scale beam made of RAC with the insert made of HSC-HPC [42].

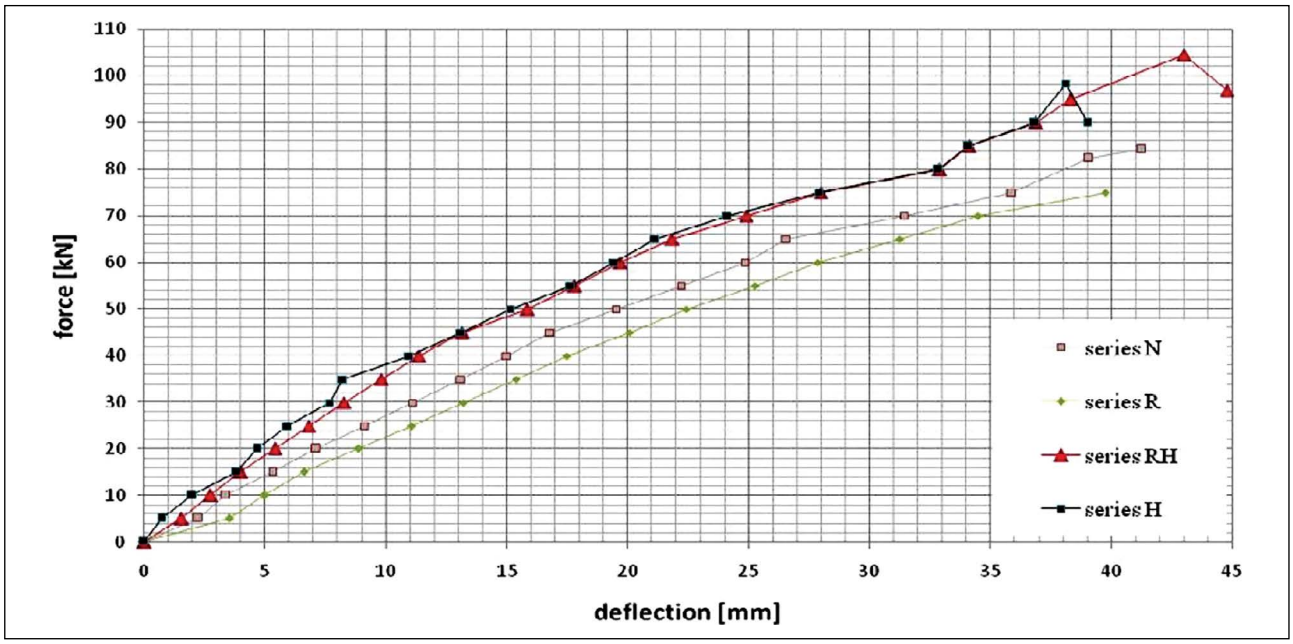


**Figure 27**. Comparison of average deflections of full-scale beams [42].

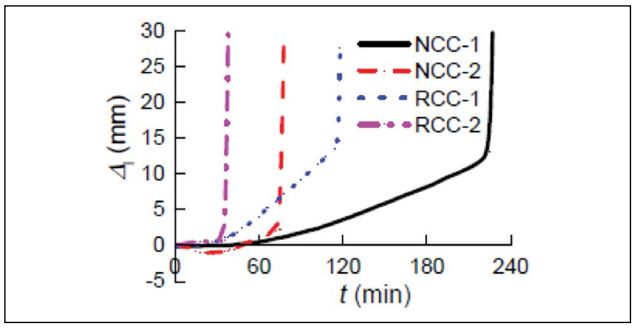


**Figure 28**. Specimen "vertical displacement to time" curves [43].

this research, the micro-plane model M4 developed by Bazant and based on kinematic constraint, and damaged plasticity model are considered in Abaqus for concrete constitutive modeling to compare the models (Fig. 24) [41]. The models are two inelastic constitutive laws and are well-established in the literature [41]. Then, it is concluded that the columns with DCLs are found suitable in reliance on a strength-reduction factor of 0.9 (Fig. 25) [41].

Lapko and Grygo [42] study on RRAC flexural members which include High Strength Concrete (HSC) - High Performance Concrete (HPC) locally (Fig. 26, 27). In this innovative concept, the non-linear FEMs are simulated in Diana FEA software and a Newton-Raphson algorithm is used in the FEM numerical solutions [42]. Also, the rebars are modeled as REBAR in Diana [42]. It is concluded that the use of HSC-HPC in compression zone of the reinforced beam considerably increase the stiffness and influence the deflections and strains [42].

Dong et al. [43] examine the effects of concrete compressive strength on the fire resistance performance of RRAC columns with C20 and C30 strength classes [43]. While the column is exposed to the fire, a constant axial force is subjected [43]. In the modeling part of the research, the four lateral sides of columns are exposed to the fire [43]. It is concluded that RRAC columns have higher fire resistance than conventional concrete if the columns have same compressive strength (Fig. 28) [43].

#### *3.1.2. Behavior Under Dynamic Loading Conditions*

Pacheco et al. [44] study on concrete structures made with RA to analysis the dynamic characterization of full-scale structures. In this paper, the two-stories3D concrete structure designed according to Eurocode 2 and 8is modeled using linear FEM in CSI SAP 2000 v.15, and elasticity modulus and modes of the structures are determined by FEM calibration (Fig. 29–31) [44]. It is concluded that the use of superplasticizers in RAC increase the elasticity modulus and is a good option, and the results of modal damping have high scatter (Fig. 32) [44].

Fu et al. [45] conduct a numeric study on seismic behavior of RRAC beams which is under torsion forces (Fig. 33). The numerical RRAC model is formed in Abaqus (Fig. 34) [45]. In the modeling part, the material behavior is defined in the plastic-damage model in Abaqus, and the stress-strain constitutive relationship of concrete is defined using Sargin model [45]. In the FEM, the rebars are embedded to the concrete and the non-linear analysis is adopted to model [45]. It is stated that the typical torsional failure in RRAC and RNAC beams are found similar [45].

Cao et al. [46] investigate the seismic performance of recycled concrete brick walls (RCBW) and study on the lateral load-displacement relations and the elastic-plastic deformation characteristics of RCBW. In the paper, vertical

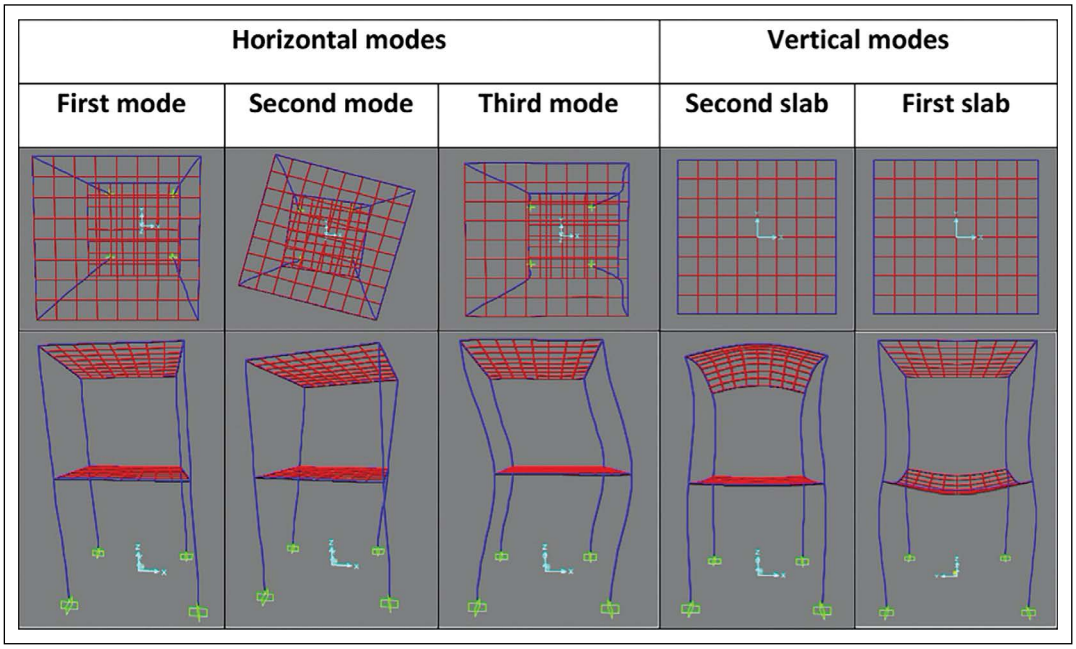


**Figure 29**. Modal configurations [44].

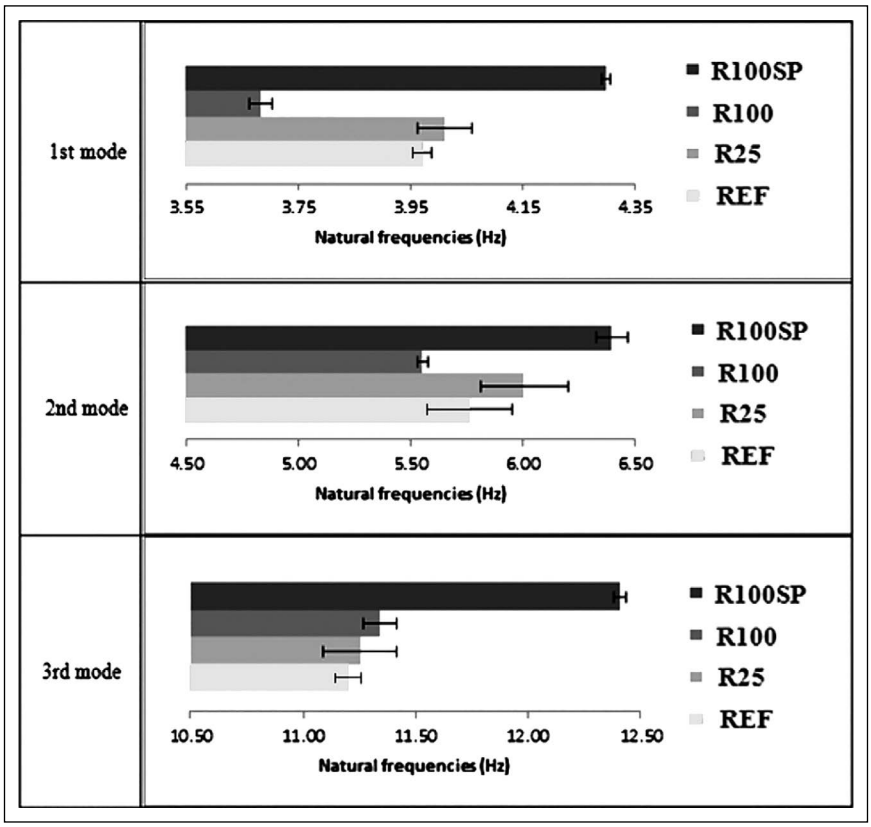


**Figure 30**. Average horizontal frequencies and confidence intervals (forced vibrations, seismograph) [44].

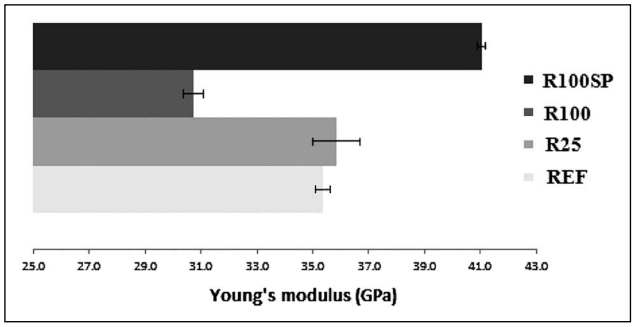


**Figure 31**. Average elasticity modulus after calibration and confidence intervals (seismograph) [44].

reinforcement is used and embedded in RCBW (Fig. 35), and RCBW FEMs are simulated in Abaqus [46]. The plastic-damage model and the plasticity model in Abaqus are considered for RCBW and the reinforcement of RCBW, respectively [46]. The contact between all the interface models is defined as hard contact and Coulomb friction model is adopted for the contact on the lateral axis [46]. As a results, it is concluded that RCBW with vertical reinforcement may be a good choice for the rural low-rise buildings when the seismic design of the low-rise buildings is considered [46].

Xiao et al. [47] study on the semi-precast column included NA and RA (Fig. 36, 37), and the columns are subjected to the low cyclic horizontal loading. In this paper, the columns are simulated in FEA software ANSYS [47]. In the modeling section, the concrete parameters are defined in the William–Warnke failure criterion and the smeared cracking model, and the double-slash elastic–plastic model is used for rebars [47]. The non-linear FE modeling demonstrates that the semi-precast RRAC and RNAC columns present a similar seismic behavior, and the bearing capacity increases when the core column RAC strength increases [47].

## 4. SUMMARY

This paper indicates a state-of-the-art review on the related investigations and results on macro-, meso- and micro-scale FE modeling of pure recycled aggregate concrete (RAC) and reinforced RAC (RRAC) under static and dynamic loadings. According to the comments stated above, generally concrete properties are able to be utilized as a non-linear parameter in FEA with various constitutive models (i.e., concrete damaged plasticity and concrete smeared cracking models in Abaqus), and hence this concept ensures to get closer results to reality and to puts out material behavior clearly. This phenomenon is valid for not only pure RAC but also RRAC. On the other hand, many simulation studies are conducted using FEA, some branches of science on pure and reinforced RAC stay short in the literature (i.e., micro-scale behavior of RAC). As a result, the followings can be drawn:

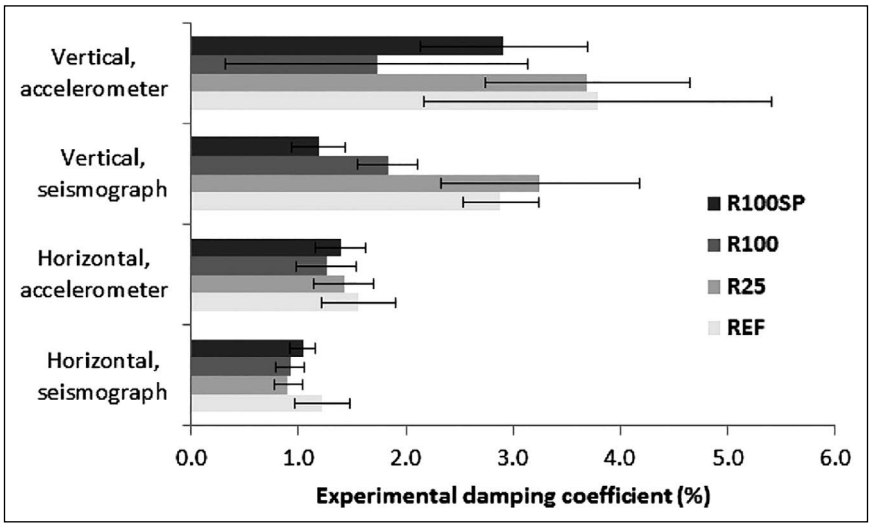


**Figure 32**. Average damping estimation and confidence intervals [44].

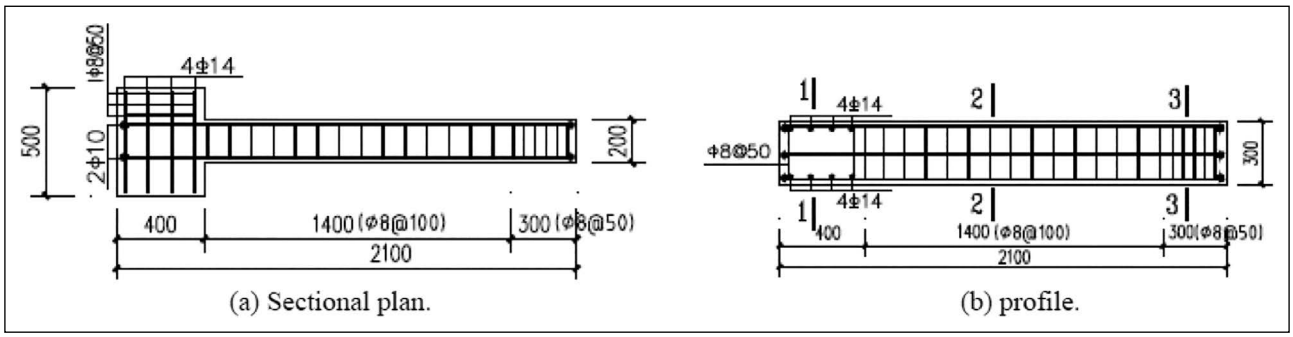


**Figure 33**. Specimen configuration and reinforcement details [45].

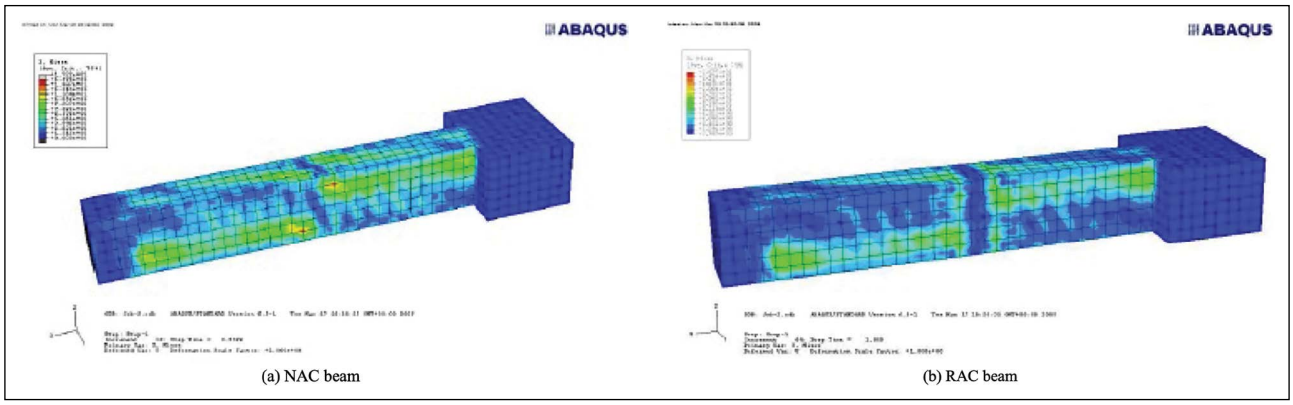


**Figure 34**. Von Misses stress of the two kinds of specimens [45].

**(1) RAC**

- It is necessary to determine the micro-scale behavior of RAC and the micro-scale behavior of RAC can be modeled in FEM.
- The harmful environment effects on RAC can be modeled in FEM considering macro-, meso- and micro-scale behavior of RAC (i.e., freeze-thaw and chemical attack effects).
- The properties of RAC and its components (attached old mortar, new and old ITZ etc.) should be determined after a fire effect, a chemical attack, etc. subjected to RAC. Here, the gradient of the properties of RAC and its components under the effects commented before can be determined, and then RAC can be modeled properly in FEM. It is thought that the next features of RAC are substantial as much as the initial features of RAC, especially for the durability properties of RAC.
- The chemical and mineral additions effects on mi-

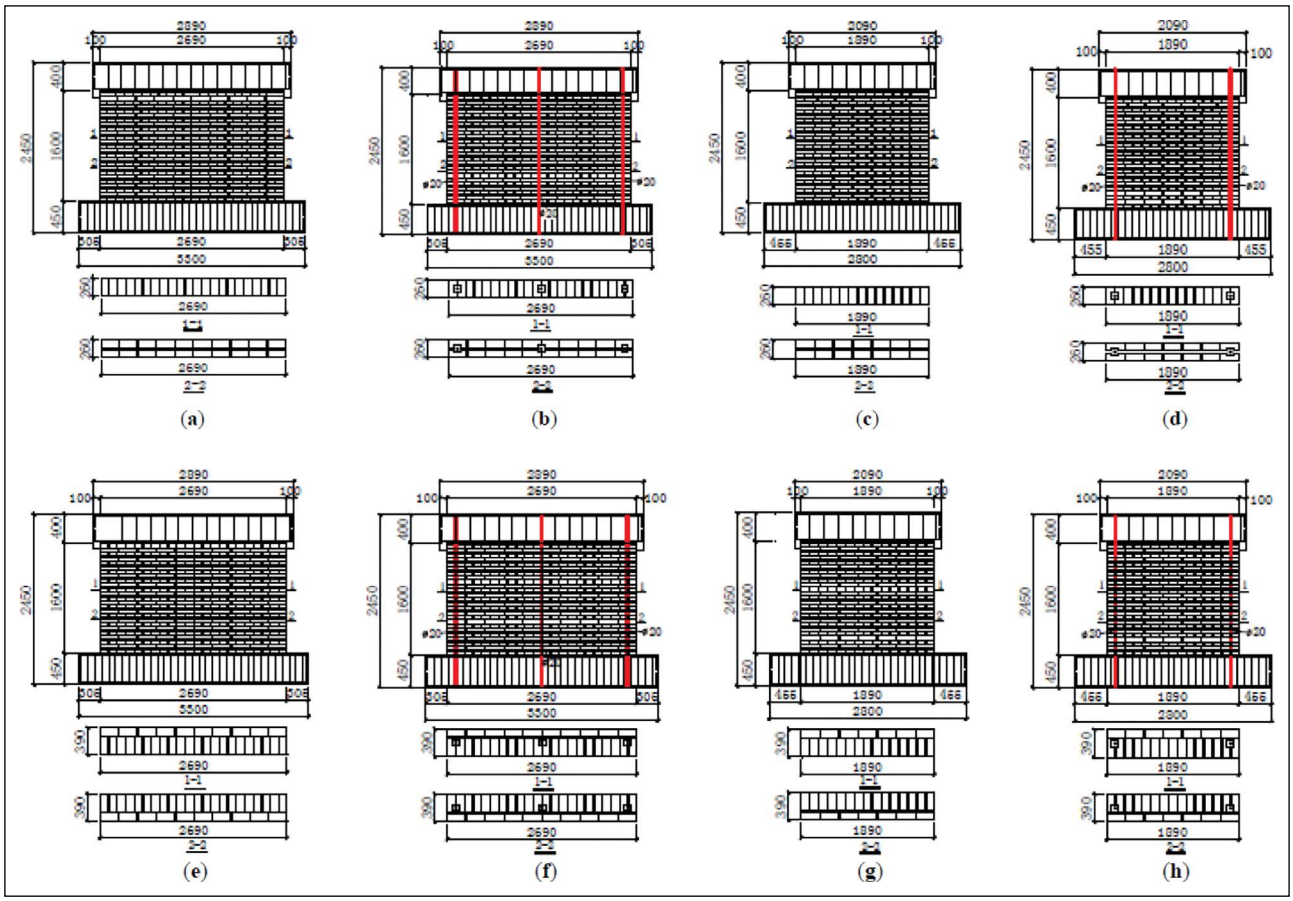


**Figure 35**. The dimensions and details of all the specimens: **(a)** MWA-1; **(b)** MWB-1; **(c)** MWA-2; **(d)** MWB-2; **(e)** MWA-3; **(f)** MWB-3; **(g)** MWA-4; **(h)** MWB-4. (Unit: millimeter) [46].

cro-scale behavior of RAC can be analyzed and modeled. For instance, the mineral additions improve the quality of mortar due to the formation of additional silicate gels (C-S-H) and this phenomenon can be modeled in micro-scale.

- RAC subjected to the cyclic loading conditions can be examined and RA effect on the macro-, meso- and micro-scale behavior of RAC can be determined. Also, the crack propagation in the RAC mass due to the cyclic loading can be modeled and the effective factors can be examined in FEM.

**(2) RRAC**

- Under the consideration of RRAC seismic behavior, the factors enhance the RAC structure seismic performance can be determined and modeled in FEM. Especially, starting from element to structure (from micro-scale to macro-scale), the rebar design in cross-sections should be properly considered and then experiments can be conducted to verify the results or both can be done.
- Stirrup effect on RRAC under various loads and moments conditions should be determined and FEM models can simulate the conditions. Hence, it can be seen how the probable situations affect the structural performance.
- The harmful environment effects on RRAC can be modeled in FEM and its effect on structural performance can be determined.
- RRAC subjected to the cyclic loading conditions can be examined and RA effect on the micro-, meso- and macro-behavior of RRAC can be determined. Also, the crack propagation in the RAC mass of RRAC and the interface between the rebars and RAC of RRAC due to the cyclic loading can be modeled and hence, it can be seen how the probable situations affect the structural performance.

## DATA AVAILABILITY STATEMENT

The author confirm that the data that supports the findings of this study are available within the article. Raw data that support the finding of this study are available from the corresponding author, upon reasonable request.

## CONFLICT OF INTEREST

The author declare that they have no conflict of interest.

## FINANCIAL DISCLOSURE

The author declared that this study has received no financial support.

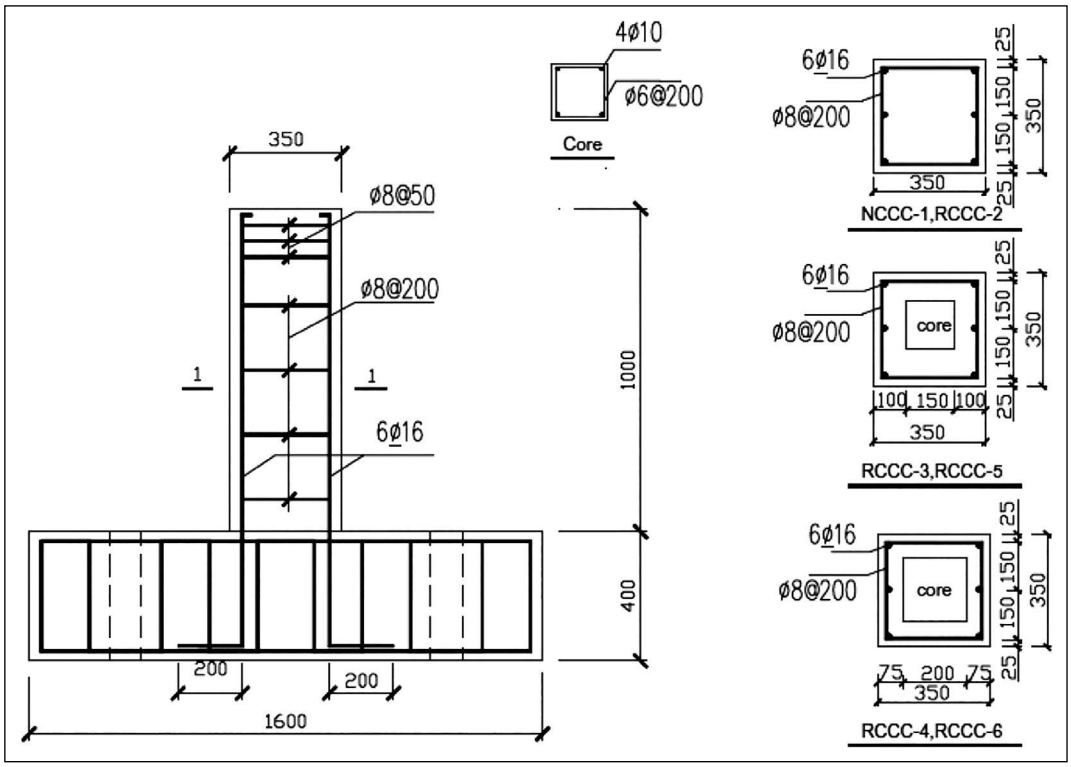


**Figure 36**. Reinforcement diagram of specimens [47].

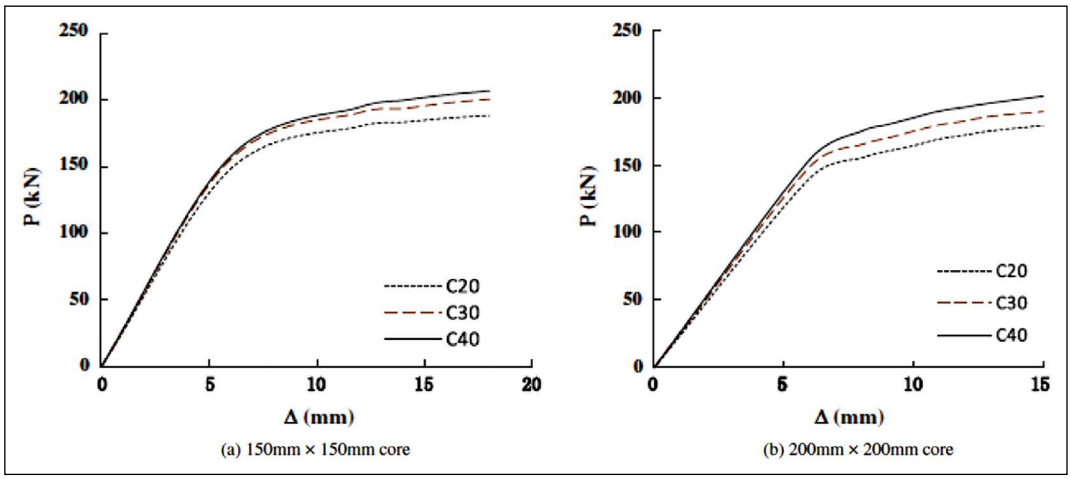


**Figure 37**. Effect of core compressive strength on the load – deflection (P-Δ) relationship [47].

## PEER-REVIEW

Externally peer-reviewed.

## REFERENCES

[1] Dilbas, H., Şimşek, M., Çakır, Ö. (2014). An Approach for Construction and Demolition (C&D) Waste Disposal through Concrete Using Silica Fume, in: EurAsia Waste Management Symposium, Istanbul, Turkey.

[2] Xiao, J., Li, W., Fan, Y., Huang, X. (2012). An overview of study on recycled aggregate concrete in China (1996–2011). *Construction and Building Materials*, 31, 364–383. [CrossRef]

[3] European Parlement (2008), Directive 2008/98/EC of The European Parliament and of The Council of 19 November 2008 on Waste and Repealing Certain Directives (text with EEA relevance). Brussels, Belgium.

[4] Dilbas, H. (2014). *An examination on mechanical behaviour of a cantilever beam produced with recycled aggregate concrete* [Unpublished master disser-

tation], Yıldız Technical University.
[5] Dilbas, H., Şimşek, M., Çakır, Ö. (2014). An investigation on mechanical and physical properties of recycled aggregate concrete (RAC) with and without silica fume. *Construction and Building Materials*, 61, 50–59. [CrossRef]
[6] Akça, K., Çakır, Ö., İpek, M. (2015). Properties of polypropylene fiber reinforced concrete using recycled aggregates. *Construction and Building Materials*, 98, 620–630. [CrossRef]
[7] Çakır, Ö. (2014). Experimental analysis of properties of recycled coarse aggregate (RCA) concrete with mineral additives. *Construction and Building Materials*, 68, 17–25. [CrossRef]
[8] Duan, Z.H., Poon, C.S. (2014). Properties of recycled aggregate concrete made with recycled aggregates with different amounts of old adhered mortars. *Materials and Design*, 58, 19–29. [CrossRef]
[9] Gaedicke, C., Roesler, J., Evangelista, F. (2012). Three-dimensional cohesive crack model prediction of the flexural capacity of concrete slabs on soil. 94, 1–12. [CrossRef]
[10] Ying, J., Xiao, J., Tam, V.W.Y. (2013). On the variability of chloride diffusion in modelled recycled aggregate concrete. *Construction and Building Materials*, 41, 732–741. [CrossRef]
[11] Wang, C., Xiao, J., Zhang, G., Li, L. (2016). Interfacial properties of modeled recycled aggregate concrete modified by carbonation. *Construction and Building Materials*, 105, 307–320. [CrossRef]
[12] Xiao, J., Li, W., Poon, C.S (2012). Recent studies on mechanical properties of recycled aggregate concrete in China-a review. *Science China Technological Sciences*, 55, 1463–1480. [CrossRef]
[13] Dilbas, H., Çakır, Ö. (2016). Fracture and Failure of Recycled Aggregate Concrete (RAC)–A Review. *International Journal of Concrete Technology*, 1, 31–48.
[14] Shi, C., Li, Y., Zhang, J., Li, W., Chong, L., Xie, Z. (2015). Performance enhancement of recycled concrete aggregate – A review. Journal of Cleaner Production, 112, 466–472. [CrossRef]
[15] Behera, M., Bhattacharyya, S.K., Minocha, A.K., Deoliya, R., Maiti, S. (2014). Recycled aggregate from C&D waste & its use in concrete - A breakthrough towards sustainability in construction sector: a review. *Construction and Building Materials*, 68, 501–516. [CrossRef]
[16] Hansen, T.C. (1986). Recycled aggregates and recycled aggregate concrete second state-of-the-art report developments 1945-1985. *Materials and Structures*, 19, 201–246. [CrossRef]
[17] Xiao, J.-Zh., Li, J.-B., Zhang, Ch. (2007). On relationships between the mechanical properties of recycled aggregate concrete: An overview. *Materials and Structures*, 39, 655–664. [CrossRef]
[18] Genikomsou, A.S., Polak, M.A. (2015). Finite element analysis of punching shear of concrete slabs using damaged plasticity model in ABAQUS. *Engineering Structures*, 98, 38–48. [CrossRef]
[19] Dilbas, H., Çakir, Ö., Şimşek, M. (2017). Recycled aggregate concretes (RACs) for structural use: an evaluation on elasticity modulus and energy capacities. *International Journal of Civil Engineering*, 15, 247–261. [CrossRef]
[20] Dilbas, H., Çakır, Ö., Şimşek, M. (2015). Kentsel Dönüşüm Sonucu Oluşan Molozların Geri Dönüşümle Betonda Kullanımı – Silis Dumanı Katkılı Geri Kazanılmış Agregalı Betonlar, 9. Ulusal Beton Kongresi, Antalya. pp. 387–398.
[21] Etse, G., Vrech, S.M., Ripani, M. (2016). Constitutive theory for Recycled Aggregate Concretes subjected to high temperature. *Construction and Building Materials*, 111, 43–53. [CrossRef]
[22] Choubey, R.K., Kumar, S., Chakradhara Rao, M. (2016). Modeling of fracture parameters for crack propagation in recycled aggregate concrete. *Construction and Building Materials*, 106, 168–178. [CrossRef]
[23] Musiket, K., Vernerey, F., Xi, Y. (2016). Numeral modeling of fracture failure of recycled aggregate concrete beams under high loading rates. *International Journal of Fracture*, 203, 263–276. [CrossRef]
[24] Ripani, M., Etse, G., Vrech, S. (2017). Recycled aggregate concrete: Localized failure assessment in thermodynamically consistent non-local plasticity framework. *Computers and Structures*, 178, 47–57. [CrossRef]
[25] Ceia, F.M.A.P.M. (2013). *Shear strength in the interface between normal concrete and recycled aggregate concrete* [Unpublished master dissertation], Tecnico Lisboia. [CrossRef]
[26] Vivian, T. Wang. W.Y.Z., Tao, Z. (2014). Behaviour of recycled aggregate concrete filled stainless steel stub columns. *Materials and Structures*, 47, 293–310. [CrossRef]
[27] Yang, Y., Zhang, Z., Fu, F. (2015). Experimental and numerical study on square RACFST members under lateral impact loading. *Journal of Constructional Steel Research*, 111, 43–56. [CrossRef]
[28] Xiao, J., Huang, Y., Yang, J., Zhang, C. (2012). Mechanical properties of confined recycled aggregate concrete under axial compression. *Construction and Building Materials*, 26, 591–603. [CrossRef]
[29] Xiang, X., Cai, C.S., Zhao, R., Peng, H. (2016). Numerical analysis of recycled aggregate concrete-filled steel tube stub columns. *Advances in Structural Engineering*, 19, 717–729. [CrossRef]
[30] Yang, Y., Zhang, L., Dai, X. (2016). Performance of

recycled aggregate concrete- filled square steel tubular columns exposed to fire. *Advances in Structural Engineering*, 20, 1340–1356. [CrossRef]

[31] Geng, Y., Wang, Y., Chen, J. (2016). Time-dependent behaviour of steel tubular columns filled with recycled coarse aggregate concrete. *Journal of Constructional Steel Research*, 122, 455–468. [CrossRef]

[32] Du, X., Jin, L., Ma, G. (2014). A meso-scale numerical method for the simulation of chloride diffusivity in concrete. *Finite Elements in Analysis and Design*, 85, 87–100. [CrossRef]

[33] Kim, S., Lee, D., Lee, J., You, S.-K., Choi, H. (2012). Application of recycled aggregate porous concrete pile (RAPP) to improve soft ground. *Journal of Material Cycles and Waste Management*, 14, 360–370. [CrossRef]

[34] Xiao, J., Li, W., Corr, D.J., Shah, S.P. Effects of interfacial transition zones on the stress–strain behavior of modeled recycled aggregate concrete. *Cement and Concrete Research*, 52, 82–99. [CrossRef]

[35] Xiao, J., Ying, J., Shen, L. (2012). FEM simulation of chloride diffusion in modeled recycled aggregate concrete. *Construction and Building Materials*, 29, 12–23. [CrossRef]

[36] Xiao, J., Li, W., Asce, S.M., Corr, D.J., Shah, S.P., Asce, M. (2013). Simulation study on the stress distribution in modeled recycled aggregate concrete under uniaxial compression. *Journal of Materials in Civil Engineering*, 25, 504–518. [CrossRef]

[37] Jeong, J., Ramézani, H., Leklou, N. (2016). Why does the modified Arrhenius' law fail to describe the hydration modeling of recycled aggregate? *Thermochimica Acta*, 626, 13–30. [CrossRef]

[38] Xiao, J., Sun, C., Jiang, X. (2015). Flexural behaviour of recycled aggregate concrete graded slabs. *Structural Concrete*, 16, 249–261. [CrossRef]

[39] Pacheco, J., De Brito, J., Ferreira, J., Soares, D. (2015). Flexural load tests of full-scale recycled aggregates concrete structures. *Construction and Building Materials*, 101, 65–71. [CrossRef]

[40] Francesconi, L., Pani, L., Stochino, F. Punching shear strength of reinforced recycled concrete slabs. *Construction and Building Materials*, 127, 248–263. [CrossRef]

[41] Zhao, X., Wu, B., Wang, L. (2016). Structural response of thin-walled circular steel tubular columns filled with demolished concrete lumps and fresh concrete. *Construction and Building Materials*, 129 216–242. [CrossRef]

[42] Lapko, A., Grygo, R. (2013). Studies of RC beams made of recycling aggregate concrete strengthened with the HSC-HPC inclusions. *Procedia Engineering*, 57, 678–686. [CrossRef]

[43] Dong, H., Cao, W., Bian, J., Zhang, J. (2014). The fire resistance performance of recycled aggregate concrete columns with different concrete compressive strengths. *Materials*, 7, 7843–7860. [CrossRef]

[44] De Brito, J., Soares, D. (2017). Dynamic characterization of full-scale structures made with recycled coarse aggregates. *Journal of Cleaner Production*, 142, 4195–4205. [CrossRef]

[45] Fu, J., Liu, B., Ma, J., Zhou, H. (2015). Experimental study on seismic behavior of recycled aggregate concrete torsion beams with Abaqus. *Advanced Materials Research*, 1079, 220–225. [CrossRef]

[46] Cao, W., Zhang, Y., Dong, H., Zhou, Z., Qiao, Q. (2014). Experimental Study on the seismic performance of recycled concrete brick walls embedded with vertical reinforcement. *Materials*, 7, 5934–5958. [CrossRef]

[47] Xiao, J., Huang, X., Shen, L. (2012). Seismic behavior of semi-precast column with recycled aggregate concrete. *Construction and Building Materials*, 35, 988–1001. [CrossRef]